U.S. Department
of Transportation
**National Highway
Traffic Safety
Administration**

NHTSA
www.nhtsa.gov

DOT HS 812 051A

August 2014

Methodology for Evaluating Fleet Protection of New Vehicle Designs: Application to Lightweight Vehicle Designs

DISCLAIMER

Suggested APA Format Citation:

Samaha, R. R., Prasad, P., Marzougui, D., Cui, C., Digges, K., Summers, S., Patel S., Zhao, L., & Barsan-Anelli, A. (2014, August). *Methodology for evaluating fleet protection of new vehicle designs: Application to lightweight vehicle designs.* (Report No. DOT HS 812 051A). Washington, DC: National Highway Traffic Safety Administration.

Technical Report Documentation Page

1. Report No.	2. Government Accession No.	3. Recipients's Catalog No.	
DOT HS 812 051A			
4. Title and Subtitle Methodology for Evaluating Fleet Protection of New Vehicle Designs: Application to Lightweight Vehicle Designs		5. Report Date August 2014 6. Performing Organization Code	
7. Author(s) Randa Radwan Samaha, Priya Prasad, Dhafer Marzougui, Chongzhen Cui, Kennerly Digges, Stephen Summers, Lixin Zhao, Aida Barsan-Anelli		8. Performing Organization Report No.	
9. Performing Organization Name and Address The National Crash Analysis Center The George Washington University 45085 University Drive Ashburn, VA 20147		10. Work Unit No. (TRAIS)n code 11. Contract of Grant No. DTFH61-09-D-00001, TOPR No. 16	
12. Sponsoring Agency Name and Address National Highway Traffic Safety Administration 1200 New Jersey Avenue SE. Washington, DC 20590		13. Type of Report and Period Covered Technical Report, 2010-2013 14. Sponsoring Agency Code	
15. Supplementary Notes			

16. Abstract

The National Crash Analysis Center (NCAC) has developed a systems modeling approach to assess real-world safety of vehicle designs in a virtual environment. This effort was to support NHTSA's research for assessing the effects of future vehicle design on safety, in particular, future lightweight vehicle designs. The approach includes estimating the real-world level of safety in a vehicle for its own occupants (self-protection) and for the occupants in vehicles with which it collides (partner protection). This approach will be referred to as EFP—Evaluating Fleet Protection—in this report. EFP is particularly useful for assessing innovative and new designs, and has the potential of becoming a powerful tool to study countermeasure strategies to improve and set priorities for both pre-crash and integrated safety and crashworthiness. As an initial implementation, EFP was applied to drivers in frontal crashes where the systems modeling was driven by finite element structural and rigid body occupant modeling, and real-world crash and full scale test data; however, the EFP approach can be extended to all crash modes and occupants.

EFP was applied to assess frontal crash safety performance of engineering models of concept lightweight vehicle designs developed in projects by the California Air Resources Board (CARB), Environmental Protection Agency (EPA), and National Highway Traffic Safety Administration as part of the Corporate Average Fuel Economy (CAFE) research efforts.

17. Key Words	18. Distribution Statement		
Fleet systems modeling, real-world crashes, self-protection, partner protection, societal injury risk, finite element structural modeling, rigid body occupant modeling, frontal crash simulations	Document is available to the public from the National Technical Information Service www.ntis.gov		
19. Security Classif. (of this report) Unclassified	20. Security Classif. (of this page) Unclassified	21. No of Pages 120	22. Price

Form DOT F1700.7 (8-72) **Reproduction of completed page authorized**

TABLE OF CONTENTS

LIST OF FIGURES

LIST OF TABLES

1 EXECUTIVE SUMMARY

The National Crash Analysis Center (NCAC) has developed a systems modeling approach to assess real-world safety of vehicle designs in a virtual environment. This effort was to support NHTSA's research for assessing the effects of future vehicle design on safety, in particular, future lightweight vehicle designs. The approach includes estimating the real-world level of safety in a vehicle for its own occupants (self-protection) and for the occupants in vehicles with which it collides (partner protection). This approach will be referred to as EFP—Evaluating Fleet Protection—in this report. EFP is particularly useful for assessing innovative and new designs, and has the potential of becoming a powerful tool to study countermeasure strategies to improve and set priorities for both pre-crash and integrated safety and crashworthiness. As an initial implementation, EFP was applied to drivers in frontal crashes where the systems modeling was driven by finite element structural and rigid body occupant modeling, and real-world crash and full scale test data; however, the EFP approach can be extended to all crash modes and occupants.

EFP was applied to assess frontal crash safety performance of engineering models of concept lightweight vehicle designs developed in projects by the California Air Resources Board (CARB), Environmental Protection Agency (EPA), and National Highway Traffic Safety Administration as part of the Corporate Average Fuel Economy (CAFE) research efforts.

1.1 Background

Innovative vehicle designs with new power trains and advanced lightweight materials like aluminum, magnesium, and advanced lightweight steels, plastics, and composites are being introduced into vehicle designs at a faster rate than in the past. There are anticipated changes in the composition of the U.S. vehicle fleet in response to the proposed CAFE Regulation where the average mass of the fleet is expected to get substantially lighter in order to meet higher fuel economy goals set by the regulation. The real-world crash safety implications resulting from future changes in fleet segment composition and mass reduction are difficult to estimate based on past experience.

The state-of-art in finite element (FE) modeling, encompassing both sophisticated software and powerful computers, is advanced enough that detailed models of a vehicle are now developed first in the pre-prototype stage of the vehicle and exercised in the various crash modes required by existing regulations and or consumer information crash tests. Several such research concept vehicle designs using advanced lightweight materials and manufacturing processes have been made public through projects sponsored by NHTSA, EPA, and CARB. The regulatory and consumer information tests are representative of real-world single-vehicle crash configurations but are performed at high speeds and the dummy occupant is generally a mid-size male. In the real-world, crashes occur at various impact velocities, configurations, impact partners (e.g., rigid obstacles, lighter or heavier vehicles), and involve occupants of various sizes and ages. To date, real-world interactions of new vehicle designs with both the existing and future fleets and the roadway environment had not been attempted through simulations because a systematic approach had not been developed or defined.

1.2 Methods/Analyses

The EFP methodology uses FE simulations (vehicle and occupants) of real-world crashes at various speeds and crash modes with occupants of various sizes to estimate the level of self-protection in single-vehicle crashes and both self- and partner-protection in two-vehicle crashes. A measure of societal injury risk, i.e., both self- and partner-protection, is calculated from the various simulations. The initial implementation of EFP was in various modes of frontal crashes as shown in Figure 1-1.

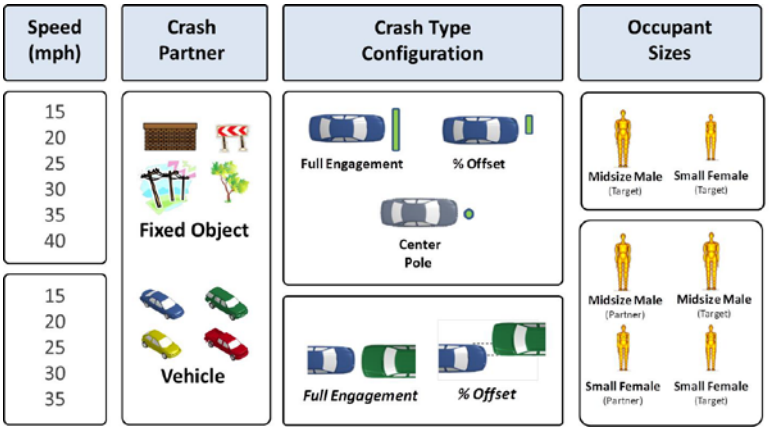

Figure 1-1. Frontal crash modes for initial implementation of EFP

$$\boldsymbol{SIR_{frontal}(v)} = \sum_{k=1}^{Kevent} \sum_{l=1}^{Loccsize} \sum_{m=1}^{Mconfig} \sum_{n=0}^{Npartner} \sum_{o=1}^{T/P} \sum_{p=1}^{Pspeed} \boldsymbol{w_{klmnop}(v)} * \boldsymbol{CIR_{klmnop}(v)}$$

The computed societal injury risk (SIR) for a target vehicle $\boldsymbol{v}$ in frontal crashes is an aggregate of individual serious crash injury risks weighted by real-world frequency of occurrence $\boldsymbol{w_{klmnop}(v)}$ of a frontal crash incident. A crash incident corresponds to a crash with different partners (*Npartner*) at a given impact speed (*Pspeed*), for a given driver occupant size (*Loccsize*), in the target or partner vehicle (*T/P*), in a given crash configuration (*Mconfig)*, and in a single- or two-vehicle crash (*Kevent*). $CIR_{klmnop}(v)$ represents the combined injury risk (by body region) in a single crash incident. $w_{klmnop}(v)$ designates the weighting factor, i.e., percent of occurrence, derived from National Automotive Sampling System Crashworthiness Data System (NASS CDS) for the crash incident. A driver age group of 16 to 50 years old was chosen to provide a population with a similar, i.e., more consistent, injury tolerance.

The following provides a summary of the analyses performed in this study:

1. The initial application of EFP was focused on planar frontal crashes in light vehicles, based on real-world prevalence of fatalities in frontal crashes (Figure 1-2). The available FE models were developed for light vehicles in planar, i.e., non-rollover, impacts.

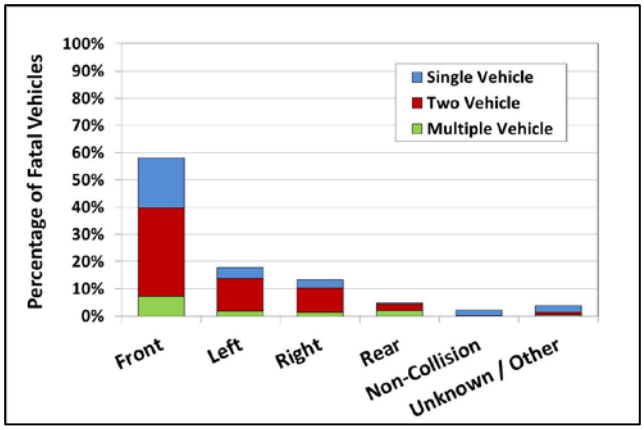

Figure 1-2. Fatal Vehicles (Passenger Cars and LTVs)

2. Frontal crash configurations (Full Engagement, Between Rail, Offset, Corner, and Other) were identified for simulation based on structural engagement from real-world distributions in NASS CDS (Figure 1-3 and Table 1-1).

3. Representative velocities based on NASS CDS were established to capture a large proportion of the occupant safety problem.

4. The fleet was classified by vehicle type and size to capture a majority of the crashes. Partner FE vehicle models were set up and verified to represent existing vehicle fleet segments.

   A selected subset of available NCAC FE models (Table 1-2) was chosen to be further refined and to undergo extensive crash validation for frontal crash configurations in order to represent segments of the existing fleet in this research. These models were selected as surrogate vehicles for crash partners to represent a midsize passenger car, small passenger car, midsize sport utility vehicle, and a full size pickup truck.

5. Vehicle structural modeling was performed to:

   - Simulate single- and two-vehicle crashes of target and fleet vehicles in representative crash configurations (Table 1-3 and Table 1-4).
   - Predict crash pulse, dynamic crush, and intrusions in self and partner vehicles.

   In this study, there were eight target vehicles as follows:

   - Taurus FE baseline model (BL) and two simple design variants, 25 percent lighter (LW3) and overall stiffer (LW4), selected by the NCAC for the EFP proof-of-concept

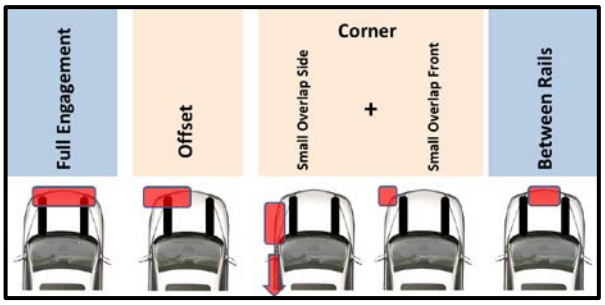

Figure 1-3. Frontal Crash Groups Based on Structural Engagement

Table 1-1. Frontal Crash Involvement and Serious Injury (MAIS3+F) Distributions

All Crashes					
Frontal Taxonomy	All Crashes	MAIS 3+F	% All	% MAIS 3+F	Risk (Rate of MAIS 3+F)
Between Rail	202010	4471	7.5%	11.0%	2.2%
FullEng	1243912	15336	46.0%	37.7%	1.2%
Offset	968395	16319	35.8%	40.1%	1.7%
Other(Front)	143552	147	5.3%	0.4%	0.1%
Sml Offset F&S	148376	4421	5.5%	10.9%	3.0%
Total	2706246	40694	100.0%	100.0%	1.5%

Table 1-2. FE Models for Representing Fleet Vehicles (NCAC)

Vehicle Model (NCAC)		FE Weight No. Parts/Elements	
Taurus (MY 2000 – 2007)			**1505 kg 802/ 973,351**
Yaris (MY 2005 – current)			**1100 kg 917/ 1,514,068**
Explorer (MY 2002 – 2005)			**2025 kg 923/ 714,205**
Silverado (MY 2007 – current)			**2270 kg 719/ 963,482**

Table 1-3. Single-Vehicle Crash Simulations

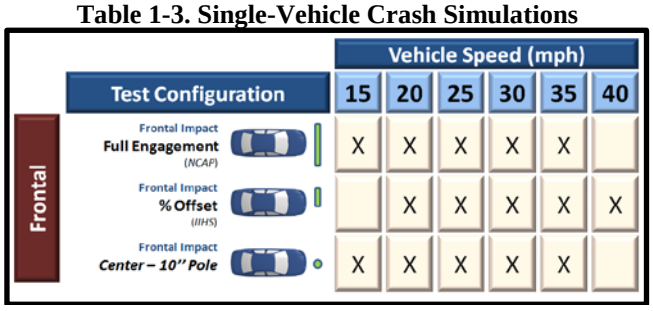

- Honda Accord FE baseline model (BL) and its lightweight design by Electricore Inc. (LW)
- Toyota Venza FE baseline model (BL) and its low (LWLO) and high option (LWHO) designs, by FEV GmbH and Lotus Engineering.

Table 1-4. Two-Vehicle Frontal Crash Simulations

Partner Vehicle	Target Vehicle	Vehicle Speed [Closing Speed]	Test Setup
Explorer		15 mph [30]	Full Engagement
Silverado		20 mph [40]	
Yaris		25 mph [50]	
Taurus		30 mph [60]	50 % Offset
		35 mph [70]	

In the future, an FE model of any new vehicle design being introduced into the fleet (e.g., with lightweight advanced materials, next generation gasoline vehicle, EV, PHEV, etc.) can be used as a target vehicle. An FE model of an existing vehicle could also be used as a target vehicle.

Performing all the LS-DYNA FE vehicle structure and MADYMO rigid body occupant simulations for the eight target vehicles involved a large number of simulation runs. A total of 440 LS-DYNA runs and 1,520 MADYMO runs were conducted, broken down as follows.

- Single-vehicle crash simulations:
  - 120 LS-DYNA runs
  - 240 MADYMO runs
- Two-vehicle crash simulations
  - 320 LS-DYNA runs
  - 1,280 MADYMO runs

6. Occupant models were developed and verified for the crash configuration of interest.

   As the available FE vehicle models lacked sufficient detail of the vehicle interior and restraint components to perform integrated FE vehicle and occupant simulations, the occupant modeling needed to be decoupled from the vehicle structural modeling and performed separately using MADYMO rigid body simulations (Figure 1-4). Generic occupant models were obtained from restraint manufacturers and then modified to reflect the interior geometry of the desired target or partner vehicle. The restraint characteristics and dummy positioning were adjusted in an iterative process until the simulation results proved to be a realistic match of the corresponding crash test data and exhibited reasonable trends in the robustness check simulations (Figure 1-5).

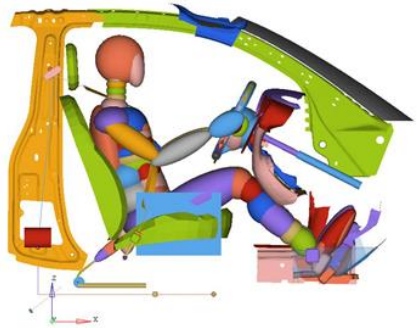

Figure 1-4. MADYMO Occupant Environment

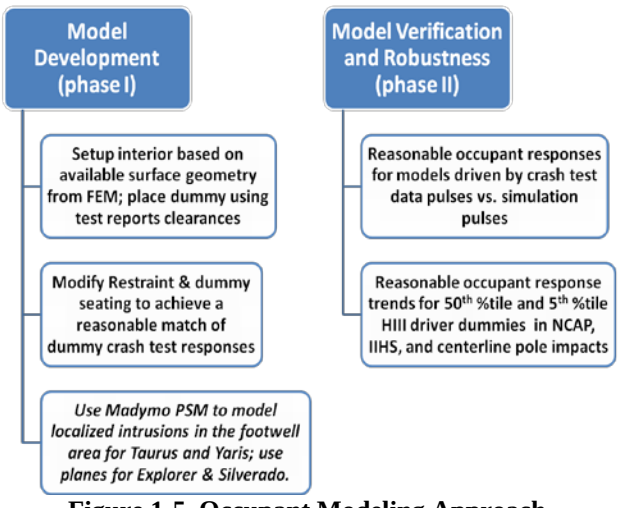

Figure 1-5. Occupant Modeling Approach

7. Occupant modeling was performed, followed by estimation of injuries.

   Vehicle responses, like the passenger compartment accelerations and intrusions, predicted by the FE simulations, were used as inputs to detailed 3-D models of the occupant in a vehicle interior environment (MADYMO) to generate occupant kinematics and responses. The occupant responses were translated into risks of injury to various parts of the body: head, neck, chest, and lower extremities.

8. The injury risks (AIS3+) to the occupants of the target and partner vehicles were summed across all crash scenarios, for both single- and two-vehicle crash configurations, with appropriate weighting factors, determined from NASS CDS, to estimate the societal injury risk associated with the target vehicle in an existing fleet (Figure 1-6 and, as an example for single-vehicle crashes, in Figure 1-7).

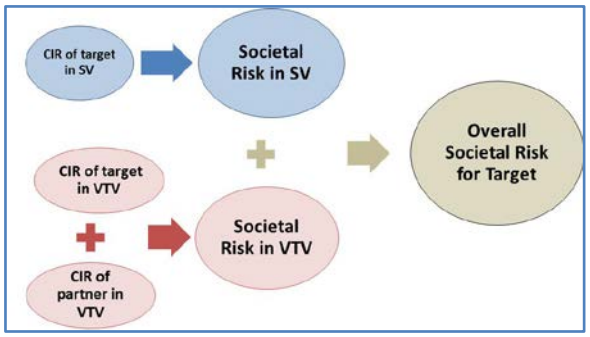

Figure 1-6. Overview of Societal Risk Computation

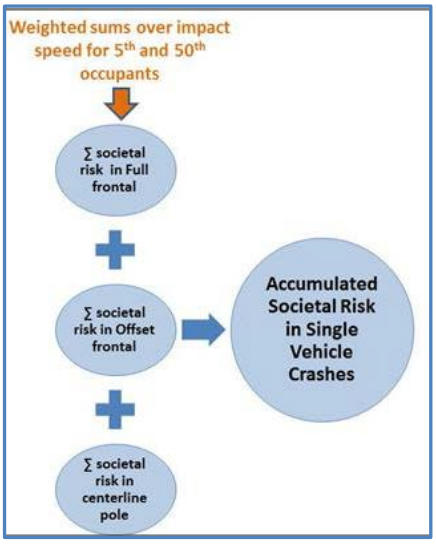

Figure 1-7. How an Individual Injury Risk is Weighted in Single-Vehicle Crashes

1.3 Main Results

The main observation from the initial application of EFP to frontal crashes is that there was an increase in societal injury risk for the light-weighted vehicle designs as compared to their baselines (Table 1-5). This trend was observed for the two simple design variants of the proof-of-concept midsize vehicle as well as the lightweight vehicle design concepts developed through projects sponsored by NHTSA, EPA, and CARB. With the proof-of-concept FE vehicle model design variants, EFP was able to isolate the effect of mass and stiffness changes in vehicle designs on societal injury risk and showed that both the decrease in mass and increase in stiffness resulted in increased societal injury risk. Isolation of effects of mass and stiffness changes could not have been achieved by physical experimentation.

Table 1-5. Fleet Injury Risk for Target Vehicles

Target Vehicle	Taurus Baseline	LW3	LW4	Accord Baseline	Accord LW	Venza Baseline	Venza Low Option	Venza High Option
Weight (lbs)	3339	2508	3339	3681	2964	3980	3313	2537
reduction		831			716		668	1444
% mass reduction		**25%**	**0%**		**19%**		**17%**	**36%**
Societal Risk I	1.25%	1.41%	1.48%	1.56%	1.73%	1.36%	1.43%	1.57%
Risk Increase		12%	18%		11%		5%	15%
Societal Risk II	1.01%	1.14%	1.22%	1.43%	1.57%	1.14%	1.20%	1.30%
Risk Increase		13%	21%		10%		5%	14%
Societal Risk IIP	1.01%	1.16%	1.23%	1.44%	1.59%			
Risk Increase		14%	21%		10%			
Societal Risk I - Target + Partner Combined AIS3+ risk of Head, Neck, Chest & Femur								
Societal Risk II - Target + Partner Combined AIS3+ risk of Head, Neck, and Chest								
Societal Risk IIP - Target + Partner Combined AIS3+ risk of Head, Neck, and Chest with A-Pillar Intrusion Penalty								

Although the same restraint systems were used for both the baseline and lightweight vehicles in this study, future trends in restraint systems are not be expected to be drastically different than those observed in this study. Vehicle restraint systems are normally designed for good performance in federal safety standard and consumer information tests; however lighter weighted vehicles will always encounter a more severe crash environment in vehicle-to-vehicle crashes comparing to heavier vehicles with same restraint system due to conservation of momentum. NHTSA plans to continue studies to support development of future restraint systems that can mitigate the increased risk for lightweighted vehicle designs in the future phases of this study. But at this time, some increase in occupant safety risk is expected.

The societal injury risks predicted by EFP are in good agreement with the real-world crash outcomes. The range of the predicted risks for the baseline vehicles is from 1.25 percent to 1.56 percent, with an average of 1.39 percent, for the NASS frontal crashes that were simulated. The serious injury (MAIS3+F) rate in air bag equipped vehicles of model year 1985 or later is 1.5 percent in 1998 to 2010 NASS CDS data years (Table 1-1). Considering the generic nature of the restraints used in this study, various assumptions and weighting factors, the predicted baseline societal injury risks are consistent with those observed in NASS.

Table 1-6. Societal Injury Risk for Single- and Two-Vehicle Crashes for Target Vehicles

Societal Risk I- Target
Combined AIS3+ risk of Head, Neck, Chest & Femur

	Target	Overall Risk in SV	Total Risk 50th male	Total Risk 5th female
Single Vehicle Crashes	Taurus BL	0.15%	0.10%	0.28%
	LW3	0.18%	0.14%	0.31%
	LW4	0.19%	0.17%	0.24%
	Accord BL	0.22%	0.20%	0.25%
	Accord LW	0.25%	0.24%	0.29%
	Venza BL	0.20%	0.12%	0.44%
	Venza Low Option	0.21%	0.14%	0.44%
	Venza High Option	0.22%	0.15%	0.42%

Societal Risk I - Target + Partner
Combined AIS3+ risk of Head, Neck, Chest & Femur

	Target	Overall Risk in VTV	Total Risk 50th male	Total Risk 5th female
Two Vehicle Crashes	Taurus BL	1.10%	0.82%	1.96%
	LW3	1.23%	0.91%	2.17%
	LW4	1.29%	1.05%	2.00%
	Accord BL	1.34%	1.13%	1.98%
	Accord LW	1.48%	1.30%	2.04%
	Venza BL	1.16%	0.81%	2.20%
	Venza Low Option	1.22%	0.84%	2.35%
	Venza High Option	1.35%	0.87%	2.77%

The results from the first phase application of the EFP process shows that the trend of increased societal injury risk for light-weighted vehicle designs, as compared to their baselines, occurs for both single-vehicle and two-vehicle crashes (Table 1-6). In general, the societal injury risk associated with the small size driver is substantially elevated when compared to that of the mid-size driver. However, both occupant sizes had reasonable injury risk in the simulated impact configurations that are representative of the regulatory and consumer information testing.

The main limitation for the frontal implementation of EFP is the availability of newer fleet vehicle FE models. The current FEMs representing the fleet span model years 2001 to 2012, thus the results are more representative of transitional fleet safety effects. As light-weighted vehicles become more available in the fleet and corresponding validated FE models of such vehicles are developed, EFP can used to assess the fleet performance and societal injury risk of a more modern fleet. In addition, the current vehicle interiors are mainly generic in nature. More detailed and improved characterization of the interior components and restraint systems will better model intrusions and occupant interactions with the vehicle interior.

1.4 Conclusions

A new and operative method for EFP for new vehicles using crash simulation was developed and demonstrated for frontal crash modes. EFP used finite element analysis and rigid body dynamics, in combination with real-world crash and test data, to evaluate self-protection, i.e., crashworthiness, and partner-protection, i.e., compatibility and fleet effects of vehicle designs.

The initial implementation of methodology to frontal crashes and proof-of-concept results demonstrated EFP's capability of using crash simulations to evaluate the crash safety for an existing or new vehicle design at different crash configuration and speeds representing the real-world. Changes in overall societal, target, or partner injury risk between baseline and modified vehicle designs could be established and evaluated to guide future safety research efforts. With further development, EFP can be extended to include other crash modes like side and rear impacts.

EFP advances the state of the art of systems modeling in crash safety simulation and address limitations identified for the previous system modeling efforts (as discussed Section 2.1.3). This method can serve as a powerful tool to assess and introduce particular designs in the fleet and make corresponding decisions on a societal level.

There are many assumptions made throughout the study as with any scientific researches and studies. The results from this study should be interpreted based on the assumptions made throughout the study and should not be taken out of context.

2 INTRODUCTION

The National Crash Analysis Center of the George Washington University has developed a methodology for **e**valuating **f**leet, i.e., self and partner, **p**rotection (EFP) of new vehicle designs through structural modeling and analytical simulations. The study is funded by the National Highway Traffic Safety Administration. The overall scope, research approaches, and data needs were defined and established in consultation with NHTSA. The study is in support of NHTSA's research for assessing the effects of future vehicle designs on safety and should support investigating potential countermeasures to address safety consequences of new designs. The overall goal is to develop a model to simulate the real-world crash environment, i.e., different types of vehicles, impact velocities, impact directions, impact types, etc. A proposed concept vehicle could be introduced in this virtual crash environment, and the safety of the occupants of such a vehicle and those of other vehicles involved in crashes with it could be evaluated using EFP.

As an initial application of EFP, the methodology was used to assess the effects of several lightweight vehicle designs on occupant safety in a variety of vehicle-to-fixed objects and vehicle-to-vehicle frontal crash simulations. NHTSA, the Environmental Protection Agency, and the California Air Resources Board (CARB) had recently completed vehicle design projects to develop detailed designs and cost estimates for future lightweight vehicles (FEV GmbH, 2012; Singh et al.; 2012; Lotus Engineering, 2012). While each of these projects were conducted by different research groups and had slightly different research goals and requirements, they all required the development of FE models to demonstrate compliance with major federal safety standards and consumer information safety requirements. Each of the sponsoring organizations agreed to support and to advise NHTSA on the use of their resulting finite element models for evaluating vehicle-to-vehicle and vehicle-to-object crash safety.

Potential near-term applications of the methodology have been identified as driven by insight gained from the initial application of EFP in frontal crash simulation. Potential refinements and expansions of the current implementation of the methodology have also been identified and outlined.

2.1 Motivation

2.1.1 Shift to Fuel Efficient Vehicle Designs

The overall study was motivated by the paradigm shift being experienced in the automotive industry towards a more fuel efficient vehicle fleet. Vehicle manufacturers are introducing innovative technologies, materials, and manufacturing processes, including new power trains and more mass reduction technologies, to meet CAFE standards, stringent greenhouse gas (GHG) standards, and increasing demand for more fuel efficient and cleaner vehicles.

With the recent CAFE requirements being based on vehicle "footprint," a measure of vehicle size determined by multiplying the vehicle's wheelbase by its average track width, an expected trend in vehicle design in the United States is to retain the vehicle size while reducing its mass by using advanced, lighter weight materials. Some such

vehicle designs have already been introduced in the fleet. These vehicles increasingly use aluminum, ultra-high-strength steels, and other advanced materials such as composites such as carbon-fiber-reinforced plastics.

The marketplace is also leading to the growth of the smaller car vehicle segments in the United States and the rest of the world. About 20 percent of all new cars sold in the United States in 2012 were small cars (Market Data Center, 2013). An analysis of vehicle sales indicated that the small car segment will steadily increase to a 23.2 percent projected market share in 2014 (Doggett, 2011).

2.1.2 Opportunities to Support CAFE and Future Safety Research with Engineering Models

Several research concept vehicle designs using advanced lightweight materials and manufacturing processes have been made public through various projects sponsored by NHTSA, EPA, and CARB. These designs are in the pre-prototype stages of development, i.e., detailed finite element engineering models of such concepts exist and have been offered as proofs of concept, but much more work would need to be done to validate these designs for production. Most of these concepts meet the existing crashworthiness standards as demonstrated through the use of computer-aided engineering (CAE) simulations of these concept designs in various regulatory and consumer information crash tests. However, the real-world interactions of these vehicles with the existing and future fleets have not been evaluated through simulations because, prior to this study, such a systematic approach had not been available. The real-world scenario involves crashes at various impact velocities, configurations, impact partners (e.g., rigid obstacles, lighter or heavier vehicles, pedestrians, and motorcycles), and vehicle occupants of various sizes and ages.

Throughout the CAFE research efforts, NHTSA sought to focus on the safety of future lightweight vehicles. The research projects undertaken by CARB, EPA, and NHTSA provided a unique opportunity to work with engineering models of future vehicle designs. While all of the models were designed to perform well in regulatory tests and some to also perform well in consumer information tests, the availability of these models provides an opportunity to explore whether this translates into good safety performance in real-world driving. In particular, it is important to evaluate the safety of these lightweight vehicles as the U.S. fleet transitions from existing vehicle designs to lightweight vehicles with improved fuel economy. The engineering models permit simulation of a range of vehicle-to-vehicle crash conditions and can evaluate the change in vehicle crash characteristics. A predictive analysis, in a methodology such as EFP, has the potential to provide insight into new occupant safety concerns and could be used to direct future research efforts throughout the model years 2017-2025 CAFE final rule implementation period (NHTSA, 2013). Such a methodology also has the potential to provide insight into crash safety implications resulting from future changes in fleet segment composition such as market driven shifts due to fuel prices or consumer preferences.

2.1.3 Summary and Limitations of Previous Studies

Assessing the safety performance of the vehicle fleet has been long recognized as an integral study area of vehicle safety research by the safety community. Several studies have used statistical modeling of the fleet and traditionally available crash data, and have attempted to predict the effects of changes in the fleet (stiffness, mass and size) on overall safety. A major shortcoming of such studies is that the inherent assumption that historical vehicle designs (for which real-world crash data is available) will continue into the future.

The seminal research addressing fleet safety was performed by Ford Motor Company (1978) for NHTSA in the mid-1970s and resulted in the Safety Systems Optimization Methodology (SSOM), which was further refined by the University of Virginia (White, 1986). SSOM first introduced the approach for assessing fleet safety using approximating functions and applied the methodology to identify structural characteristics that would maximize the safety performance of a mid-1970s 3,000 lb. car from the mid-1970s in the existing fleet. In the late 1990s, Volpe National Transportation Systems Center developed a fleet system modeling approach in support of vehicle aggressivity studies at NHTSA (Kuchar, Greif, & Neat, 2000; Kuchar, 2000). Volpe partitioned the fleet into two vehicle types, extracted one-dimensional lumped mass vehicle models from full frontal crash test data, and used these models to drive three-dimensional rigid body articulated models for occupant simulations to predict overall head and chest injuries. In the mid-2000s, TNO Automotive of the Netherlands performed research to study the potential of multi-body vehicle models to develop strategies for crashworthiness optimization for NHTSA, the European Commission, and the Dutch Ministry of Traffic (Kellendonk, 2005; Van Der Zweep, 2005). TNO implemented three-dimensional articulated rigid body structural models of several vehicle types that had been constructed from existing finite element models and included an integrated occupant. Laituri et al. constructed a three-dimensional rigid body occupant model of an "average" car based on extensive crash test data and driven by vehicle crash pulses from a one-dimensional lumped mass model (Laituri et al., 2003). Laituri developed an accumulated injury risk metric for drivers in full engagement frontal crashes over a range of impacts speeds and occupants sizes based on real-world frequency of occurrence.

Limitations of Previous Studies – While SSOM introduced the fleet safety concept for a single vehicle and used a combination of crash modes, SSOM pre-dated the National Automotive Sampling System (NASS) accident files, biomechanical injury risk functions, abbreviated injury scale (AIS), nonlinear finite element codes, and the more developed articulated multi-body occupant models. While the University of Virginia first included AIS in their revisions to the SSOM model in the early 1980s and Volpe added the concept of multiple vehicle types and implemented biomechanical injury risk functions at multiple severity (i.e., AIS) levels for the fleet injury risk computation, Volpe applied full frontal structural one-dimensional models with the assumption that these models are sufficient to simulate frontal offset and narrow object crashes, and their analysis of the crash environment did not account for vehicle class or structural engagement. Volpe performed simulation of impact speeds up to 88 km/h, which is far beyond the range of 56 km/h for which the one-dimensional models were developed and validated. Volpe also oversampled the simulations at higher impact speeds based on the premise of higher occurrence of serious injuries (AIS 3+), while in reality over 90 percent of AIS3+ occur in changes in velocity (delta-Vs) under 56 km/h. TNO simulated a range of vehicle overlap (25 to 80%) with potentially unrealistic predictions as the approximated rigid body vehicle models did not have the needed details to capture the dynamic structural responses at low overlap ranges. Also, the base FE models from which the TNO models were extracted were not verified in frontal offset mode for any range of overlap. Similarly to Volpe, the TNO models were simulated at 20-80 km/h impact speeds where the high end is an extrapolation beyond the performance range of the original FE models as those were not tested beyond 35 mph. Also, TNO's simulation matrix was not based on observed real-world crash frequencies but designed per a statistical approach based on permutation of crash scenarios for the seven vehicles modeled. That resulted in a small number of cases from the NASS database for comparison; thus a detailed analysis of separate scenarios was not possible and all passenger cars were taken as one group and SUVs and MPVs were not considered.

3 METHODOLOGY

EFP implements a CAE process using vehicle structural and occupant modeling, in combination with real-world crash and test data analyses, to assess the crashworthiness for self-protection, partner-protection, and the fleet safety effects (i.e., self plus partner protection) of new vehicle designs.

3.1 Methodology Overview

An overview of the EFP approach is shown in Figure 3-1. The goal is to develop a CAE process to consistently evaluate real-world fleet safety using quantifiable measures through vehicle structural and occupant modeling for current and new vehicle designs.

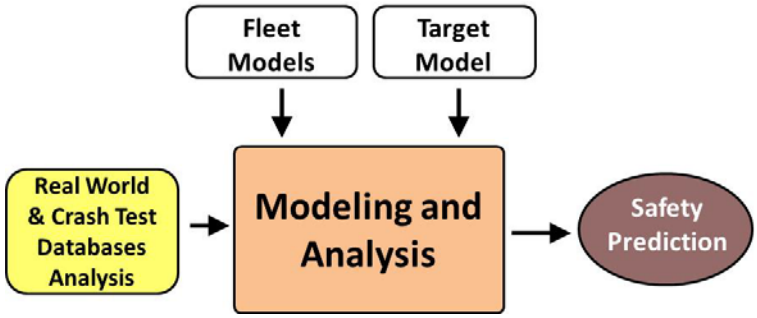

Figure 3-1. EFP Overview

3.1.1 Fleet Societal Injury Risk

The fleet societal injury risk in EFP is defined as the total safety of occupants in the target vehicle and crash partner vehicles. The governing equation to compute the societal injury risk is formulated as follows:

$$SIR(v) = \sum_{i=1}^{Nmode} \sum_{j=1}^{Jevent} \sum_{k=1}^{Koccloc} \sum_{l=1}^{Loccsize} \sum_{m=1}^{Mconfig} \sum_{n=0}^{Npartner} \sum_{o=1}^{T/P} \sum_{p=1}^{Pspeed} w_{ijklmnop}\ (v) * CIR_{ijklmnop}\ (v)$$

The Societal Injury Risk (SIR) for a target vehicle $\boldsymbol{v}$ is defined as an aggregate of individual crash serious injury risks weighted by real-world frequency of occurrence $\boldsymbol{w_{ijklmnop}(v)}$ of a crash incident discretized over the following.

- P impact speeds
- Target/partner vehicle
- N crash partners
- M crash configurations
- L occupant sizes
- K occupant seating locations (*weighting factor accounts for occupancy rates*)
- J crash events (single-vehicle, two/multiple-vehicle)
- I crash modes

$CIR_{ijklmnop}(v)$ represents a combined serious injury risk (CIR) for the head, neck, chest, and lower extremities body regions in a single crash incident. A crash incident corresponds to a crash event at a given impact speed for a given occupant size in a given seating position, in the target or partner vehicle, in a given crash configuration, in a single- or two-vehicle crash, and in a given crash mode. $w_{ijklmnop}(v)$ designates the weighting factor, percent of occurrence, derived from the National Automotive Sampling System Crashworthiness Data System (NASS CDS) for the crash incident.

The formulation of the governing equation for proposed societal injury risk is based on the following hypotheses:

- Societal injury risk should be segregated by the predominant crash modes, i.e., frontal, side, rollover, and rear crashes, to address different structural engagement, varying vehicle and occupant kinematics, and varying occupant injury mechanisms and risks in different crash environments.

- Societal injury risk computation should be segregated by single and two (or more) vehicle crash events. This will allow assessment of safety in the events for which the countermeasures were designed and how well they translate to the more predominant multiple-vehicle crash events. To-date, the safety community has been conducting single-vehicle regulatory and consumer information crash tests to develop safety countermeasures and occupant restraint systems for each crash mode.

- Societal injury risk computation should be segregated by occupant size to allow safety assessment for a wide population of occupants in the real-world. To-date, safety countermeasures and restraints systems have been primarily for the average size male occupant.

The above is an overview of the EFP methodology. In this study, EFP was implemented for the frontal crash mode, where only frontal crashes are analyzed. The fleet models consisted of FE vehicle structural models (LS-DYNA) that were coupled with rigid body occupant modeling (MADYMO).

3.1.2 Outline of EFP Processes

The following sections outline the EFP processes shown in Figure 3-1.

3.1.2.1 Real-World and Crash Test Databases Analysis Process

1. Establish crash configurations and exposure for a target vehicle based on real-world distribution in the NASS CDS.

2. Select and set up the fleet partner vehicles to represent existing vehicle fleet segments.

3. UsUse data from crash tests representative of the crash configurations of interest to validate and verify the vehicle and occupant models.

3.1.2.2 Modeling and Analysis Process

1. Perform vehicle structural modeling:
    - Simulate single- and two-vehicle crashes of representative crash configurations up to speeds of current regulations and consumer information testing.

- Predict crash pulse, dynamic crush, and intrusions in target and fleet partner vehicles.

2. Estimate occupant injury risk for each crash configuration:
   - Use occupant modeling to predict probabilities of serious-to-fatal injuries in target and partner vehicles for restrained occupants over the crash configurations and impact speeds under investigation.

3.1.2.3 Safety Prediction Process

With a baseline or modified/new vehicle design as the target, the total safety of occupants in the target vehicle and partner vehicles, called fleet societal injury risk in this study, is estimated in single- and two-vehicle crash configurations. The individual crash injury risks are combined to compute the total injury risk for a given target vehicle as follows:

1. Use frequencies of real-world crash occurrence to establish the weight of injury risk for each crash event:
   - A crash event is a given configuration at a given impact speed for a given occupant size in a given seating position.
   - The weighting factors are derived from NASS CDS.

2. Sum the risk of serious injuries (AIS 3+) in both the target and partner vehicles for each crash event to calculate the societal injury risk of the crash event.

3. Calculate total fleet safety, i.e., fleet societal injury risk, by computing an accumulated injury risk, i.e., the weighted sum of the injury risks for all vehicles across all simulated crash events.

Changes in overall societal, target, or partner injury risk between baseline and modified vehicle designs could be established and evaluated to guide future safety research efforts.

3.1.3 Integral Components of EFP

Real-world "sanity" checks and availability of validated vehicle structural and occupant models are integral components of the EFP methodology.

3.1.3.1 Real-World "Sanity" Checks

An integral feature of EFP is the real-world sanity checks, i.e., continuous checks with real-world data (NASS CDS and crash test databases), which are necessary to verify and guide the procedure. As such, the crash configurations to be simulated must be based on real-world crash distributions and exposure based on NASS CDS analyses. Also, crash test data that are representative of the crash configurations of interest should be available to validate and verify the vehicle and occupant models which are the cornerstone of the methodology. The main strength and predictive potential of EFP is that the approach is based on physical and realistic models, configurations and exposure, injury risks, etc.

3.1.3.2 Finite Element Models

A critical component for this process is that FE models of the target vehicles, both the baseline and the modified/new vehicle designs, as well as the partner vehicles representing the fleet are available, and validated in the representative crash configurations under investigation. The results of EFP depends on the credibility of these

FE models, such as how well these models represent real-world crashes, how realistically the material and technologies are modeled in these FEMs, etc.

3.1.3.3 Occupant Response Models

Another critical component for this process is that occupant models with current restraint systems for the partner vehicles and for both the target baseline and modified/new vehicle designs are available and validated in the representative crash configurations under investigation. Similarly to the vehicle models, the results of EFP also depend on the credibility of the occupant and restraint models, whether developed as finite element or rigid body dynamics models, such as how realistically the restraint systems are modeled and the fidelity of the dummy interactions with the vehicle environment, including the restraints, in the pertinent crash configurations.

3.2 What to Study? Crash Configuration Selection

To study real-world safety effects of future light-weighted vehicle designs, the simulated crash configurations need to represent real-world crashes. Under this section, the approach used to identify, define, and select the target crash configurations to be simulated in this study is presented. When the project began, there was a need to establish which crash configurations would be the focus of the study. During that process, data from two national crash databases, the Fatality Analysis Reporting System (FARS) and NASS, were analyzed as presented in this section. After analyzing these two databases, the researchers decided to study frontal crash configurations in this initial implementation of EFP.

3.2.1 Overview of Crash Involvement and Fatalities

To provide the background for the crash configurations modeled in this study, data from FARS and the NASS General Estimate System (GES) were initially analyzed for an overview of crash involvement and traffic fatalities in recent model year vehicles on U.S. roads. FARS is a census of all crash fatalities on U.S. roads. FARS data are obtained from police accident reports (PARs) and contain basic information about the crash, vehicle, and persons involved. NASS GES data are a nationally representative probability sample selected from all police-reported crashes (around 55,000 cases per year with major property damage, injury, or death from the several million police-reported crashes). GES data incorporate pre-event, occupant, vehicle, environment, and limited injury information. The vast majority of cases in GES involve property-damage-only (PDO). The police report does not investigate the extent of injuries or their causes. A principal benefit of GES is to determine the frequency of crashes of various categories, regardless of their severity.

This project started in late 2010. When the project started, the distribution of fatalities in 2009 on U.S. roads was examined and the result is shown in Figure 3-2. This study is focused on analysis of planar crashes, i.e., non-rollover, for drivers restrained with 3-point belts in recent model year (MY) light vehicles, excluding motorcycles. To better represent the future on-road fleet, the analysis focused on belted occupants in MY 1998+ vehicles designed to meet requirements of the current Federal Motor Vehicle Safety Standard (FMVSS) for frontal and side impact crash protection (albeit not the most recent FMVSS No. 214, Side Impact, which incorporates the oblique pole test and will be fully effective in the 2016 model year).

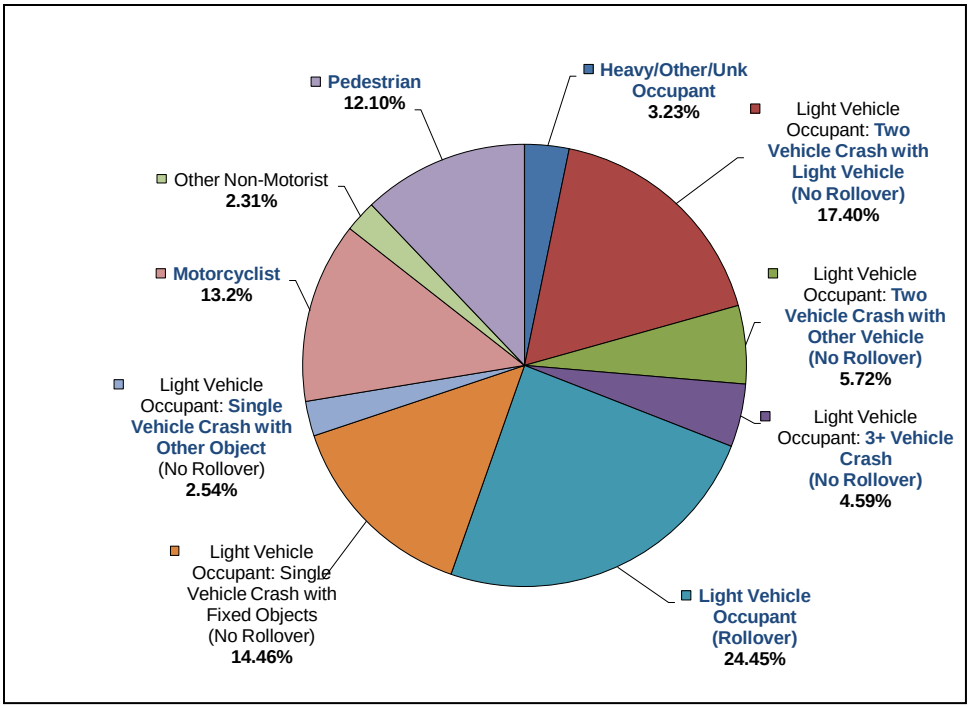

Figure 3-2. 2009 FARS- U.S. Traffic Fatalities (Total: 33,808)

Although EFP can be applied to any crash mode with any vehicle type, a critical component for the methodology, as discussed in Section 3.1.3.2, is that FE models of the involved vehicles are available and validated in the representative crash configurations under investigation. The FE models available for this study were developed for light vehicles in planar impacts, i.e., non-rollover, and consequently, the initial application of EFP was focused on planar crashes in light vehicles, excluding motorcycles. Crashes with pedestrians were beyond the scope of this study. Crashes involving 3+ vehicles are not well defined and too varied for simulation. The crashes considered for this study represent 32 percent of all 2009 traffic fatalities, shown in Figure 3-2, including 14.5 percent for single-vehicle crashes with fixed objects (no rollover) and 17.4 percent for two-vehicle crashes with light vehicles (no rollover). This amounts close to 50 percent of all planar crashes involving light vehicles.

In general the data selection criteria for the population of interest for the overview analysis were as follows.

- GES and FARS crash data in calendar years 1998-2008
  - GES – Vehicle Involvement and Injury
  - FARS – Vehicle Fatalities
- Light vehicles involved in planar, non-rollover crashes
- Vehicle model years 1998 or later
- Crashes with at least one restrained (with 3-point belt) occupant within the vehicle
- Single- or two-vehicle crashes
- Vehicle injury outcome based on restrained occupants

Figure 3-3 shows the distributions of all crash-involved vehicles by initial point of impact for single- and two-vehicle crashes. The distributions of all crash-involved vehicles with fatalities are presented in Figure 3-4. As stated earlier, crashes with more than two vehicles involved were excluded from the study. Such multiple vehicle

crashes account for 7.2 percent of frontal and 1.8 percent of side fatal crashes as shown in Figure 3-4. Crash-involved vehicles include vehicles with injury and PDO from GES and vehicles with fatalities from FARS.

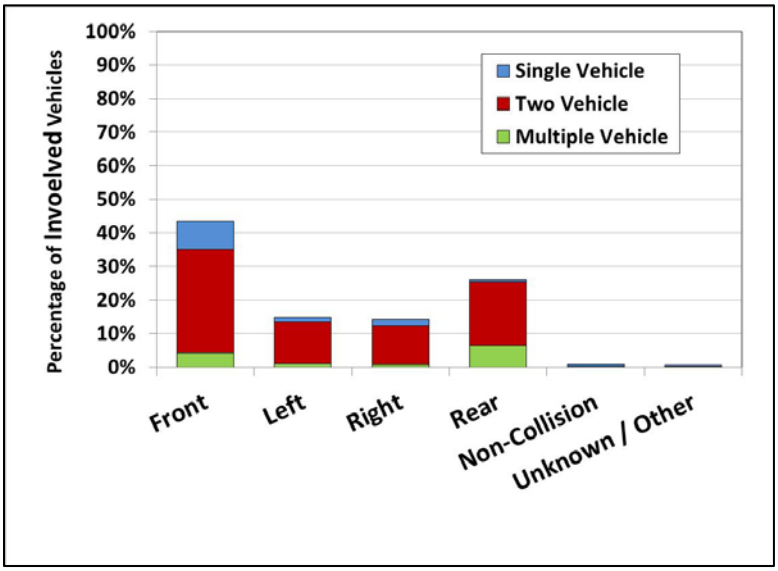

Figure 3-3. Crash-Involved Vehicles (Passenger Cars and LTVs) by Initial Point-of-Impact (MY1998+, planar non-rollover crashes with restrained occupants)

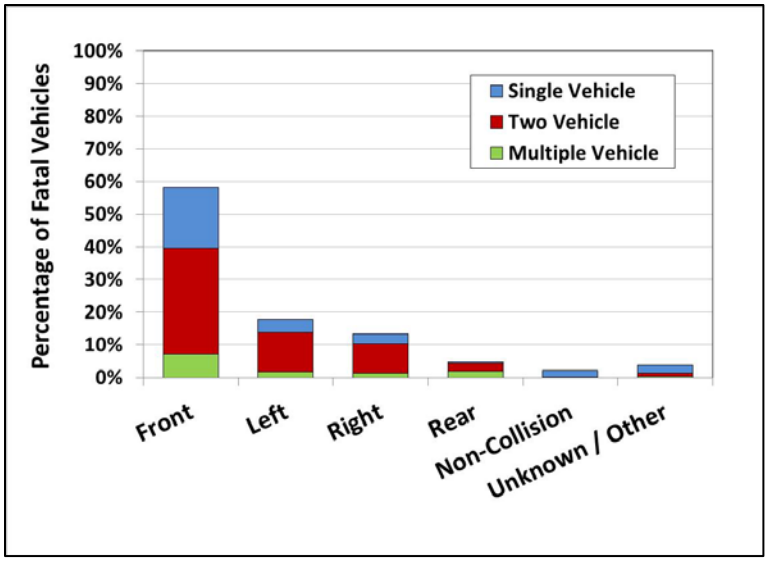

Figure 3-4. Fatal Vehicles (Passenger Cars and LTVs) by Initial Point-of-Impact (MY1998+, planar non-rollover crashes with restrained occupants)

For passenger cars (PCs) and light trucks and vans (LTVs), frontal crashes account for 58.1 percent of fatal vehicle crashes followed by side crashes (including both left and right side) at 31.1 percent as shown in Figure 3-4. Even though rear impacts are 26.1 percent of all crashes for PCs and LTVs as shown in Figure 3-3, they make up only 4.9 percent of fatal crashes as shown in Figure 3-4. Frontal crashes account for the highest numbers of fatalities and are thus an important subset of the crash population. Frontal crashes are also most readily

addressed with the available simulation models and injury metrics. Once EFP feasibility has been established by application to frontal crashes, the methodology can be extended to apply to multiple crash configurations, i.e., side and rear impacts. The actual number of fatal vehicles addressed by this study for frontal crashes is presented in Figure 3-5.

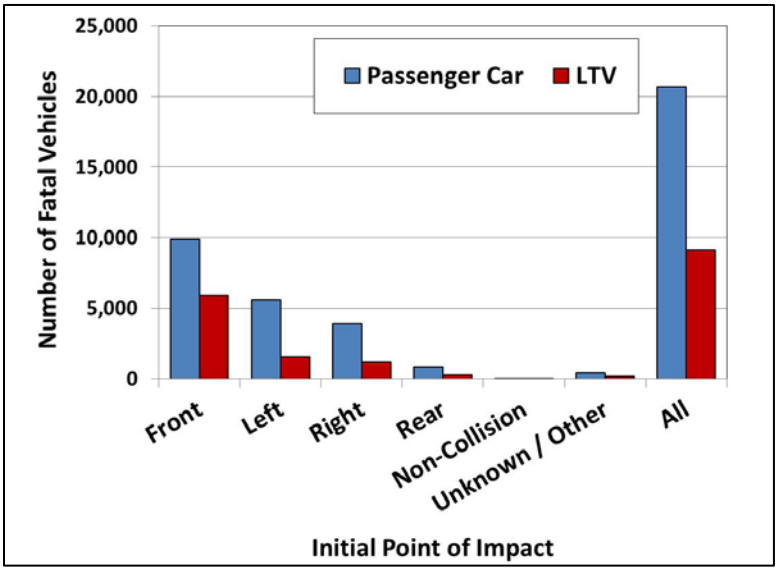

Figure 3-5. Fatal Vehicles by Body Type and Initial Point of Impact- 1998-2008 FARS (MY1998+, planar non-rollover crashes with restrained occupants)

3.2.2 Background NASS CDS Analysis

The following background analysis from the NASS CDS was conducted to establish and assess data selection criteria and sample size for the population groups in the main study. NASS CDS data were used to identify crash speeds to be simulated and injured occupant body regions to be evaluated for the crash scenarios represented by the vehicles modeled. NASS CDS was also used to estimate cumulative injury and fatality risks in real-world crashes represented by the simulation matrix.

NASS CDS is a nationally representative sample of tow-away crashes of light vehicles on U.S. roads with around 4,500-5,000 cases per year. In addition to police-reported information, CDS includes detailed information such as scene diagrams and photographs, vehicle damage, occupant injury, and injuring contacts that allow for the study of injury mechanisms. NASS CDS also includes estimates of delta-V and crash severity metrics as computed by crash investigators using crash reconstruction codes. The Abbreviated Injury Scale (AIS), ranging between 1 (minor injury) to 6 (maximum severity injury), is used to code the severity of each individual injury to head, face, neck, thorax, abdomen, spine, lower extremities, and upper extremities, based on the threat to life posed by the particular injury. In NASS CDS data, national estimates are calculated by applying a weighting factor for each case, the product of inverse probabilities of selection in a three stage sampling process.

To establish real-world baseline conditions for this study, a snapshot of real-world crashes for recent model year vehicles was analyzed. The preference was to include vehicles with the most recent model years (designed to current standards and consumer information test requirements), but that was balanced with the need to have a

sufficient sample size for the population of crashes to be binned for the different crash configurations and speeds for the vehicle segments being simulated.

The real-world crash environment, i.e., NASS CDS data, is used in this study to develop the weighting factors, i.e., percent of occurrence, for the different configurations to be simulated. The methodology for selecting the weighting factors is developed in this study. In future studies, the real-world crash environment could be used to verify the accumulated risk of serious-to-fatal injuries predicted by the methodology for the simulated matrix.

For the purposes of this study, the overall occupant injury risk is based upon the risk of sustaining a serious (MAIS 3+) injury or a fatality, referred to as the MAIS 3+F risk. The highest recorded injury to a given body region, irrespective of the total number of injuries sustained to that body region, is referred to as the Body Region AIS (BAIS). Also, the results presented are based on the NASS national estimates, i.e., weighted sample data (unless otherwise stated).

The initial population background analysis was done in 2010. During this background analysis, the following case selection criteria were applied to establish and assess data selection criteria and sample size for the population groups. As the project progressed, further population analysis was performed in 2011 as discussed in section 3.2.3.1. In the 2011 analysis, the criteria were further refined to establish the main study population. Also in the 2011 analysis, the 2010 calendar year data was available and was included in the main study. The following is a list of population analysis done in the initial analysis in 2009.

CRASH

- NASS CDS 1998-2009 data

VEHICLE

- Light vehicles model year 1998+, curb weight ≤ 10,000 lbs.
- General area of damage to the front of the vehicle
- Vehicles were classified into four categories (based on body type and curb weight):
    - Passenger Car (< 3,000 lbs.)
    - Passenger Car (≥ 3,000 lbs.)
    - SUV (≤ 10,000 lbs.)
    - Pickup Truck (≤ 10,000 lbs.)
- Vehicles that resulted in a rollover or fire were excluded from the analysis

OCCUPANT

- Front row drivers 16 to 50 years old
- Front seated occupants restrained by a 3-point belt system
- Occupants who were fully ejected from the vehicle were excluded
- Documented occupant injury

The passenger cars were divided into two groups depending on the vehicle's curb weight, <3,000 lbs. and ≥3,000 lbs. A driver age group of 16 to 50 years old was chosen to provide a population with a similar, i.e., more consistent, injury tolerance. It has been shown that adult occupant injury tolerance decreases with age and the elderly group has a higher risk of injury than the younger age group at any given crash delta-V. (Zhou, Rouhana,

& Melvin, 1996; Augenstein et al., 2005) (Digges, Dalmotas, & Prasad, 2013) This requires different risk functions for the elderly group, which is not included in this phase of the project.

Based on these selection criteria there were 5,872 cases (2,427,224 weighted) available for analysis. Table 3-1 provides an overview of the number of cases that were available in NASS CDS by vehicle classification and occupant injury severity.

Table 3-1. NASS CDS 1998-2009: Number of non-weighted cases available for analysis by vehicle classification and driver injury severity (weighted data in parentheses)

	MAIS 0-2	MAIS 3+F	ALL
Passenger Car <3000lb	1,817 (839,587)	150 (10,926)	1,967 (850,513)
Passenger Car >3000lb	1,746 (763,351)	141 (14,876)	1,887 (778,227)
Pickup	747 (272,025)	56 (6,556)	803 (278,580)
SUV	1,142 (514,273)	73 (5,631)	1,215 (519,904)
	5,452 (2,389,236)	**420 (37,988)**	**5,872 (2,427,224)**

To provide insight into which body regions to focus on in developing the EFP occupant injury risk functions, serious injury by body region was examined for the four vehicle classes in the study population. The graph in Figure 3-6 presents the BAIS 3+ injury risk of sustaining injuries to the head, neck, thorax, and lower extremities by vehicle class.

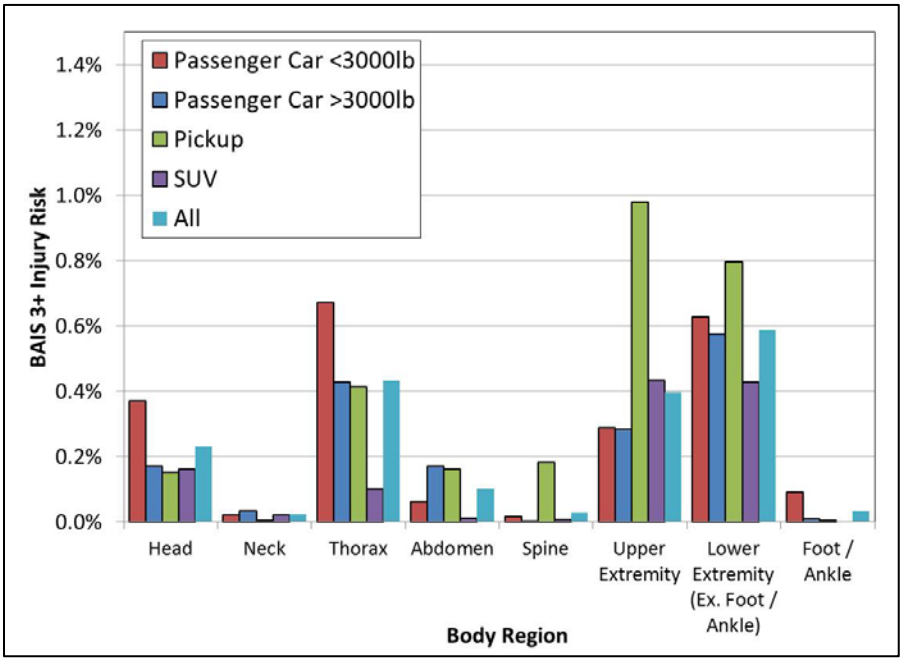

Figure 3-6. NASS CDS 1998-2009: BAIS 3+ Injury Risk by Vehicle Class (weighted data)

Note: The raw sample sizes are small for some of the body regions for the pickup

As a measure of crash severity for frontal crashes, both the delta-V and the barrier equivalent speed (BES) were initially considered. BES is the speed with which the crashed vehicle would have to strike a rigid barrier to absorb the same amount of crush energy as it did in the actual impact. The data in Table 3-2 provides the weighted

distribution of the presence of the delta-V and BES for frontal crash involved drivers in NASS CDS. The BES was coded in over two-thirds (68%) of NASS CDS cases compared to 59 percent in which the delta-V was coded.

Table 3-2. Distribution of Coded Delta-V and Barrier Equivalent Speed for Frontal Crash Involved Vehicle Drivers (weighted)

		Barrier Equivalent Speed		
		Missing	Coded	**Total**
Delta V	Missing	32%	9%	**41%**
	Coded	0%	59%	**59%**
	Total	**32%**	**68%**	**100%**

This study considers various degrees of frontal engagement (i.e., full engagement, offset, small offset). As such, the delta-V for crashes under consideration would be not directly comparable. The associated crash pulse for an offset crash with a delta-V of 25 km/h, for example, would be less severe than the crash pulse associated with a full engagement crash with the same delta-V. In contrast, given that BES is based only on the crush energy of the crashed vehicle and normalized to the corresponding energy absorbed by the vehicle in a rigid barrier strike, BES provides a more comparable severity measure across different frontal crash configurations in the speeds of interest. In addition, the BES was coded in more CDS cases and thus provided about 15 percent larger population than if delta-V were used for this study.

Logistic regression analysis was used to generate injury risk curves based on the probability of sustaining either an MAIS+F or BAIS injury. These injury risk curves were calculated based upon the entire range of NASS CDS BES values reported for each of the frontal crash involved vehicles. For the purposes of presentation, the injury risk curves were truncated to show the risk of injury between the BES range 10 km/h to 90 km/h.

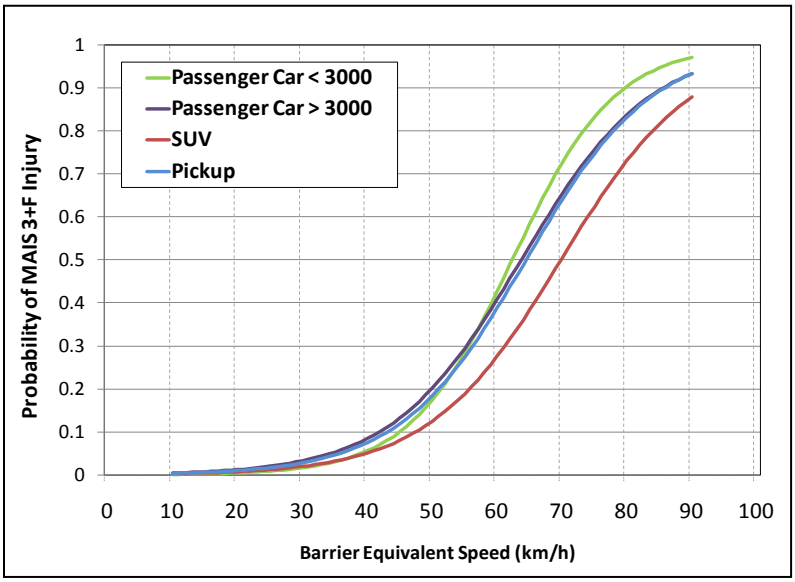

Figure 3-7. NASS CDS 1998-2009 – MAIS 3+F Injury Risk by Vehicle Class and Barrier Equivalent Speed (weighted)

Figure 3-7 shows the MAIS 3+F injury risk curve for each of the vehicle class groups by BES. At higher BES (60 km/h or greater) there is a greater probability of sustaining an MAIS 3+F injury for drivers in passenger cars with curb weight less than 3,000 lbs. compared to the other vehicle types considered. The risk of MAIS 3+F injury for passenger cars with curb weight greater or equal to 3,000 lbs. was slightly higher than those associated with pickup trucks across the entire BES speed range 10 to 90 km/h. The lowest risk of serious or fatal injury in frontal crashes greater than 40 km/h was to drivers of SUVs (which include the crossover utility vehicles [CUVs] for this study).

Table 3-3 provides an overview of the maximum, minimum, median, mean, and standard deviation of the vehicle curb weight for each of the vehicle classifications in the NASS CDS study population.

Table 3-3: Summary Vehicle Weight Statistics (lbs.) for Belted Drivers by Vehicle Class (weighted)

		Injury Severity		Injury Severity		ALL
		MAIS 0-1	MAIS 2+F	MAIS 0-2	MAIS 3+F	
Passenger Car <3000lb	Mean	2,635	2,603	2,633	2,679	2,633
	StdDev	219	202	219	187	218
	Max	2,998	2,998	2,998	2,998	2,998
	Min	1,786	1,984	1,786	1,984	1,786
	Median	2,624	2,601	2,624	2,734	2,624
Passenger Car >3000lb	Mean	3,301	3,305	3,300	3,340	3,301
	StdDev	252	264	251	335	253
	Max	6,305	4,696	6,305	4,674	6,305
	Min	3,020	3,020	3,020	3,020	3,020
	Median	3,263	3,241	3,263	3,197	3,263
Pickup	Mean	4,176	4,195	4,174	4,319	4,177
	StdDev	957	762	951	754	947
	Max	9,193	7,011	9,193	6,415	9,193
	Min	2,579	2,668	2,579	3,042	2,579
	Median	4,189	4,321	4,211	4,497	4,211
SUV	Mean	3,943	3,918	3,943	3,877	3,942
	StdDev	937	632	926	704	924
	Max	7,187	6,283	7,187	5,842	7,187
	Min	2,315	2,381	2,315	2,381	2,315
	Median	4,012	3,990	4,012	3,660	4,012

3.2.3 Frontal Crash Configuration Mapping

The objective of the crash configuration mapping was to determine and prioritize the frontal crash configurations to be simulated for the target and partner vehicles in the fleet simulation matrix. Also the weighting factors, i.e., percent of occurrence, for each frontal crash scenarios was derived and used in weighting the injuries for each frontal configuration to calculate the total injury for each vehicle.

The distribution of both single- and two-vehicle crashes was determined from NASS CDS based on a classification of post-crash damage profile to the front end. A frontal crash taxonomy based on post-crash damage and its location relative to the longitudinal frame rails was first introduced by Sullivan et al. in 2008 (Sullivan, Henry, & Laituri, 2008). The Sullivan classification was later refined by Scullion et al. in 2010 to address frontal crashes with damage in between the frame rails and included "Full Engagement," "Offset," "Moderate Offset," "Small Offset," "Between Rail," and "Underride" frontal crash groupings (Scullion et al., 2010). In the current study, the taxonomy was further expanded to include frontal small offset impacts with side damage, as coded by NASS CDS, in the definition of overall frontal impact crashes. The new expanded taxonomy was implemented to

ensure that all front crashes were captured and to overcome the CDS coding challenges relative to frontal crashes with narrow overlap that has been highlighted by recent research (Pintar, Yoganandan, & Maiman, 2008; Sherwood, Nolan, & Zuby, 2009). A different grouping of frontal impacts was also incorporated in the current study to include corner impacts as shown in Figure 3-8. "Corner impacts" are defined as the combination of "Small Overlap Side" and "Small Overlap Front." The new expanded taxonomy allows the assessment of the contribution of corner impacts and the other defined groups ("Full Engagement," "Offset," "Between Rail," and "Other") to the overall frontal crash populations.

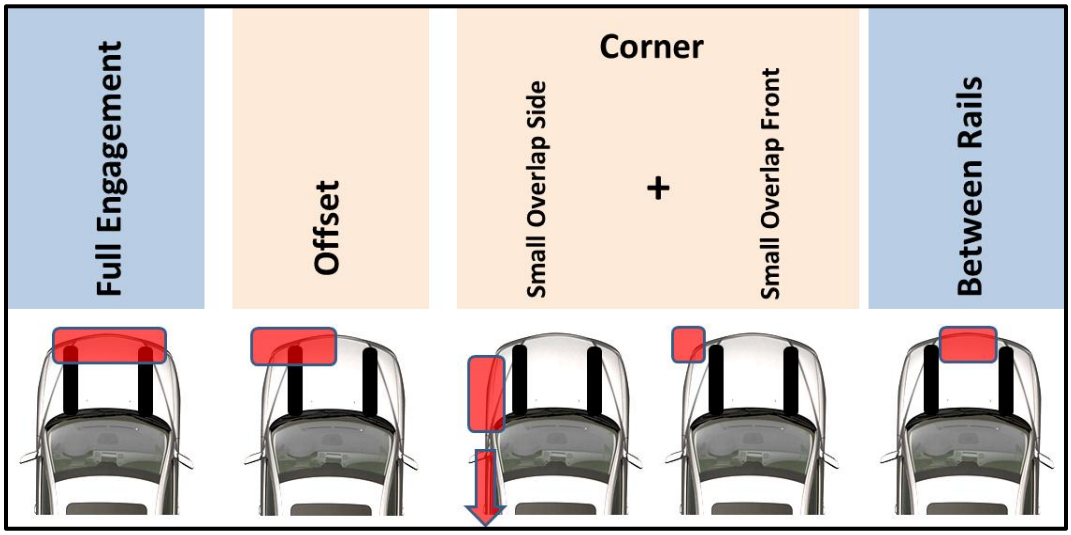

Figure 3-8. Expanded Taxonomy Frontal Crash Groups

3.2.3.1 NASS CDS Study Population

The data selection criteria for the main study population are outlined below. These are similar to the criteria used for the background analysis in section 3.2.2 above, but are refined to address impact speeds up to current regulations and consumer information testing, increase sample size, and allow the implementation of the expanded frontal taxonomy. Differences are highlighted in *italics*. In particular, to increase sample size, crashes involving MY 1985 and later vehicle with frontal damage that are equipped with frontal air bags were considered.

CRASH

- NASS CDS Data: Calendar years 1998-2010 data
- Direction of Force (DOF) 11, 12, or 1 o'clock

VEHICLE

- *MY 1985 and later vehicles that are equipped with frontal air bags*
  - Vehicles are divided into four categories (curb weight ≤ 10,000 lbs.)
  - Passenger Car above and below 3,000 lbs.
  - Sports Utility Vehicles
  - Pickup Trucks
- General Area of Damage: Front of vehicle (*and to side of vehicle forward of A-pillar close to front end to capture small frontal offset angular collisions*)

- *Cases with BES available, BES ≤40 mph (i.e., up to speeds of current regulations and consumer information testing)*
- Single- or two-vehicle crashes only (multiple excluded)
- Vehicles involved in a rollover excluded
- Vehicles with secondary impact with extent of damage greater than 2 excluded

OCCUPANT

- Belted front-seat occupants, nearside, 16 to 50 years old
- Vehicles with occupants fully ejected from the vehicles excluded

3.2.3.2 Crash Involvement and Injury Distributions and Injury Rates

Descriptive statistics for the crash distributions for the identified frontal crash groups are highlighted in Table 3-4. The predominant groups are the configurations of full engagement, offset, and between the rail front end damage accounting for 46 percent, 35.8 percent, and 7.5 percent of the frontal crash population under study. Full engagement frontal crashes result in 37.7 percent of all serious injuries to belted front seat occupants; offset frontal crashes result in 40.1 percent; and between the rail crashes result in 11 percent. In the current implementation, EFP will address 89.3 percent of all frontal crashes and 88.8 percent of all serious injuries under study including full frontal engagement, offset, and between rails configurations.

Table 3-4. Frontal Crash Involvement and Serious Injury (MAIS3+F) Distributions and Injury Rate: Air-Bag-Equipped Fleet Vehicles, MY 1985+, 1998-2010 NASS CDS

All Crashes - Unweighted Data			All Crashes -Weighted Data (National Estimates)					
Frontal Taxonomy	All Crashes	MAIS 3+F	Frontal Taxonomy	All Crashes	MAIS 3+F	% All	% MAIS 3+F	Risk (Rate of MAIS 3+F)
Between Rail	554	67	**Between Rail**	202010	4471	7.5%	11.0%	2.2%
FullEng	2767	145	**FullEng**	1243912	15336	46.0%	37.7%	1.2%
Offset	1859	133	**Offset**	968395	16319	35.8%	40.1%	1.7%
Other(Front)	299	6	**Other(Front)**	143552	147	5.3%	0.4%	0.1%
Sml Offset	321	36	**Sml Offset**	148376	4421	5.5%	10.9%	3.0%
Total	5800	387	**Total**	2706246	40694	100.0%	100.0%	1.5%

Note: The "Other" group includes vehicles with underride or frontal damage and 9, 10, 2, or 3 direction of force.

A breakdown of the frontal groups by single-vehicle versus two-vehicle crashes is presented in Table 3-5. Overall, single-vehicle crashes make up 19 percent of the frontal crash population under study while two-vehicle crashes are 81 percent of total. Of the three predominant crash configurations, single-vehicle "Full Engagement" and "Offset frontal crashes" account for 38 percent and 27 percent of all single-vehicle crashes and two-vehicle "Full Engagement" and "Offset frontal crashes" account for 48 percent and 38 percent of all two-vehicle crashes, respectively. In contrast, single-vehicle "Between the Rail" frontal crashes account for 19 percent of all single-vehicle crashes and 5 percent of two-vehicle crashes.

Table 3-5. Frontal Crash Involvement: Single- and Two-Vehicle Crash Configurations: Air-Bag-Equipped Fleet Vehicles, MY 1985+ (weighted), 1998-2010 NASS CDS

						of Total	
Frontal Taxonomy	All Crashes	Single Vehicle	Two Vehicle	Single Vehicle	Two Vehicle	Single Vehicle	Two Vehicle
Between Rail	202010	97579	**104431**	**19%**	**5%**	**3.6%**	**3.9%**
FullEng	1243912	195458	**1048454**	**38%**	**48%**	**7.2%**	**38.7%**
Offset	968395	138660	**829735**	**27%**	**38%**	**5.1%**	**30.7%**
Other(Front)	143552	48420	95132	9%	4%	**1.8%**	**3.5%**
Sml Offset F&S	148376	30544	117833	6%	5%	**1.1%**	**4.4%**
Total	2706246	510661	2195584	100%	100%	**19%**	**81%**

3.2.4 Simulation Matrix Based on Frontal Crash Configuration Mapping

The simulation matrix for this study using EFP is designed to address the predominant real-world frontal impact configurations. The schematic for the crash configurations included in the simulation matrix is provided in Figure 3-9. The EFP approach is to simulate the two major crash classes, single- and two-vehicle crashes. The approach will also establish the weighting factors ($\mathbf{W_i}$ in Figure 3-9) for each occupant type, crash type, and impact speed for the target and partner vehicles in the fleet simulation matrix (refer to section 3.1.1 for definition of SIR).

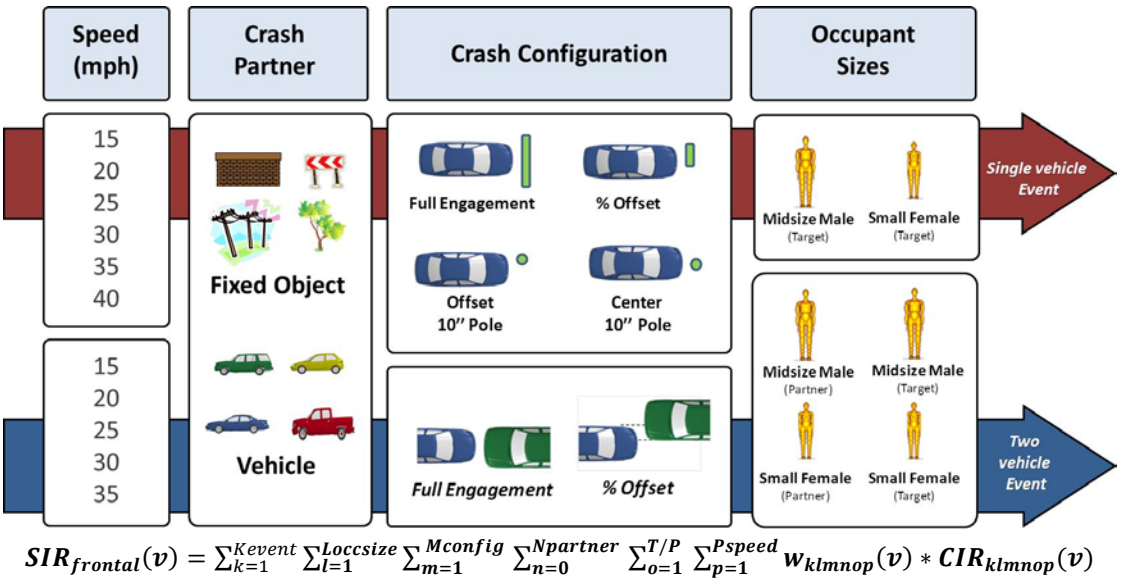

$$SIR_{frontal}(v) = \sum_{k=1}^{Kevent} \sum_{l=1}^{Loccsize} \sum_{m=1}^{Mconfig} \sum_{n=0}^{Npartner} \sum_{o=1}^{T/P} \sum_{p=1}^{Pspeed} w_{klmnop}(v) * CIR_{klmnop}(v)$$

Figure 3-9. Schematic of Accumulated Injury Risk for Modeled Single- and Two-Vehicle Frontal Crashes

3.3 What to Study? Fleet Vehicle FE Model Selection and Development

As shown in Figure 3-5, both passenger car and LTV vehicle segments are needed to represent a virtual fleet to model the real-world frontal crash safety problem. As indicated in section 3.1.3, validated finite elements models for target vehicles and the partner vehicles representing the fleet need to be available to implement EFP.

LS-DYNA finite elements models for a small and midsize passenger car, a midsize sport utility vehicle, and a full size pickup truck are used as surrogates to represent the fleet crash partner vehicles. Extended validation efforts were undertaken to enhance the models and assess their robustness in full, offset, and centerline pole frontal crash engagements. The FE models were enhanced to improve the correlation with available crash test data, including FMVSS No. 208 and U.S. New Car Assessment Program frontal tests and Insurance Institute for Highway Safety (IIHS) offset deformable barrier (ODB) frontal tests. Single- and two-vehicle crashes up to speeds of consumer information testing were simulated to predict the crash pulse, dynamic crush, and intrusions in self and partner vehicles. The level of effort for the extended FE vehicle model development and verification in frontal crash configuration involved more than 90 LS-DYNA simulations and developmental iterations.

3.3.1 Vehicle FE Model Availability

Since the mid-1990s, the NCAC has developed finite element models for crash simulations by reverse engineering more than a dozen passenger cars, SUVs, pickups, and single-unit and tractor-trailer combination trucks for NHTSA and the FHWA. These models, shown in Table 3-6, with status at the start of this project, vary in complexity and size depending on their applications. They are available in the public domain on the NCAC Web site (www.ncac.gwu.edu/vml/models.html) and have been used successfully by the NCAC, FHWA, NHTSA, and many researchers worldwide. The NCAC model development process is documented in Appendix 1 of this report. A selected subset of the available FEMs was chosen to be further refined and to undergo extended crash validation for frontal crash configurations in order to represent segments of the existing fleet in this study.

Table 3-6. Vehicle FE Models Developed by the NCAC as Available at the Start of This Study (www.ncac.gwu.edu/vml/models.html)

Year, Make and Model	FE Model Picture	Number of Elements	Validation and Verification Tests
2010 Toyota Yaris		Under develop-ment	Frontal NCAP (NHTSA Tests 5677 and 6221) planned
2007 Chevy Silverado		929,131	Frontal NCAP (NHTSA Test 5877) Suspension modeled in greater detail
2006 Ford F250		730,000	Full Frontal High Resolution Barrier Test (NHTSA Test 5820) Over Ride Barrier Test (NHTSA Test 5881)
2003 Ford Explorer		620,000	Frontal NCAP Test (NHTSA Test 3730) Full Frontal High Resolution Barrier Test (NHTSA Test 5034) Roof crush component test (NHTSA test C0139 and C0140)

2001 Ford Taurus		1,060,000	<u>Separate FEMs:</u> Frontal NCAP Tests (NHTSA Tests 3248 and 4776) Side NCAP Test (NHTSA Test 3263) Roof crush component test (NHTSA test C0287)
1999 Ford Econoline		300,000	Frontal NCAP test (NHTSA Test 3021)
1998 Chevrolet S10		220,000	Frontal NCAP test (NHTSA Test 3252)
1997 Toyota Rav4		500,000	Frontal NCAP Test (NHTSA Test 2496)
1997 Dodge Caravan		335,000	Frontal NCAP test (NHTSA Test 2335)
1997 Geo Metro		194,000	Frontal NCAP test (NHTSA Test 2239) Several oblique impacts into roadside hardware Oblique impact into F-shape barrier Suspension validated to F-shape concrete barrier.
1996 Dodge Neon		270,000	Frontal NCAP test (NHTSA Test 2320)
1994 Chevrolet C1500		58,000	Frontal NCAP test (NHTSA Test 1741) Suspension validated to component tests conducted at FOIL Several roadside hardware impacts including impacts into PCB, W-beam guardrail, sign posts etc.
1995 Ford F800 SUT	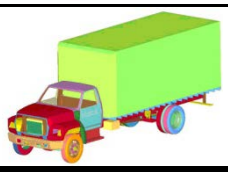	22,000	Oblique impact into Rigid F-shape barrier, crash test conducted at FOIL

3.3.2 Vehicle FE Model Initial Status and Applicability to this Study

Based on availability, the FEMs of the fourth-generation Taurus (MY 2000 – 2007), second-generation Yaris (MY 2005 – current), third-generation Explorer (MY 2002 – 2005), and GMT900 platform Silverado (MY 2007 – current) were selected as surrogate vehicles for crash partners for this study. They are used to represent a midsize passenger car, small passenger car, midsize SUV, and full size pickup, respectively, in the existing vehicle fleet. NHTSA reports the median age of a passenger vehicle on U.S. roads to be 13.8 years and of a light truck to be 14.5 years (Lu, 2006). Thus these four popular vehicles are expected to provide a reasonable representation of their vehicle segments in the current on-road fleet. The selected vehicle models and their initial status, prior to the extended validation efforts of this project, are outlined in Table 3-7. In response to high fuel economy demands and more stringent greenhouse gas and CAFE standards, the light-duty vehicle fleet might transition into a lighter fleet. These partner vehicle models will be a good representation of the current on-road vehicles before the transition starts. NHTSA is concerned that the new lighter vehicles will have a higher delta-V when crashing with heavier vehicles and thus have higher injury and fatality risk. This is especially important as the heavier legacy vehicles will remain in the fleet during the transition to lighter and smaller vehicles (Medford, 2011).

Table 3-7. Initial Status for Selected FE Models for Representing Partner Vehicles

Initial Status		
2001 Ford Taurus • Different versions validated to frontal NCAP, side NCAP, IIHS ODB, and roof crush tests • **Model includes vehicle interior components**		
2003 Ford Explorer • Validated to frontal NCAP • **Interior components available but not included**		
2007 Chevy Silverado • Validated to frontal NCAP test • **Interior digitized but not yet incorporated in the model**	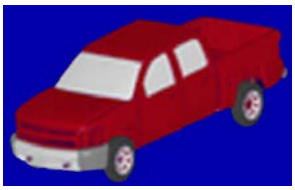	
2010 Toyota Yaris • Validated to frontal NCAP test		

It is worth noting that both the Taurus and the Explorer were rated "Good" in the IIHS 40 percent offset tests at 40 mph. The Explorer rails were lowered compared to the previous model to provide geometrical compatibility with cars and meets the guidelines agreed to by the Industry to improve crash compatibility under the voluntary "Enhancing Vehicle-to-Vehicle Crash Compatibility Agreement" (EVC) established in 2003. Current and future

designs are not expected to be radically different from the two vehicles in question. The Explorer was a body-on-frame design and the trend is towards unitized body for SUVs. However, pickups are expected to continue as body-on-frame vehicles, and some will be in the same weight class as the Explorer. Future studies will include more modern vehicle designs like the Accord or the Camry replacing the 2000-2007 Taurus from the fleet, and potentially adding a unitized body SUVe.g., such as theVenza into the fleet model. The results of a follow-up study will shed some light on the robustness of the results of this initial study. When FE models of new vehicles with light-weighted designs and new powertrains are developed for the different vehicle segments, the methodology developed in this study can be applied to assess safety effects in the future fleet.

3.3.3 Extended Vehicle FE Model Development and Validation

For this study, prior to performing the matrix of simulations, extended model validations were performed for the four surrogate vehicle models to ensure the models demonstrate reasonable responses in non-standard crash configurations. In addition, as available, vehicle interior components were incorporated into the models. Each of the four vehicle models were run in different crash modes and the results compared to crash test data, including exterior vehicle crush data and intrusion responses as available and feasible. The following crash tests were identified and the test information (reports, video clips, and test data) was collected.

- Frontal NCAP
- Side NCAP
- IIHS frontal ODB
- IIHS frontal pole research tests

After the models were validated to crash test data, a robustness study was performed to ensure that the model would be stable under the most severe crash conditions to be simulated. The Yaris, Taurus, Explorer, and Silverado models were subjected to a centerline pole impact at 35 mph. This impact was chosen because it involved large deformations, which would cause a simulation to abort if the model is not robust. Additionally, the Taurus and the Yaris models were tested for robustness in vehicle-to-vehicle full and 50 percent offset impacts with the Silverado model. The results from these robustness simulations were used to further develop and stabilize the FE models as needed.

Last, all four vehicle models were run at low and high speeds within a given crash configuration to verify expected trends (i.e., a higher speed impact would lead to more severe occupant injury). These simulations would also serve to further develop the MADYMO occupant models based on the assessment of the trends in the occupant responses and injury risk. The following simulations were run for the verification study.

- NCAP rigid wall at 25 mph and 35 mph
- IIHS ODB at 25 mph and 40 mph
- Centerline pole at 25 mph and 35 mph

The extended validation, robustness, and verification studies for the four models to support this project are documented in NCAC working papers (www.ncac.gwu.edu/research/reports.html) and provided as Appendices 2

to 5 to this report. Specific focus was placed on the Taurus model since it is the midsize passenger car and candidate vehicle for proof-of-concept light-weighting for this study.

3.3.4 Vehicle Interior Detail for Vehicle FE Models

The NCAC FE vehicle models have been traditionally developed, as specified by NHTSA, to match vehicle accelerations (e.g., compartment crash pulse, engine and brake caliper accelerations), barrier load force, and overall energy balance in a full barrier NCAP frontal test, thus the models typically have minimal detail for vehicle interiors (e.g., seat, door panels, dash). To conduct occupant simulations, the relevant vehicle interiors need to be modeled. Not all the FE models used in this study had the needed interiors modeled to effectively perform occupant simulation in the frontal crash configurations of interest. Given the lack of available FE interior and FE restraint models for this implementation of the EFP methodology, the occupant modeling was decoupled from the vehicle structural modeling and was performed separately using MADYMO rigid body simulations. The available FE interior components were supplemented with generic surfaces and characteristics from generic MADYMO occupant model environments as outlined in Section 3.5 below.

Overall, when vehicle FE models are used in simulations of various vehicle-to-structure and vehicle-to-vehicle crashes in non-standard conditions, e.g., offset, pole, and far side impact configurations, model responses such as localized intrusions and occupant/restraints interactions become important. Seats and restraints also become more relevant as they affect structural loading and occupant trajectories in certain crash modes. For side impact configurations, which is a potential future application of EFP, the door panels and seats (structure and cushion) are critical. For studies involving occupants seated in the second row in frontal and side impact configurations (a current/upcoming focus for crashworthiness studies), the rear seats, front seat backs, B-pillar structure, and pad/cover are important. Therefore in order to use the FE vehicle models in EFP, there is a need to model the vehicle interior, such as detailed geometry of interior, material thickness and properties, etc., as part of the initial FE vehicle model development. For frontal simulations we would need detailed instrument panel geometry and material data. Additionally, all the components behind the surface of the IP and the steering column components and their attachment to the cross-car beams would have to be modeled. This would make it possible to study occupant kinematics and responses resulting from contact with vehicle interior surfaces, and interaction with restraints and seats, in the same FE simulation.

3.4 Target Vehicle FE Models: Proof-of-Concept and Lightweight Vehicle Design Studies

In order to evaluate the feasibility, cost, and safety of future lightweight vehicle designs, NHTSA, the EPA, and the CARB initiated vehicle design projects to develop detailed designs and cost estimates for future lightweight vehicles. While each of these studies were conducted by different research groups and had slightly different research goals and requirements, the studies all required the development of finite element models to demonstrate compliance with the major safety requirements. Each of the sponsoring organizations agreed to support NHTSA's use of the resulting finite element models for evaluating vehicle-to-vehicle and vehicle-to-object crash safety. The development of these three unique finite element models for future lightweight vehicle designs provides an excellent opportunity to apply EFP to evaluate the safety implications of introducing lightweight vehicle designs into the existing U.S. fleet and vehicle crash safety in crash conditions beyond the standard vehicle safety tests. In this study, FE models of the three lightweight designs were used as target vehicles in EFP. Although the goal was not to judge the design of each light-weighted vehicle, it is important to note that the study results will depend on

how realistic these models are, such as how realistic the designs are, how realistically the material and design are modeled, etc.

3.4.1 Ford Taurus (EFP Proof-of-Concept)

When the project was started in 2010, none of the light-weighted vehicle models from EPA, CARB, and NHTSA were available. As a first step to develop and assess the feasibility of EFP, it was decided to use one of the existing GWU vehicle models and to develop two simplistic new vehicle designs to compare the safety performance against the baseline vehicle. The goal of the proof-of-concept designs was to assist in the development and evaluation of the EFP methodology to be applied to light vehicles models and other new vehicle design as those become available. The researchers understand that these simplistic designs are not practical but the results will give the researchers a good indication about the sensitivity of EFP. The NCAC/GWU chose the existing model of a 2001 Ford Taurus as the baseline for new vehicle models for the proof-of-concept of EFP.

3.4.2 Taurus LW3 and LW4 FEM Designs

Initially, four strategies were considered for simplistic light-weighting and design changes for the Taurus FEM. The strategies are outlined below and compared to the baseline (Table 3-8).

- **Taurus Baseline:** The FE model of MY 2001 Taurus
- **LW1 (15%Off_DP500):** The weight is 15 percent less than baseline model; DP500 high strength steel used in all steel materials in Taurus except Engine and Transmission, with 20 percent less thickness.
- **LW2 (25%Off_DP500):** The weight is 25 percent less than baseline model; DP500 high strength steel used in all steel materials in Taurus except Engine and Transmission, with 40 percent less thickness.
- **LW3 (25%Off):** The weight is 25 percent less than baseline model, with same thickness and lower density of steel parts.
- **LW4 (DP500):** The weight is same as baseline model with DP500 high strength steel replacing all steel materials in Taurus except Engine and Transmission.

Table 3-8. Four Simplistic Light-weighting Design Strategies: FEM Weights

	Baseline	15% Off_DP500	25%Off_DP500	25%Off	DP500
Mass(kg)	1504	1266	1127	1127	1504

The NCAC decided to use LW3, a 25 percent light-weighted design, and LW4, an overall stiffer design, to assess the feasibility of EFP for comparing the safety performance of a new vehicle design against a baseline vehicle. The LW3 and LW4 designs were chosen for this study to allow better discrimination between the effects of weight and stiffness changes. These designs were intended to serve as a proof of concept of EFP.

LW3 implemented a 25 percent light-weighting strategy by simplistically reducing the density[1] of all steel parts in the Taurus by approximately one third, including a reduction of 100 kg from the engine (powertrain components). The Taurus vehicle design was not otherwise changed. The LW3 design is a surrogate of a strategy where the vehicle has been light-weighted while the front end stiffness remains the same. In LW4, all of the steel parts were replaced with a dual phase ltra-high-strength steel, except the engine and transmission, as compared to the baseline. The vehicle design was not otherwise changed in the LW4 design. The LW4 design is a surrogate of a strategy where the weight of the vehicle has not changed while the front end stiffness has increased. These new designs of the Taurus vehicle were not meant to be realistic designs, but were rather intended to evaluate if the developed EFP was sensitive enough to detect changes in occupant risk related to vehicle design modifications. Additionally, the selected designs will independently examine safety effects related to changing vehicle weight and stiffness. The following sections provide detailed background and supporting information about how LW3 and LW4 are implemented.

3.4.2.1 Weight Distribution of 2001 Ford Taurus

Initially, an analysis of the weight distributions of the 2001 Taurus was performed as follows.

- Body-in-white
- Body components: Doors, hood, trunk lid, bumpers, fenders, fuel tank, battery, wind screen, and rear glass
- Power train system: Engine, transmission, fuel tank, battery, exhaust system, and heating/cooling system
- Chassis: Suspension, tires, steering system, and brake assembly
- Interior: Seats, instrument panel, and interior trim
- Other: Electric system and padding materials

Then the weight distribution of the 2001 Ford Taurus model was compared to that of a 2011 Honda Accord. As shown in Table 3-9, the FE Taurus model has reasonable weight distribution when compared to a more modern popular midsize vehicle.

[1] The researchers understand that the density of AHSS is similar to regular steel. The main reason for light-weighting by using AHSS is reducing the gauge of the material. The approach used here is just for simplicity and to prove the concept.

Table 3-9. Comparison of Mass Distribution of 2011 Accord and 2001 Taurus

		2011 Honda Accord		2001 Ford Taurus	
		Mass(kg)	Percentage	Mass(kg)	Percentage
Body Structure		372	24.6%	375.0	24.4%
	Body	310	20.5%	316.4	20.6%
	Bumpers	23	1.5%	27.3	1.8%
	Subframe	32	2.1%	24.4	1.6%
	Fenders	7	0.5%	7.0	0.5%
Closures		164	10.8%	199.6	13.0%
	Doors	110	7.3%	134.8	8.8%
	Glasses	22	1.5%	25.2	1.6%
	Hood	17	1.1%	22.2	1.4%
	Trunk Lid	15	1.0%	17.3	1.1%
Interior		97	6.4%	127.6	8.3%
	Seats	66	4.4%	85.4	5.5%
	Instrument Panel	31	2.0%	42.2	2.7%
Chassis		322	21.3%	227.2	14.8%
	Suspension	160	10.6%	65.0	4.2%
	Brakes	58	3.8%	55.5	3.6%
	Wheels	77	5.1%	93.0	6.0%
	Steering	27	1.8%	13.7	0.9%
Powertrain		331	21.8%	419.6	27.3%
	Engine & Transmission	260	17.2%	302.8	19.7%
	Exhaust	35	2.3%	27.9	1.8%
	Fuel System	24	1.6%	51.2	3.3%
	Engine Cooling System	12	0.8%	37.8	2.5%
Others		229	15.1%	189.7	12.3%
	HVAC, Lighting, Electrical, Wiper System, Airb & Belt Sysmte, pedal, trim, others	229	15.1%	189.7	12.3%
Total		1515	100.0%	1538.7	100.0%

	Similar Mass (<20kg Difference)
	20-40kg Difference
	20-40kg Difference (Mass difference may be due to mis-grouping)
	More than 40kg Difference

3.4.2.2 Mixed-Material Strategies for Mass Reduction of Current Vehicles

Manufacturers have been focusing on changing vehicle designs and/or increasing the use of materials such as high-strength steel (HSS), ultra-high-strength steel, aluminum, and composites to achieve mass reduction. Experts indicate that vehicle mass reduction using lighter and stronger materials requires a systems approach. Overall, the systems approach centers on increasing usage of advanced high-strength steels (AHSS) for the body-in-white and aluminum for the closures, and possibly structural and chassis applications. Examples of current vehicles with AHSS and aluminum are listed in Table 3-10 (Brooke & Evans, 2009).

Recently, the use of AHSS has grown over 15 percent per year and is expected to continue to grow at 10 percent per year, as the industry is learning how to engineer and produce more vehicle parts in AHSS. Prime candidate components are rockers, sills, pillars, cross members, and bulkheads (using martensitic, boron, and dual-phase advanced high-strength steels). For closure applications, such as hoods and decklids, aluminum offers substantial mass savings. In 2009, 22.3 percent of vehicle production had aluminum hoods. Steady growth is also expected in aluminum use in suspension and driveline components. Experts expect aluminum will make up over 10 percent of the average curb weight of vehicles in 2020 (Brooke & Evans, 2009).

Table 3-10. Examples of Current Vehicles With AHSS and Aluminum

Model	% AHSS
2009 BMW X6	32% of body in-white & closures
2009 Altima	32%
2010 Lincoln MKT and F-150	16%
Volkswagen- all	100% of bumper beams boron (hot-stamping process)
Chrysler – all	20-30% (→ 60% by 2012)
2009 Acura MDX, Honda Pilot, GM Lambda crossovers	High proportion in bodies-in-white
2008 Audi TT Couple	Body shell weighs 206 kg (68% Aluminum and 32% AHSS)

3.4.2.3 Strategies and Modeling Implementation

Figure 3-10 presents examples of stress-strain curves for different steels, ranging from mild steel to the ultra-high-strength, dual-phase (DP) steels.

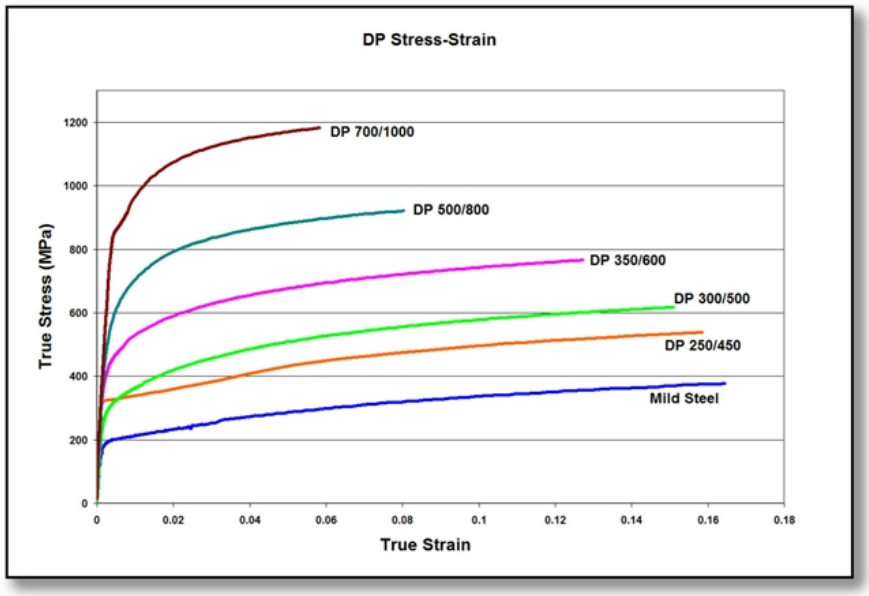

Figure 3-10. Stress-Strain Curves of Different Steels
(Reference: www.worldautosteel.org/Applications/Manufacturing/Stress-Strain-Curves.aspx)

In the Taurus baseline FEM, the material properties for the steel in the Taurus baseline are as follows.

- Density = 7,850 kg/m^3,
- Elastic Modulus = 210 GPa,
- Yield Stress = 140 ~ 400 MPa

For the LW3 design, the density of the all steel parts was simplistically reduced by approximately one third. The engine body was reduced by 100kg.

For the LW4 design, the baseline steel was replaced by a high strength steel (Dual Phase-DP 500) with the following material properties.

- Density = 7,850 kg/m^3,
- Elastic Modulus = 210 GPa,
- Yield Strength = 500 MPa

In LW4, all steel materials in the Taurus FE model, except the engine and transmission, were replaced to DP500.

3.4.3 Toyota Venza (Low and High Options)

In March 2010, Lotus Engineering released a report to identify potential mass reduction opportunities for a crossover utility vehicle based on a MY 2009 Toyota Venza (Lotus Engineering Inc., 2010). A Phase 2 project was subsequently awarded to Lotus Engineering to further refine the cost and design of the high option, a 32 percent light-weighted design for the crossover vehicle (Lotus Engineering Inc., 2012). This project included more detailed engineering and cost evaluations for body and closure. The project also required the development of finite element models for body and closures to demonstrate predicted crash safety of the lightweight vehicle design in safety assessment testing.

In January 2011, the EPA awarded a contract to FEV GmbH to conduct a Phase 2 study for the low option in the original Lotus Phase 1 study, a 20 percent light-weighted design for the crossover vehicle (FEV GmbH, 2012). This project was similar in scope to the project for the high option lightweight vehicle. The project included more detailed engineering, cost evaluation, and the development of finite element models for body and closures to demonstrate predicted crash safety of the lightweight vehicle design in safety assessment testing.

3.4.4 Honda Accord

NHTSA also awarded a contract for lightweight vehicle design to Electricore Inc. (Singh et al., 2012). This project was different than the CARB and EPA projects in two important aspects. First, a midsize vehicle, the Honda Accord, was selected to evaluate lightweight opportunities for a different vehicle segment. Second, it was stipulated that the resulting vehicle design should achieve the maximum amount of mass reduction appropriate for high-volume production (200,000 vehicles per year) while limited to no more than a 10 percent cost increment compared to the baseline vehicle. Other than these two requirements, the Honda Accord project had similar goals and outputs to the other two projects. The final lightweight vehicle achieved 23 percent mass reduction. A detailed FEM was developed for the vehicle body, closure, and chassis.

3.5 What to Study? Occupant Model Development

As noted earlier, not all the FE models used in this study had the needed interiors to effectively perform occupant simulation in the frontal crash configurations of interest. Given the lack of available FE interior and FE restraint models for this implementation of the EFP methodology, the occupant modeling was decoupled from the vehicle structural modeling. The occupant simulations were performed separately using MADYMO rigid body modeling

where the available FE interior components were supplemented with generic surfaces and characteristics from generic MADYMO occupant model environments as outlined below.

MADYMO occupant models were developed for the four partner vehicles (baseline Taurus, Yaris, Explorer, Silverado) using generic restraint systems designed to meet current regulations and consumer information testing, and were verified to frontal crash test data. These occupant models were also implemented in the target vehicles (baseline and modified lightweight designs of the Taurus, Accord, and Venza) and verified to crash test data as available. The models were set up with initial restraint systems from generic models supplied by automotive suppliers, with interior geometry adapted from the FEM, as available, for each vehicle. The models were driven by compartment pulses from crash test data or FEM simulations, and footwell intrusions from the FEM simulations. These models were used to evaluate the effect of acceleration and intrusion on occupant safety. The MADYMO prescribed structural motion (PSM) approach was used to model localized intrusions at the footrest and the accelerator pedal areas for the small and midsize passenger cars while planes were used for the SUV and pickup truck, with the respective motion extracted from finite element simulation outputs (LS-DYNA). It was anticipated that for the two large vehicles, the SUV and pickup truck, there would not be excessive localized intrusion and that the planar approach would effectively capture any intrusion that was seen in the FE simulation. The models were then used to predict probabilities of serious injuries in target and partner vehicles for restrained midsize male and small size female drivers in the single- and two-vehicle crashes of representative crash configurations up to speeds of current regulations and consumer information testing.

3.5.1 Occupant Restraint Modeling Approach

The overall approach to the occupant modeling is illustrated in Figure 3-11. Data from the FEM simulations, including the occupant compartment geometry, crash pulse, and toe pan intrusions, were imported into MADYMO to evaluate the occupant response. However, before the occupant simulation matrix could be executed, it was necessary to validate each occupant model to actual crash test data to make sure the estimated injury risks were realistic and the injuries were as close as possible to real-world injuries.

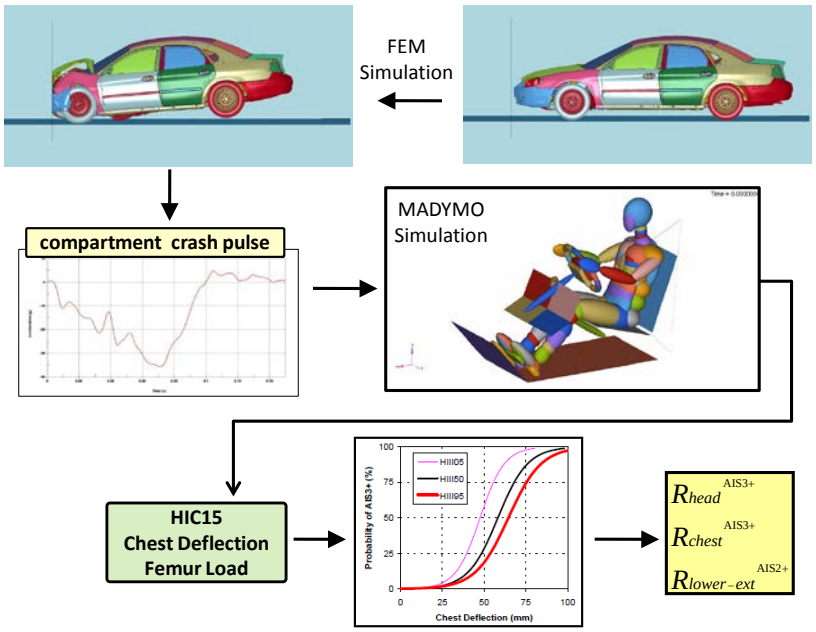

Figure 3-11. Overall Approach to Occupant Simulations

The occupant model validation was approached in two phases: model development (phase I) and model verification and robustness validation (phase II). This approach is outlined in Figure 3-12 and will be described in further detail in the following sections. The level of effort involved over 250 MADYMO runs to develop and establish baseline models for the Taurus, Yaris, Accord, Explorer, and Silverado. The occupant model development and validation are documented in NCAC working papers posted on the NCAC Web site (www.ncac.gwu.edu/research/reports.html) and are provided as Appendices 6-11 to this report. Due to limited time and test data availability, the Venza occupant model did not undergo the outlined phase I and II development; however the model was verified for the 50th percentile male dummy in the NCAP configuration at 35 mph. The resulting baseline occupant models will be placed in the public domain and become available from the NCAC Web site (www.ncac.gwu.edu/vml/models.html).

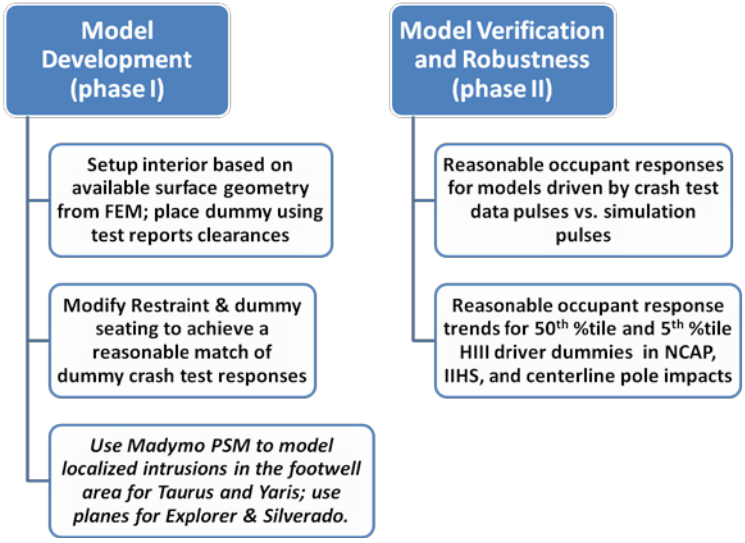

Figure 3-12. Outline of Occupant Modeling Approach, Phase I and Phase II

3.5.2 Phase I: Occupant Model Development

Phase I of the occupant modeling approach was Model Development. In this phase, generic occupant models obtained from restraint manufacturers were modified to reflect the interior geometry and clearances of the desired target or partner vehicle. The occupant models were run and the restraint characteristics and dummy positioning were adjusted in an iterative process until the simulation results proved to be a reasonable match of the corresponding crash test results.

Crash test data were used to modify and validate the generic occupant models. Crash test data were fundamental in verifying the results of the baseline simulations for the occupant modeling. The available crash test data were mainly regulatory and consumer information tests and research vehicle-to-object tests performed by NHTSA, IIHS, and Transport Canada in support of developing new safety regulations and advanced crash safety studies. As such, these tests are typically representative of the real-world crash environment.

3.5.2.1 Generic Occupant Restraint System Models

For this study, the NCAC contacted restraint manufacturers to obtain generic occupant restraint models. The NCAC received restraint system models for a MY 2009 pickup truck, a MY 2006 midsize SUV, a MY 2011 small car, and a MY 2007 midsize car. The models of the restraint systems represented designs currently in production in terms of pretensioners, load limiters and air bag inflators. It is worth noting that in general, current driver air bags are similar in most vehicles. Although differences in vent size might exist and tether lengths may be different, the inflators are designed for out-of-position (OOP) performance. As a result, driver air bag parameters are generally similar. Additionally, the NCAC was able to obtain knee bolster stiffness functions and frontal interior plane geometry of a MY 2004 sedan from an automotive manufacturer, which were used to enhance the foundation models provided by the restraint manufacturers.

The occupant models used in this study were built off of these generic foundation models supplied by the restraint manufacturers. It was by intention to use generic systems as the foundations for the models so that the models would be more representative of a vehicle class rather than a specific vehicle. It was also opted, in consultation with NHTSA, to use the same restraint systems for both the baseline and lightweight vehicles to provide insight on how restraint systems would need to evolve for the lightweight designs variants of the baseline vehicles. As the MY 2011 small car model includes a modern restraint system, it was used as the foundation for the Taurus occupant model, supplemented by the knee bolster stiffness functions and frontal interior plane geometry of the MY 2004 sedan. This generic midsize car model was also used as the foundation for the target and partner passenger car baseline and modified designs of the Yaris, Accord, and Venza. The Venza has a knee air bag, which was not included in the occupant simulation models in this initial study. It is expected that the presence/absence of the knee bag could substantially affect occupant responses and will be considered in future studies. However, the femur loads were similar and low in the Venza simulations and, therefore, the femur injury risks were equivalent as the changes from the baseline were of interest. The MY 2006 SUV model was the foundation for the Explorer, with the addition of the more modern air bag model from the MY 2009 pickup model. The MY 2009 pickup truck restraint model was used as the foundation for the Silverado.

A summary of model characteristics for the three light-weighted vehicle models are shown in Table 3-11.

Table 3-11. Summary of Model Characteristics

Vehicle	Firing Time Rule	Air Bag Vent Size (mm)	Pretensioner Pull Length (mm)	Stage 1 Load Limiter (N)	Stage 2 Load Limiter (N)
Taurus	5-30	30	40 mm	5,000	--
Accord	5-30	30	40 mm	4,000	3,000
Venza	5-30	30	40 mm	4,000	--

3.5.2.2 Vehicle Interior Geometry and Dummy Positioning

For vehicles in which interior geometry were available from the FE models, interior components were imported into MADYMO to guide the positioning of the model. Otherwise, the generic vehicle interior components and dummy in the occupant models were positioned according to the test report data on clearances and angles. A summary of these parts is shown in Table 3-12.

Table 3-12. Summary of FE Parts Used to Develop MADYMO Occupant Models

Occupant Model	FE Parts Used for Positioning	FE Parts Used for Simulations
Taurus	None	Driver side toe pan
Yaris	None	Driver side toe pan
Accord	*Digitized data:* dashboard, A-pillar, knee bolster, accelerator pedal, brake pedal, roof, seat back, seat bottom, steering wheel *FE model data:* toe pan, floor, steering wheel, side panel	Driver side toe pan
Venza	Toe pan, floor, windshield, A- and B-pillar	Toe pan, floor, windshield, A- and B-pillar
Explorer	Toe pan	Toe pan
Silverado	Toe pan	Toe pan

The occupant models for the Taurus, Yaris, and Accord included the driver side toe pan geometry from the corresponding FE model, which would allow the inclusion of prescribed structural motion to capture localized intrusions in the toe pan. The Taurus and Yaris were positioned according to the test report data, with no additional guidance from FE model geometry. Efforts were made to generally validate dynamic intrusions in the FE models with post-test intrusions; however, measurement of dynamic intrusions is not currently available in existing crash test data (Appendices 2 to 5).

To position the generic interior geometry of the Accord model, basic data of the dashboard, A-pillar, knee bolster, accelerator pedal, brake pedal, roof, seat back, seat bottom, and steering wheel were digitized from a physical vehicle. Interior geometry data was also available from the FE model and included the toe pan, floor, steering wheel, and side panel (Figure 3-13). The digitized data and FE model data were combined and overlaid onto the MADYMO model (Figure 3-14). The generic interior components were then repositioned according to the digitized parts, FE parts, and test report data. While these digitized and FE components were used for positioning, the final occupant model only included the generic interior components (appropriately positioned) and the FE toe pan with PSM.

Figure 3-13. Digitized Parts (left) and FE Model Parts (right) That Were Used to Position the MADYMO Model

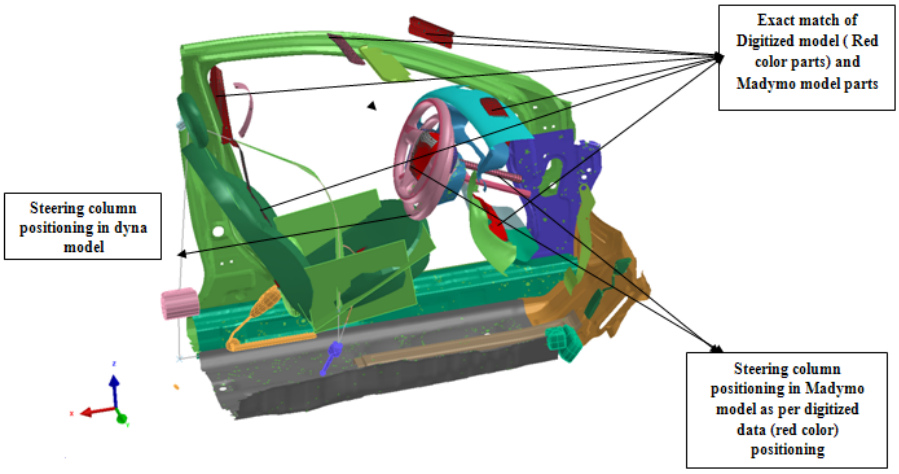

Figure 3-14. Overlay of Digitized Parts and FE Model Parts Onto Generic MADYMO Model

The Venza occupant model included the entire toe pan FE part, as well as the floor, windshield, and A- and B-pillar (Figure 3-15).

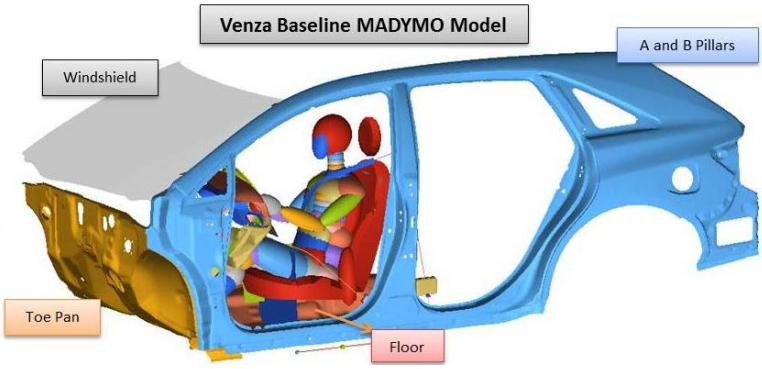

Figure 3-15. Venza MADYMO Model With Imported FE Parts

The Explorer and Silverado models used rigid planes as representations of the toe pans. The FE toe pan was imported into the models to serve as guidance for the positioning of the rigid planes, but no contacts were defined for these FE parts (Figure 3-16).

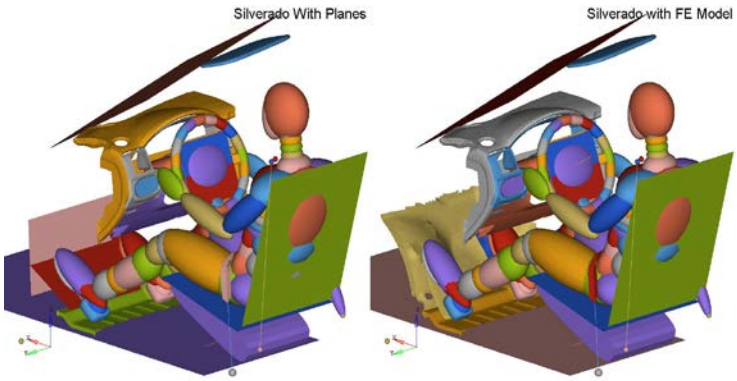

Figure 3-16. Comparison of Positioning of Silverado Model With Planes (left) and FE Toe Pan (right)

The first step in modifying each occupant generic model was to set up the interior based on the available surface geometry from the FEM and to position the dummy according to the test report. The Taurus, Yaris, and Accord occupant models included the toe pan geometry from the corresponding FE model, which would allow the inclusion of prescribed structural motion to capture localized intrusions in the toe pan. The Venza occupant model incorporated the prescribed structural motion of the toe pan, floor, windshield, A-pillar, and B-pillar; however the interior geometry and contact stiffnesses in the Venza model were generic. The Explorer and Silverado models included rigid planes as representations of the toe pan with prescribed joint motion. Because these two vehicles are substantially larger than the others, it was anticipated that there would not be excessive localized intrusion and that the planar approach would effectively capture any intrusion that was seen in the FE simulation.

The interior geometries of the generic models were modified to reflect measurements from crash test reports (e.g., steering wheel angle). The dummy clearances listed in the test report were used to position the dummy within the vehicle. Special attention was paid to the knee-to-dash measurement in an effort to replicate the lower extremity behavior seen in the actual crash test and to accurately predict the femur injury risk. As an example, the lower extremity positioning of the Taurus 50th percentile occupant model is shown in Figure 3-17 and the knee bolster contact characteristic is shown in Figure 3-18.

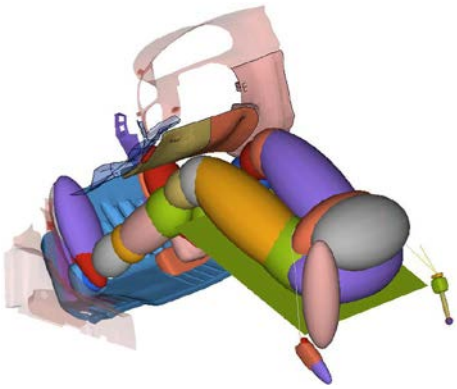

Figure 3-17. Lower Extremity Positioning of the 50th Percentile Dummy in the Taurus Occupant Model

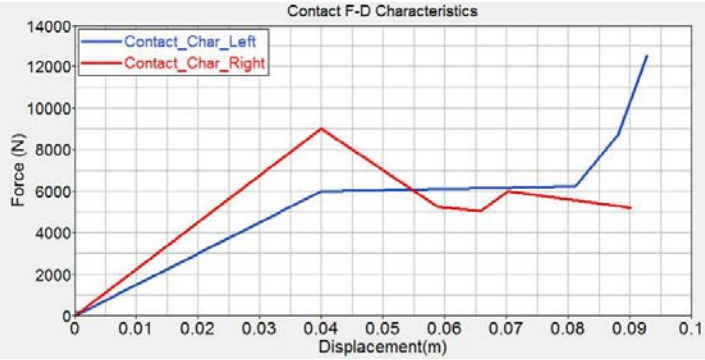

Figure 3-18. Taurus Knee Bolster Contact Characteristic

In some cases, it was difficult to match the dummy positioning exactly as prescribed in the test report. For example, there was difficulty in achieving the correct tibia angle in the Silverado model of the 50th percentile dummy. The dummy positioning in the crash test is shown in Figure 3-19. The tibia angle appears to be more acute than what was able to be achieved in the occupant model given the constraints of the FE toe pan geometry and positioning (Figure 3-20).

Figure 3-19. Dummy Positioning in Silverado Crash Test

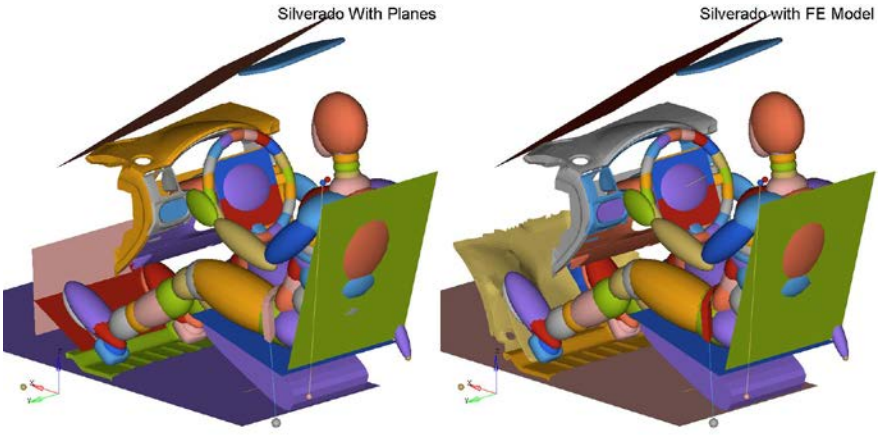

Figure 3-20. Dummy Positioning in Silverado Occupant Model, With Toe Pan Modeled With Planes (left) and With FE Geometry (right)

In addition to proper positioning, it was also important to effectively couple the dummy to the vehicle interior, specifically in the interaction of the foot with the footrest and floor. In the Taurus occupant model, the foot was not well-coupled to the floor, causing the heel to elastically bounce off the floor upon impact. To achieve tighter coupling of the foot to the floor, a "foot stop" was added to the floor, acting as a heel rest for the right foot (Figure 3-21). The addition of this foot stop allowed for more realistic lower extremity kinematics and closer correlation to test data.

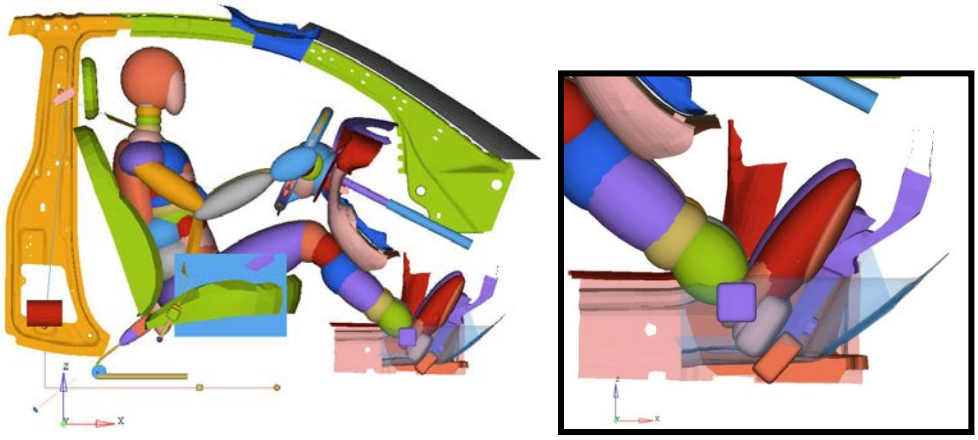

Figure 3-21. Addition of Foot Stop to Taurus Occupant Model

3.5.2.3 Air Bag and Pretensioner Firing Time Strategies

Air Bag firing algorithms are not publicly available; however, the firing times in available crash tests of each vehicle under study at various velocities were carefully studied and established. A general approach based on a vehicle design guideline and verified with crash test measurements was used to establish air bag firing strategy. The vehicle design guideline is based on free motion travel of an occupant computed from the compartment deceleration pulse as follows: apply the "5-30" rule for the firing time of the air bag and pretensioner, i.e., fire 30 ms prior to 5 inches of free motion travel of the occupant, with an earliest limit of 14 ms firing time. This guideline defines the time at which the air bag begins to generate gas. While the fill time of the air bag depends on the volume of the bag, this scenario should allow the air bag to be inflated and in place to restrain the occupant. The air bags in the models were not pre-inflated and the bag inflation time was dictated by the mass inflow rates of the inflators. Therefore, the bag/occupant interaction time was predicted in the model and not assumed. In the simulation, the air bag and pretensioner were triggered at the same time. The crash test data was checked to verify if a vehicle conformed to the design guideline, in particular if the occupant crash pulse and the shoulder belt data were available. For some vehicles, the 5-30 rule may not be achievable and the firing time is later allowing more occupant excursion. For these cases, the test data, specifically the belt pretensioner firing and compartment pulse were used to determine a rule that is specific to that vehicle. The firing strategy for each of the models is provided in the occupant model documentation, Appendices 6-11. Details for the Taurus, Yaris, and Venza models are provided in this section.

A follow-up study can be conducted with sensor suppliers in the future. In the case of the Accord lightweight design variant, the sensitivity of occupant responses to firing time was noticed. The selected firing time was the most reasonable for the vehicle considering available test data. It should be noted that the current state-of- art in

FE or any other modeling for air bag sensor responses is not predictive. The common practice in crash sensing for air bag firing relies heavily on tests supplemented by modeling.

3.5.2.3.1 TAURUS

The shoulder belt loads from the crash test data were analyzed to determine the air bag and pretensioner firing time, as shown in Figure 3-22. For NHTSA test no. 4135, the firing time was observed to be 24 ms.

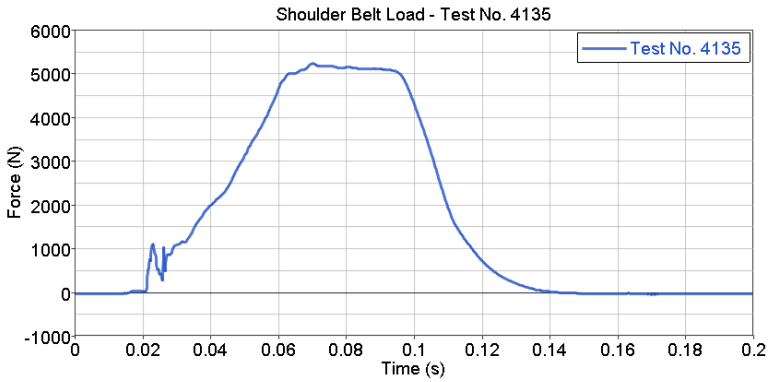

Figure 3-22. Shoulder Belt Force for NHTSA Test No. 4135

The firing time for this specific case was then used to determine a firing time rule that would be applicable to all crash speeds. The general guideline is for the 5-30 rule, i.e., 30 ms prior to 5" free motion travel of the occupant. The crash data was checked to verify that this vehicle conformed to the general guideline. The crash pulse from the test was double integrated to give the displacement time history, as shown in Figure 3-23. Five inches of displacement were observed at 54 ms, which confirmed that the 24 ms firing time matched the established 5-30 rule. For all the occupant simulations with the Taurus that were run in this study, the firing time was determined with this rule—30 ms less than the time at which 5 inches of displacement were observed.

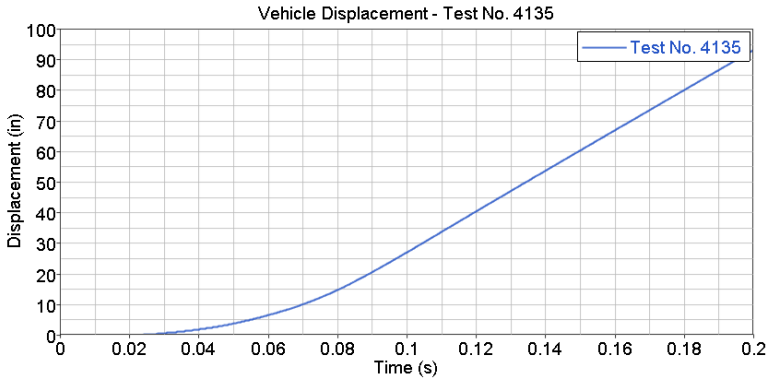

Figure 3-23. Vehicle Displacement Time History for NHTSA Test No. 4135

The firing times for the single-vehicle and vehicle-to-vehicle crashes for the Taurus are shown in Table 3-13 and Table 3-14.

Table 3-13. Taurus Single-Vehicle Crash Firing Times (seconds) by Crash Speed (mph)

		Single Vehicle		
Crash Type	Crash Speed (mph)	Baseline Firing Time (s)	LW3 Firing Time (s)	LW4 Firing Time (s)
Full Frontal	15	0.037	0.033	0.035
	20	0.030	0.026	0.026
	25	0.026	0.022	0.021
	30	0.023	0.019	0.018
	35	0.020	0.017	0.015
Offset	20	0.049	0.043	0.048
	25	0.045	0.039	0.042
	30	0.041	0.036	0.038
	35	0.038	0.033	0.034
	40	0.035	0.030	0.031
Center Pole	15	0.059	0.053	0.061
	20	0.050	0.044	0.048
	25	0.046	0.039	0.040
	30	0.040	0.036	0.034
	35	0.035	0.031	0.030

Table 3-14. Taurus Vehicle-to-Vehicle Crash Firing Times (seconds) by Crash Speed (mph)

		B to B	B to LW3		B to LW4		Taurus to Yaris			Taurus to Explorer			Taurus to Silverado		
Crash Type	Crash Speed (mph)	Baseline Firing Time (s)	Baseline Firing Time (s)	LW3 Firing Time (s)	Baseline Firing Time (s)	LW4 Firing Time (s)	Baseline Firing Time (s)	LW3 Firing Time (s)	LW4 Firing Time (s)	Baseline Firing Time (s)	LW3 Firing Time (s)	LW4 Firing Time (s)	Baseline Firing Time (s)	LW3 Firing Time (s)	LW4 Firing Time (s)
Full Frontal	15	0.034	0.034	0.029	0.034	0.035	0.036	0.031	0.034	0.029	0.024	0.027	0.035	0.030	0.032
	20	0.028	0.028	0.023	0.027	0.026	0.028	0.024	0.026	0.024	0.020	0.022	0.027	0.023	0.024
	25	0.023	0.023	0.019	0.022	0.020	0.024	0.020	0.021	0.021	0.017	0.018	0.022	0.018	0.019
	30	0.020	0.020	0.016	0.020	0.016	0.020	0.017	0.017	0.016	0.013	0.014	0.018	0.014	0.015
	35	0.017	0.017	0.014	0.017	0.014	0.018	0.015	0.014	0.014	0.010	0.012	0.014	0.011	0.011
Offset	15	0.049	0.048	0.043	0.048	0.047	0.067	0.059	0.062	0.042	0.040	0.038	0.047	0.040	0.041
	20	0.042	0.043	0.037	0.040	0.038	0.051	0.046	0.044	0.037	0.031	0.027	0.038	0.033	0.031
	25	0.037	0.038	0.032	0.034	0.031	0.041	0.036	0.035	0.033	0.028	0.023	0.034	0.028	0.026
	30	0.033	0.033	0.028	0.031	0.026	0.035	0.030	0.030	0.028	0.025	0.020	0.030	0.025	0.022
	35	0.030	0.030	0.025	0.028	0.023	0.032	0.027	0.025	0.025	0.022	0.018	0.027	0.022	0.019

3.5.2.3.2 YARIS

The shoulder belt loads from the crash test data were analyzed to determine the air bag and pretensioner firing time. For NHTSA test no. 5677, the firing time was observed to be 20 ms (Figure 3-24).

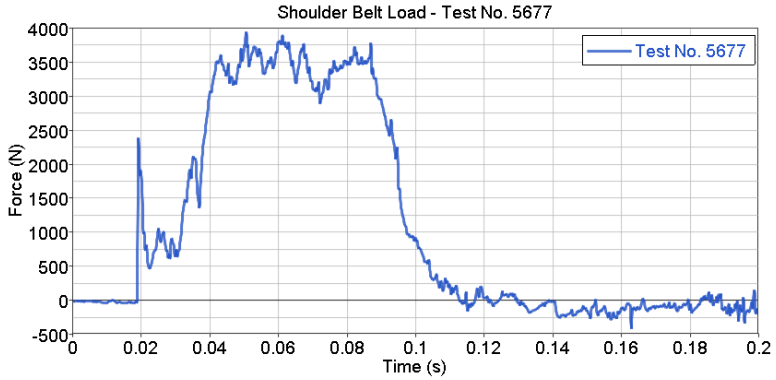

Figure 3-24. Shoulder Belt Force for NHTSA Test No. 5677

The firing time for this specific case was then used to determine a firing time rule that would be applicable to all crash speeds. The crash data showed that the firing time for this vehicle did not conform to the general 5-30 guideline. The crash pulse from the test was double integrated to give the displacement time history, as shown in Figure 3-25. Seven inches of displacement were observed at 50 ms, which would correspond to a 7-30 rule. For all simulations that were run in this study, the firing time was determined with this rule—30 ms less than the time at which 7 inches of displacement were observed.

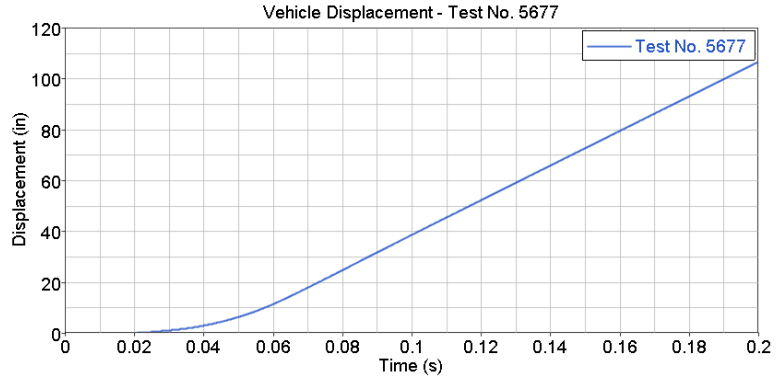

Figure 3-25. Vehicle Displacement Time History for NHTSA Test No. 5677

3.5.2.3.3 VENZA

The Venza occupant model used a generic FE model air bag. The test air bag firing time was observed to be 15 ms. For the occupant model; the 5-30 rule was used to estimate the firing times from the FE crash pulses. For the crash test conditions, this rule would correspond to a firing time of 18 ms (versus 15 ms from the test report). The firing times for the single-vehicle and vehicle-to-vehicle crashes for the Venza are shown in Table 3-15 and Table 3-16.

Table 3-15. Venza Single-Vehicle Crash Firing Times (seconds) by Crash Speed (mph)

		Single Vehicle		
Crash Type	Crash Speed (mph)	Venza Firing Time (s)	LWLO Firing Time (s)	LWHO Firing Time (s)
Full Frontal	15	0.041	0.034	0.025
	20	0.033	0.030	0.019
	25	0.029	0.026	0.015
	30	0.025	0.024	0.013
	35	0.018	0.020	0.011
Offset	20	0.048	0.050	0.051
	25	0.046	0.048	0.041
	30	0.044	0.042	0.035
	35	0.042	0.041	0.029
	40	0.031	0.030	0.024
Center Pole	15	0.050	0.055	0.042
	20	0.048	0.044	0.031
	25	0.033	0.035	0.024
	30	0.030	0.025	0.019
	35	0.025	0.020	0.015

Table 3-16. Venza Vehicle-to-Vehicle Crash Firing Times (seconds) by Crash Speed (mph)

		Venza to Taurus			Venza to Yaris			Venza to Explorer			Venza to Silverado		
Crash Type	Crash Speed (mph)	Venza Firing Time (s)	LWLO Firing Time (s)	LWHO Firing Time (s)	Venza Firing Time (s)	LWLO Firing Time (s)	LWHO Firing Time (s)	Venza Firing Time (s)	LWLO Firing Time (s)	LWHO Firing Time (s)	Venza Firing Time (s)	LWLO Firing Time (s)	LWHO Firing Time (s)
Full Frontal	15	0.034	0.032	0.031	0.044	0.044	0.033	0.035	0.033	0.027	0.030	0.029	0.028
	20	0.031	0.030	0.023	0.036	0.035	0.025	0.027	0.026	0.021	0.026	0.026	0.022
	25	0.029	0.023	0.018	0.029	0.029	0.021	0.026	0.020	0.018	0.024	0.023	0.020
	30	0.022	0.020	0.014	0.025	0.025	0.017	0.021	0.017	0.018	0.022	0.020	0.018
	35	0.021	0.018	0.013	0.022	0.021	0.015	0.021	0.015	0.017	0.018	0.018	0.016
Offset	15	0.053	0.035	0.032	0.052	0.048	0.047	0.046	0.037	0.035	0.039	0.040	0.040
	20	0.042	0.030	0.028	0.041	0.039	0.037	0.034	0.030	0.028	0.029	0.040	0.038
	25	0.042	0.028	0.025	0.035	0.032	0.031	0.027	0.030	0.024	0.028	0.033	0.030
	30	0.029	0.026	0.020	0.030	0.030	0.027	0.027	0.025	0.023	0.027	0.030	0.026
	35	0.028	0.025	0.018	0.027	0.026	0.021	0.025	0.022	0.019	0.022	0.028	0.021

3.5.2.4 Restraint System Fine Tuning

Once the dummy was reasonably positioned within the vehicle, the simulation was run and the restraints were modified through an iterative process. Because the restraint models were generic, it was necessary to fine tune the restraint characteristics within realistic value ranges to achieve a better match to the crash test data. The baseline

occupant models were developed with the ability to change belt restraint geometry, pretensioners, load limiters, and air bag size, mass-flow rate, and vent parameters. The restraint system fine tuning for each of the models is provided in the occupant model documentation, Appendices 6-11. Some details for the Taurus and Accord models are provided in this section.

3.5.2.4.1 TAURUS

The restraint system was fine-tuned through an iterative process until the model output the expected occupant accelerations according to the crash test data. Through this process, the air bag vent size and pretensioner pull function were modified. In the generic model from the restraint supplier, the air bag vent size was 25 mm. However, in order to reduce the HIC numbers to match the test results, the vent size was increased to 30 mm, which softened the air bag.

The characteristics of the belt system were determined by the shoulder belt load data from the crash test. The pretensioner was located at the outboard side in the generic model, but this was moved to the inboard side for the Taurus model.

One restraint characteristic that was modified was the belt pretensioner pull function. In the Taurus model, the pretensioner was modeled on the inboard side. The pretensioner maximum value was varied until the occupant acceleration curves matched those of the test. The values tested ranged from 25 mm to 65 mm in 5 mm increments. The physical depiction of the difference between a 25 mm and 65 mm pretensioner is shown in Figure 3-26 and the corresponding pretensioner pull functions are shown in Figure 3-27.

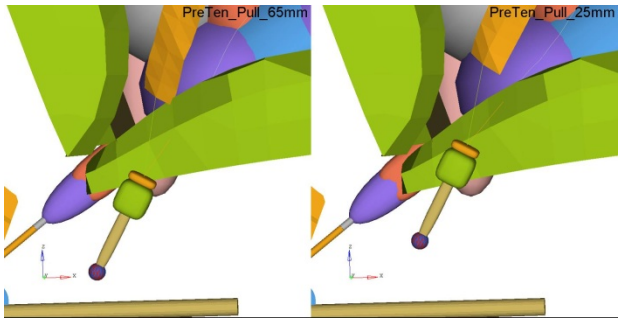

Figure 3-26. Example of Maximum Pretensioner Value of 65 mm (left) and 25 mm (right)

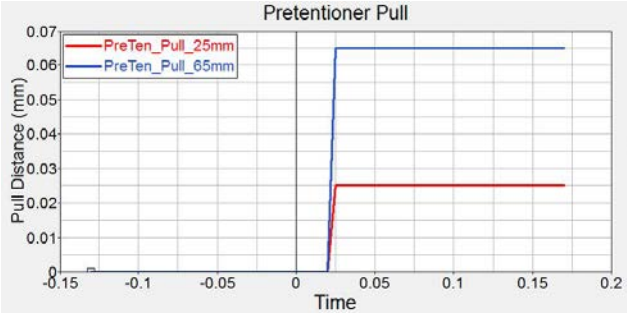

Figure 3-27. Pretensioner Pull Functions for 25 mm (red) and 65 mm (blue) Pretensioners

Last, the belt load data from the test showed that there was a load limiter at the shoulder belt. This feature was added, with load limiting set at 5,000 N. A comparison of the final belt loading curves to the test data for a 30 mph full frontal crash into a barrier with the 50th percentile dummy is shown in Figure 3-28.

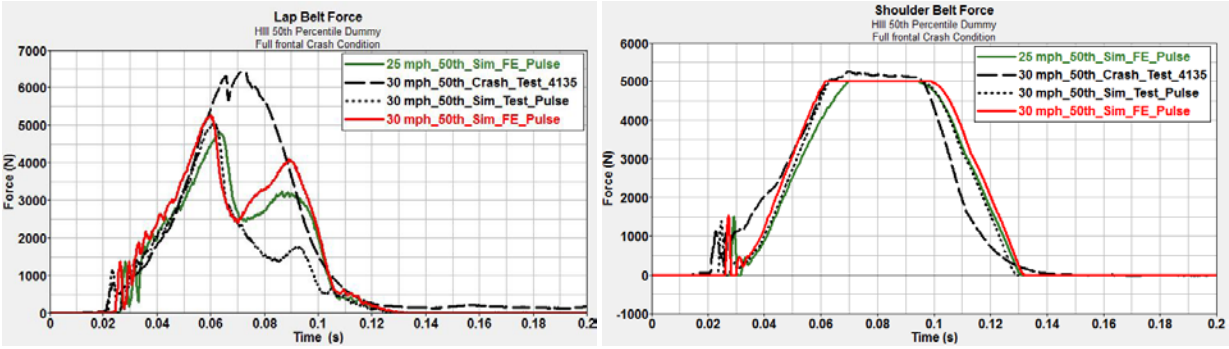

Figure 3-28. Comparison of Lap and Shoulder Belt Forces from Test and Simulations for 30mph Full Frontal Impact

3.5.2.4.2 ACCORD

For the Accord model, it was necessary to modify the retractor spool function in order to match the belt load measurements from the crash test. Figure 3-29 shows the retractor spool function that was used in the model, as well as lower and upper limits for this function, provided by the restraint manufacturer as general guidance.

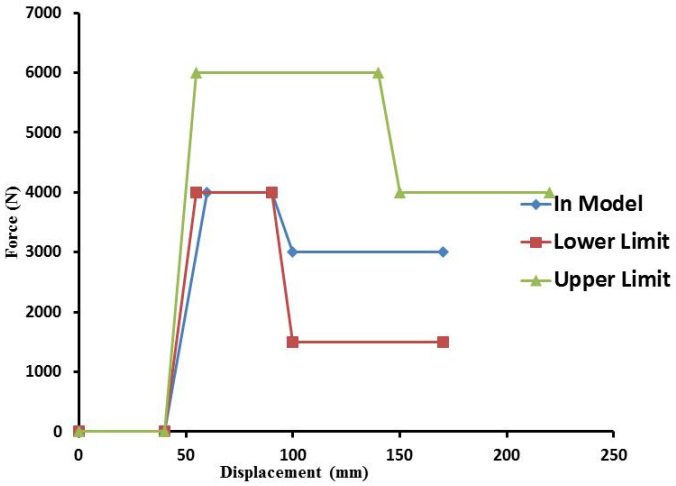

Figure 3-29. Accord Retractor Spool Function

A comparison of the final belt loading curves to the test data for a 35 mph full frontal crash into a barrier with the 50th percentile dummy is shown in Figure 3-30.

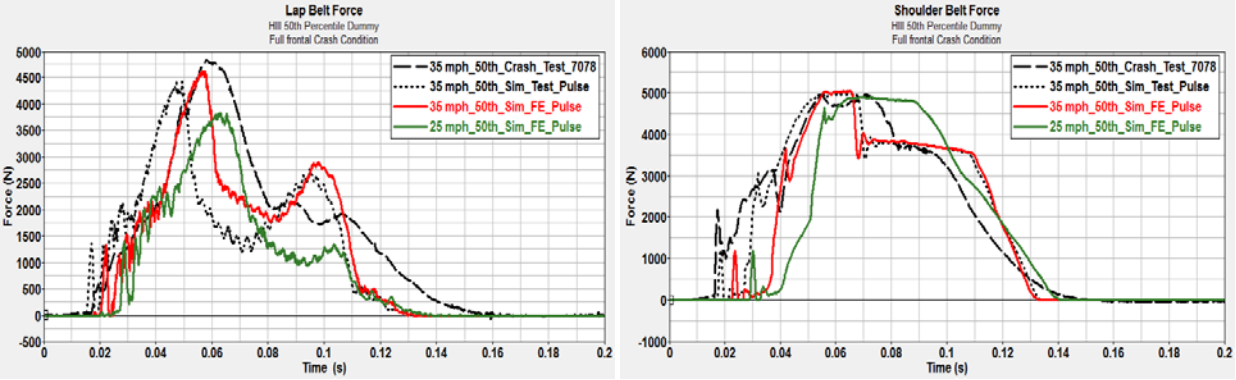

Figure 3-30. Comparison of Lap and Shoulder Belt Forces From Test and Simulations for Full Frontal Impact

3.5.3 Phase II: Occupant Model Verification and Robustness Validation

Phase II of the occupant modeling involved a verification and robustness study. In this phase, the pulses from the vehicle were used to accelerate the occupant model. The results from the simulations driven by the simulation pulses were compared to the corresponding results from the simulations driven by the test pulses. This check was performed for vehicle models with existing test results to ensure that reasonable occupant responses would be observed once the FE simulation outputs were used in the occupant models. The occupant models for any of the baseline vehicles, such as the Taurus, Accord, and Venza, were used for the light-weighted version of these vehicles. It is understood that the OEMs will refine these restraint systems in real vehicle production for light-weighted vehicles and such modification will change the injury risk results.

Verification and robustness checks were also performed, similarly structured to those of the FE models. The models were run in the NCAP, IIHS, and centerline pole impacts to confirm that reasonable occupant response trends would be observed for the 50th percentile male and 5th percentile female dummies. Due to limited time and test data availability, the Venza occupant model did not undergo the rigor of Phase II validation and robustness checks, in particular for the 5th percentile female dummy. Further information on these studies can be found in the occupant model documentation, Appendices 6 to 11.

3.6 Simulation Matrices

3.6.1 Simulated Frontal Crash Configurations

For the initial implementation of EFP, the simulation matrix was designed to address the predominant real-world frontal impact configurations identified in Section 3.2.4. The schematic for the crash configurations that were to be simulated is shown in Figure 3-31. The simulations include two major crash categories, single- and two-vehicle crashes, and represent two occupant sizes in frontal crashes up to speeds of current regulatory and consumer information testing.

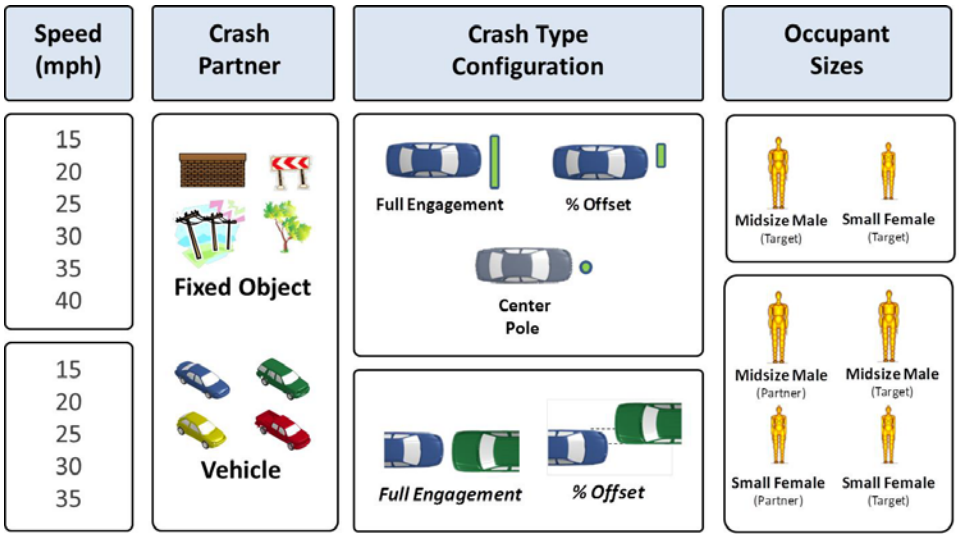

Figure 3-31. Schematic of Modeled Single- and Two-Vehicle Frontal Crashes

The conditions for the different crash configurations were guided by analyses of NASS CDS outlined in Section 3.2 and the availability of crash test data to develop and validate the FE structural and occupant models. For single-vehicle crashes, three configurations were simulated at five impact speeds. For two-vehicle crashes, two configurations were simulated at five impact speeds. The single- and two-vehicle simulation matrices for a given target vehicle are presented in Table 3-17 and Table 3-18.

Table 3-17. Single-Vehicle Crash Simulations
15 LS-DYNA Simulations per Target Vehicle
30 MADYMO (50percentile male and 5percentile female drivers) Simulations per Target Vehicle

	Test Configuration	Vehicle Speed (mph) 15	20	25	30	35	40
Frontal	Frontal Impact **Full Engagement** (*NCAP*)	X	X	X	X	X	
	Frontal Impact **% Offset** (*IIHS*)		X	X	X	X	X
	Frontal Impact ***Center – 10" Pole***	X	X	X	X	X	

Table 3-18. Two-Vehicle Frontal Crash Simulations
40 LS-DYNA Simulations per Target Vehicle
160 MADYMO (50percentile male and 5percentile female drivers) Simulations for Target and Partner

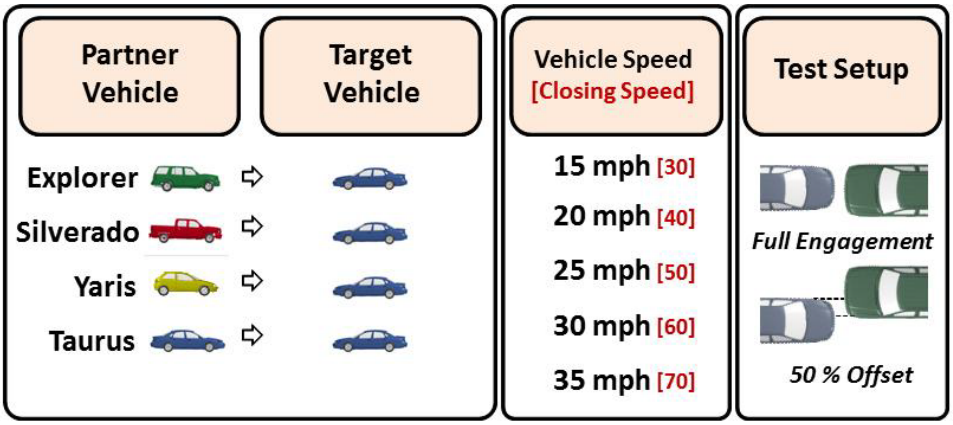

3.6.2 Study Target and Partner Vehicles

In this study, there were eight target vehicles as follows.

1. Taurus FEM baseline and its two simple design variants, LW3 and LW4
2. Honda Accord FEM baseline and its lightweight design, LW
3. Toyota Venza FEM baseline and its low and high option designs, LWLO and LWHO

In the future, an FEM of any new vehicle design being introduced into the fleet (e.g., with lightweight advanced materials, next generation gasoline vehicle, EV, PHEV, etc.) could be used as a target vehicle. An FEM of an existing vehicle could also be used as a target vehicle. As indicated earlier, the partner vehicles are the FEM surrogates of the fleet: the Yaris as a surrogate for an average small car, the baseline Taurus as a surrogate for an average midsize car, the Explorer as a surrogate for an SUV, and the Silverado as a surrogate for a pickup in the fleet. In the future, more partner vehicles representing additional vehicle segments in the fleet could be included.

3.6.3 Level of Simulation Effort

Performing all the LS-DYNA FE vehicle structure and MADYMO rigid body occupant simulations for the eight target vehicles involved a large number of simulation runs. A total of 440 LS-DYNA runs and 1,520 MADYMO runs were conducted, broken down as follows.

- Single-vehicle crash simulations:
  - 120 LS-DYNA runs
  - 240 MADYMO runs
- Two-vehicle crash simulations:
  - 320 LS-DYNA runs
  - 1,280 MADYMO runs

The FE vehicle structure simulations output the target and partner vehicles' crash pulses and intrusions in the different crash configurations. These outputs were incorporated into the MADYMO input to drive the occupant simulations. Two MADYMO simulations were run for each vehicle structure simulation, one for the 50th

percentile male and one for the 5th percentile female driver occupant configuration. The occupant responses output from MADYMO simulations were analyzed to predict probabilities of serious-to-fatal injuries in the target and partner vehicles for restrained drivers. The FE vehicle simulation outputs were also used to extract crash structural response attributes such as dynamic interior intrusions.

3.7 Injury Risk Calculation

Several occupant responses output by the MADYMO simulations were analyzed for the 50th percentile male and 5th percentile female driver occupants in each crash configuration over the range of speeds simulated. An example for the 50th percentile male dummy in one crash configuration (full frontal single-vehicle crash in this case) at the range of impact speeds for one target vehicle (Taurus baseline) illustrating the occupant responses analysis is shown in Table 3-19. The individual risk of serious injuries to the head, neck, chest, and knee-thigh-hip (KTH) complex were estimated by using injury risk functions (as described in Section 3.7.1 below) based on the relevant occupant responses HIC15 (Head Injury Criteria in 15 ms time interval), Neck Loads, Chest Deflections, and Femur Loads. The occupant responses and corresponding injury risk data for the target vehicles (baseline and modified) are tabulated in Appendices 12-19. It is worth noting that neck loads and moments are not easy to simulate with existing rigid body or finite element software given the dynamic interaction between the air bag and occupant's head and upper torso. However, the focus of this study is on trends and neck injury risks for belted occupants with supplemental air bags are low in the field and in the simulations. As such, the predicted neck injury risks did not substantially impact the predicted societal injury risks.

Table 3-19. Example Occupant Responses and Injury Risk Computations (Taurus Full Frontal Single-Vehicle Crash Simulation Results for HIII 50th Percentile Dummy)

Occupant Responses and Injury Risk Computation- Example Results for HIII 50th %ile Dummy						
Dummy Injury Measurement	***Formula***	**15 mph**	**20 mph**	**25 mph**	**30 mph**	**35 mph**
HIC15		50	83	124	146	169
Neck Tension (T)	*Upper Neck Fz Maximum*	849	1008	1264	1303	1348
Femur Left moment (My) (Nm)	*Maximum Moment*	26	49	64	58	62
Femur Right moment (My) (Nm)	*Maximum Moment*	71	64	81	93	108
Femur Left Moment (Resultant)	*Maximum Moment*	75	72	91	118	126
Femur Right Moment (Resultant)	*Maximum Moment*	77	76	92	105	117
Pelvis Acceleration (g)	*Max Resultant Acceleration*	29	36	43	53	62
Chest Deflection (mm)	*Maximum deflection*	22	24	25	26	26
Chest Acceleration (g)	*Maximum acceleration*	28	32	35	39	41
Femur Load - Left (N)	*Maximum Compressive force Fz*	417	408	926	1440	1927
Femur Load - Right (N)	*Maximum Compressive force Fz*	1696	2379	3112	4098	5273
HIC15 Risk (%)	*NORMDIST(LN(HIC15),7.45231,0.73998,1)*	0.0%	0.0%	0.0%	0.0%	0.1%
Chest Deflection Risk (%)	*1/(1+EXP(12.597-0.05861*35-1.568*((maxDef)^0.4612)))*	2%	2%	3%	3%	3%
Femur Max Rsk (%)	*1/(1+EXP(4.9795-0.326* maxFemur /1000)) -1/(1+EXP(4.9795))*	0.5%	0.8%	1.2%	1.9%	3.0%
Neck Tension(T) Risk (%)	*1/(1+EXP(10.9745-2.375*maxT/1000))*	0.0%	0.0%	0.0%	0.0%	0.0%
Combined Injury Risk I	***(1-(1-H)*(1-C)*(1-N)*(1-F))***	**0.02**	**0.03**	**0.04**	**0.05**	**0.06**
Combined Injury Risk II (No Femur)	***(1-(1-H)*(1-C)*(1-N))***	**0.02**	**0.02**	**0.03**	**0.03**	**0.03**

3.7.1 Injury Risks Functions

The head AIS3+ HIC15 risk function was the same as used by NHTSA's 2011 NCAP (Federal Register, 73 FR 40016, 2008) and is identical for both the 5th percentile female and 50th percentile male dummies, as follows:

$$P_{head}(\text{AIS}\,3+) = \Phi\left(\frac{\ln(HIC15) - 7.45231}{0.73998}\right)$$

$$where\ \ \Phi = \text{cumulative normal distribution}$$

The neck tension AIS3+ risk function was also the same as the function used in the 2011 NCAP. The functions for the two dummies are as follows:

For the 5th percentile dummy

$$P_{neck\_Tens}(AIS3+) = \frac{1}{1+e^{10.958-3.770 Neck\_Tension}}$$

For the 50th percentile dummy $$P_{neck\_Tens}(AIS3+) = \frac{1}{1+e^{10.9745-2.375 Neck\_Tension}}$$

The Normalized Neck Injury Criterion (Nij) used in the 2011 NCAP was initially considered for the neck body region. However, since the corresponding AIS3+ risk function for Nij has the threshold issue of computing a probability of 3.8 percent serious injury risk at Nij=0, the risk function for the neck tension was preferred for this study. Also, the NCAP risk function for neck tension has been shown to be a better predictor of serious neck injuries than Nij in the real-world based on NASS CDS (Prasad et al., 2010).

The chest deflection AIS3+ risk function, also the same as used in the 2011 NCAP, was calculated as follows:

For the 5th percentile dummy $$P_{chest\_defl}(AIS3+) = \frac{1}{1+e^{10.5456-1.7212*(ChestDefl)^{0.4612}}}$$

For the 50th percentile dummy $$P_{chest\_defl}(AIS3+) = \frac{1}{1+e^{10.5456-1.568*(ChestDefl)^{0.4612}}}$$

Last, the femur AIS 3+ risk curve was the same as used in the FMVSS No. 208 Advanced Air Bags Rule (Kuppa et al., 2001; NHTSA, 2006) and was calculated as follows:

For the 5th percentile dummy $$P_{femur}(AIS3+) = \frac{1}{1+e^{\left(4.9795-0.47941\frac{FemurMax}{1000}\right)}} - \frac{1}{1+e^{4.9795}}$$

For the 50th percentile dummy $$P_{femur}(AIS3+) = \frac{1}{1+e^{\left(4.9795-0.326\frac{FemurMax}{1000}\right)}} - \frac{1}{1+e^{4.9795}}$$

3.7.2 Combined Injury Risks Functions

Three Combined Injury Risks, CIR I, CIR II, and CIR IIP were computed for each single- and two-vehicle crash simulation for both target and partner vehicle occupants as demonstrated in Figure 3-32. The three combined injury risks are defined as follows.

- CIR I: injury risk of AIS3+ injury to the head, or neck, or chest, or KTH body regions
- CIR II: injury risk of AIS3+ injury to the head, or neck, or chest
- CIR IIP: injury risk of AIS3+ injury to the head, or neck, or chest with a penalty based on maximum dynamic intrusion at the mid A-pillar

As in the 2011 NCAP, the combined injury risk functions assume that the probabilities of injury to the different body regions are independent. However, in this study the AIS3+ injury risks were combined for the head, neck, chest, and femur while in NCAP, the AIS3+ injury risks for head, neck, and chest were combined with AIS2+ injury risk for the KTH region. In this study, combining AIS3+ injury risk for all the body regions was done to ensure consistency relative to threat to life of the predicted injury risks. The actual formulas for the individual and combined injury risk CIR I and CIR II functions used for the 50th percentile male driver occupant are shown in

the last two rows of the example shown in Table 3-19. The formulas for the combined injury risk functions for the 5th percentile female driver are the same.

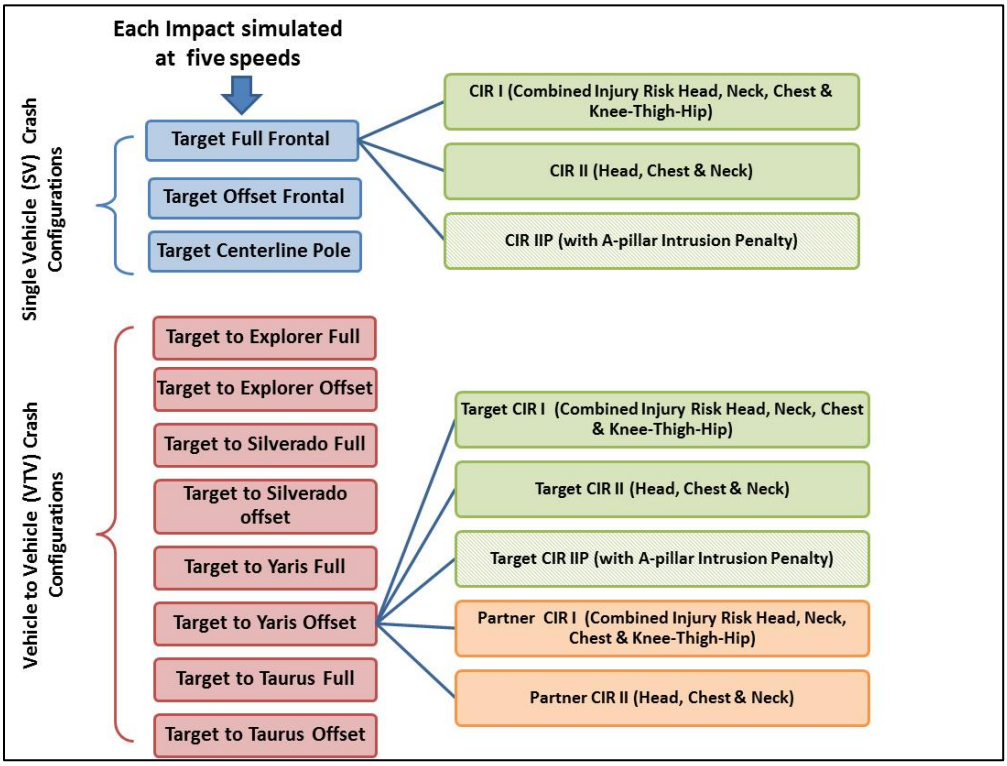

Figure 3-32. Injury Risk Computation for Every Modeled Crash Simulation

3.7.2.1 Motivation for Computing Three Combined Injury Risks

3.7.2.1.1 CIR I

CIR I was computed to address the four main body regions injured in frontal crashes.

3.7.2.1.2 CIR II

After examining the predicted risks from CIR I, it became obvious that, in certain cases, the injury risks predicted from the femur loads dominated the combined injury risk. Also, some simulations involving high toe-board intrusions showed low femur loads because the knee was driven up and knee-to-bolster interaction did not result in transmission of axial forces through the femur. It became evident that an injury risk based only on axial femur loads, such as the current KTH injury risk, is sensitive to geometry and is not as effective in predicting the safety response of a vehicle class. As such, CIR II, which excludes the KTH injury risk based on femur loads, was also computed and analyzed. In the future implementation of EFP, it would be useful to assess KTH injury risk functions that take into account femur moments.

An example of an impact with upward rotation of the knee that resulted in lower recorded femur axial loads in spite of higher intrusions is shown in Figure 3-33. This situation occurred in the vehicle-to-vehicle full

engagement of the Taurus Baseline into LW4 at 35 mph. The corresponding femur loads and dynamic intrusions are shown in Table 3-20.

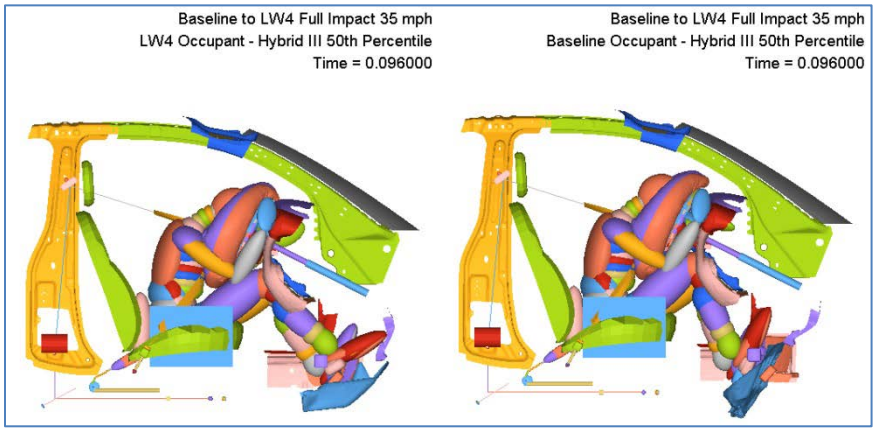

Figure 3-33. Example of Upward Knee Rotation Driven by High Intrusion in Taurus Baseline Occupant (right) as Compared With LW4 Occupant (left)

Table 3-20. Toe Pan Intrusions and Femur Loads for Example Impacts With Upward Knee Rotation

Impact Speed (mph)	Max Toe Pan Intrusion (mm)		Max Femur Load (N)	
Full Engagement VTV	Taurus Baseline	LW4	Taurus Baseline	LW4
30	160	38	4447	6562
35	264	51	4893	8598

3.7.2.1.3 CIR IIP

High magnitudes of dynamic intrusion of the A-pillar relative to the B-pillar were observed in some of the FE vehicle structural simulations, specifically in vehicle-to-vehicle crashes with a smaller vehicle crashing into a larger vehicle. In the current implementation of the occupant environment, toe-board intrusions are modeled as prescribed structural motions in MADYMO; however A-pillar intrusions are not fully modeled. Dynamic A-pillar intrusions are important in estimating injury risks for the following reasons.

- Most modern vehicles have a cross-car beam attaching the right A-pillar to the left A-pillar. Generally, the steering column is attached to the cross-car beam. If the A-pillar moves, the column will also move towards the occupant closing the gap between the occupant and the steering wheel. FMVSS No. 204 specifies requirements limiting the rearward displacement of the steering control into the passenger compartment to reduce the likelihood of chest, neck, or head injury (limit of 127 mm of rearward movement in a 30 mph perpendicular impact into a fixed barrier.) Also, the steering column rearward movement affects the effectiveness of the air bag system by reducing steering column collapse. Most vehicles rely on a combination of the air bag and steering column collapse to control head and chest loadings.

- Another important aspect of A-pillar intrusion is door openability after crash. Generally, lack of door openability after crash also increases extrication times.
- A third important aspect of A-pillar intrusion is the reduction of survival distance for the driver.

As such, CIR IIP, which combines the injury risk to the head, or neck, or chest, and includes a penalty function for A-Pillar intrusion was also computed and analyzed. The penalty function associated with A-pillar intrusions has been adopted based on the 127 mm limit in FMVSS No. 204 on the rearward displacement of the steering control. The following penalty functions were selected for the A-pillar to B-pillar intrusion, based on the above practical considerations:

- If increment is ≥ 127 mm, double the calculated risk of head and chest, since injury risk is expected to increase substantially upon rearward motion of the steering control exceeding this limit.
- If increment is ≥ 254 mm, risk of head and chest is 100 percent, as the occupant survival space becomes highly compromised.
- If 0<increment<127mm, use linear interpolation to assign risk.

In the future the occupant simulation capabilities could be expanded to incorporate dynamic A-pillar intrusions.

3.7.3 Combined Injury Risk Example for Target and Partner Vehicles

An example of computed combined injury risks (CIR I, and CIR II) for the two occupant sizes for one of the target vehicles is shown in Table 3-21 for the single-vehicle crash simulations and in Table 3-22 for the two-vehicle crash simulations. The combined injury risk functions were also computed for the occupants of the four partner vehicles in the two-vehicle crashes, generating tables similar to Table 3-22 for the partner vehicle occupants.

Table 3-21. Example of Computed CIR I and CIR II for the Occupants of a Target Vehicle in the Single-Vehicle Crash Simulations

Crash Configuration	Speed (mph)	HIII 50th %ile Dummy						HIII 5th %ile Dummy					
		HIC15 Risk (%)	Chest Deflection (%)	Femur Max (%)	Neck Tension (T)(%)	Combined Injury Risk (%)	Combined Injury Risk II (No Femur) (%)	HIC15 Risk (%)	Chest Deflection (%)	Femur Max (%)	Neck Tension (T)(%)	Combined Injury Risk (%)	Combined Injury Risk II (No Femur) (%)
Full Frontal	15	0.0%	1.8%	0.5%	0.0%	**2.3%**	**1.8%**	0.1%	3.8%	0.9%	0.3%	**5.1%**	**4.2%**
	20	0.0%	2.3%	0.8%	0.0%	**3.1%**	**2.3%**	0.1%	4.3%	1.1%	0.3%	**5.8%**	**4.8%**
	25	0.0%	2.6%	1.2%	0.0%	**3.8%**	**2.6%**	0.1%	4.3%	1.3%	0.4%	**6.0%**	**4.8%**
	30	0.0%	2.9%	1.9%	0.0%	**4.8%**	**3.0%**	0.1%	5.0%	1.4%	0.4%	**6.8%**	**5.5%**
	35	0.1%	2.9%	3.0%	0.0%	**6.0%**	**3.1%**	0.1%	5.7%	1.6%	0.4%	**7.6%**	**6.1%**
Offest Frontal	20	0.0%	1.0%	0.1%	0.0%	**1.1%**	**1.0%**	0.0%	2.4%	1.1%	0.3%	**3.8%**	**2.8%**
	25	0.0%	1.3%	0.1%	0.0%	**1.4%**	**1.3%**	0.0%	2.8%	1.2%	0.4%	**4.4%**	**3.3%**
	30	0.0%	1.5%	0.2%	0.0%	**1.7%**	**1.5%**	0.1%	3.8%	1.2%	0.5%	**5.5%**	**4.3%**
	35	0.0%	2.0%	0.4%	0.0%	**2.4%**	**2.0%**	0.1%	3.8%	1.2%	0.5%	**5.4%**	**4.3%**
	40	0.0%	2.3%	0.4%	0.0%	**2.7%**	**2.3%**	0.1%	3.8%	1.2%	0.3%	**5.3%**	**4.2%**
Center Pole	15	0.0%	0.7%	0.1%	0.0%	**0.8%**	**0.7%**	0.0%	1.8%	0.6%	0.3%	**2.7%**	**2.1%**
	20	0.0%	1.2%	0.2%	0.0%	**1.3%**	**1.2%**	0.1%	2.4%	0.7%	0.4%	**3.5%**	**2.8%**
	25	0.0%	2.0%	0.3%	0.0%	**2.4%**	**2.0%**	0.1%	3.3%	0.8%	0.7%	**4.8%**	**4.0%**
	30	0.0%	3.3%	0.6%	0.0%	**3.9%**	**3.3%**	0.2%	5.0%	1.2%	0.8%	**7.0%**	**5.9%**
	35	0.3%	3.7%	1.4%	0.0%	**5.3%**	**4.0%**	0.2%	5.7%	1.5%	0.5%	**7.7%**	**6.3%**

Table 3-22. Example of Computed CIR I and CIR II for the Occupants of a Target Vehicle in Two-Vehicle Crash Simulations

Crash Configuration	Speed (mph)	HIII 50th %ile Dummy						HIII 5th %ile Dummy					
		HIC15 Risk (%)	Chest Deflection (%)	Femur Max (%)	Neck Tension (T)(%)	Combined Injury Risk (%)	Combined Injury Risk II (No Femur) (%)	HIC15 Risk (%)	Chest Deflection (%)	Femur Max (%)	Neck Tension (T)(%)	Combined Injury Risk (%)	Combined Injury Risk II (No Femur) (%)
Explorer Full	15	0.0%	1.8%	0.5%	0.0%	**2.2%**	**1.8%**	0.1%	3.8%	1.0%	0.4%	**5.2%**	**4.2%**
	20	0.0%	2.6%	0.8%	0.0%	**3.4%**	**2.6%**	0.1%	4.3%	1.1%	0.5%	**5.9%**	**4.9%**
	25	0.0%	2.9%	2.5%	0.0%	**5.4%**	**3.0%**	0.2%	5.7%	1.1%	0.7%	**7.6%**	**6.6%**
	30	0.2%	3.3%	4.0%	0.1%	**7.4%**	**3.5%**	0.2%	6.4%	1.7%	0.3%	**8.5%**	**6.9%**
	35	0.7%	3.3%	3.1%	0.1%	**7.1%**	**4.1%**	0.2%	7.3%	2.2%	0.5%	**9.9%**	**7.9%**
Explorer Offset	15	0.0%	1.3%	0.1%	0.0%	**1.4%**	**1.3%**	0.1%	2.8%	1.2%	0.4%	**4.5%**	**3.3%**
	20	0.0%	1.8%	0.2%	0.0%	**1.9%**	**1.8%**	0.1%	4.3%	1.2%	0.8%	**6.3%**	**5.2%**
	25	0.0%	2.3%	0.7%	0.0%	**3.0%**	**2.3%**	0.2%	5.7%	1.4%	1.7%	**8.7%**	**7.5%**
	30	0.0%	3.3%	1.1%	0.1%	**4.5%**	**3.4%**	0.2%	6.4%	1.1%	1.0%	**8.5%**	**7.5%**
	35	0.6%	3.7%	1.8%	0.1%	**6.1%**	**4.4%**	0.3%	7.3%	0.9%	1.1%	**9.4%**	**8.5%**
Silverado Full	15	0.0%	1.5%	0.4%	0.0%	**1.9%**	**1.5%**	0.1%	3.3%	1.1%	0.4%	**4.8%**	**3.8%**
	20	0.0%	2.6%	1.2%	0.0%	**3.7%**	**2.6%**	0.1%	4.3%	1.0%	0.4%	**5.8%**	**4.8%**
	25	0.0%	2.9%	3.0%	0.0%	**5.9%**	**3.0%**	0.1%	5.7%	1.3%	0.4%	**7.4%**	**6.2%**
	30	0.1%	3.3%	6.9%	0.0%	**10.1%**	**3.4%**	0.2%	6.4%	1.7%	0.4%	**8.6%**	**7.0%**
	35	0.3%	3.3%	10.5%	0.1%	**13.7%**	**3.6%**	0.2%	6.4%	2.6%	0.3%	**9.3%**	**6.9%**
Silverado Offset	15	0.0%	1.5%	0.1%	0.0%	**1.6%**	**1.5%**	0.1%	3.3%	1.2%	0.7%	**5.2%**	**4.1%**
	20	0.0%	2.3%	0.3%	0.0%	**2.6%**	**2.3%**	0.1%	5.0%	1.2%	1.0%	**7.2%**	**6.0%**
	25	0.0%	2.3%	0.5%	0.0%	**2.8%**	**2.3%**	0.1%	5.7%	1.4%	1.1%	**8.1%**	**6.9%**
	30	0.0%	2.9%	0.8%	0.0%	**3.8%**	**3.0%**	0.2%	6.4%	1.1%	1.2%	**8.8%**	**7.8%**
	35	0.1%	3.3%	1.3%	0.1%	**4.7%**	**3.4%**	0.3%	7.3%	1.1%	1.4%	**9.8%**	**8.8%**
Yaris Full	15	0.0%	1.3%	0.3%	0.0%	**1.6%**	**1.3%**	0.1%	3.3%	1.1%	0.4%	**4.8%**	**3.7%**
	20	0.0%	2.0%	0.6%	0.0%	**2.6%**	**2.0%**	0.1%	3.8%	1.0%	0.3%	**5.1%**	**4.1%**
	25	0.0%	2.6%	1.5%	0.0%	**4.1%**	**2.6%**	0.1%	5.0%	1.1%	0.4%	**6.5%**	**5.4%**
	30	0.0%	2.6%	2.0%	0.0%	**4.6%**	**2.7%**	0.1%	5.0%	1.4%	0.3%	**6.7%**	**5.3%**
	35	0.1%	3.3%	3.5%	0.0%	**6.8%**	**3.4%**	0.2%	5.7%	1.5%	0.5%	**7.7%**	**6.3%**
Yaris Offset	15	0.0%	0.3%	0.1%	0.0%	**0.4%**	**0.3%**	0.0%	0.9%	0.8%	0.2%	**1.9%**	**1.1%**
	20	0.0%	0.6%	0.1%	0.0%	**0.7%**	**0.6%**	0.0%	1.8%	0.9%	0.3%	**3.0%**	**2.1%**
	25	0.0%	1.5%	0.1%	0.0%	**1.6%**	**1.5%**	0.1%	3.3%	1.1%	0.6%	**5.0%**	**3.9%**
	30	0.0%	1.8%	0.3%	0.0%	**2.1%**	**1.8%**	0.1%	3.8%	1.3%	0.5%	**5.5%**	**4.3%**
	35	0.1%	2.3%	0.6%	0.0%	**2.9%**	**2.4%**	0.1%	5.0%	1.3%	0.9%	**7.2%**	**6.0%**
Taurus Full	15	0.0%	1.3%	0.3%	0.0%	**1.6%**	**1.3%**	0.1%	2.8%	1.1%	0.3%	**4.2%**	**3.2%**
	20	0.0%	2.0%	0.6%	0.0%	**2.6%**	**2.0%**	0.1%	3.8%	1.0%	0.4%	**5.3%**	**4.3%**
	25	0.0%	2.3%	1.0%	0.0%	**3.3%**	**2.3%**	0.1%	4.3%	1.2%	0.3%	**5.9%**	**4.8%**
	30	0.0%	2.9%	2.1%	0.0%	**5.0%**	**3.0%**	0.1%	5.0%	1.4%	0.4%	**6.8%**	**5.5%**
	35	0.1%	2.9%	2.8%	0.0%	**5.8%**	**3.0%**	0.1%	5.0%	1.6%	0.3%	**6.9%**	**5.4%**
Taurus Offset	15	0.0%	0.9%	0.1%	0.0%	**0.9%**	**0.9%**	0.0%	2.1%	1.2%	0.4%	**3.7%**	**2.5%**
	20	0.0%	1.2%	0.1%	0.0%	**1.2%**	**1.2%**	0.0%	2.8%	1.2%	0.5%	**4.6%**	**3.4%**
	25	0.0%	1.8%	0.1%	0.0%	**1.9%**	**1.8%**	0.1%	3.3%	1.2%	0.5%	**5.0%**	**3.8%**
	30	0.0%	2.3%	0.5%	0.0%	**2.8%**	**2.3%**	0.1%	3.8%	1.3%	0.3%	**5.4%**	**4.2%**
	35	0.2%	2.9%	0.8%	0.1%	**4.0%**	**3.1%**	0.1%	5.0%	1.2%	0.6%	**6.8%**	**5.6%**

3.7.4 Societal Injury Risk for a Target Vehicle

The societal injury risk for each target vehicle was computed at each speed for each crash configuration for each of the two occupant sizes, based upon the risk of sustaining a serious (MAIS 3+) injury or a fatality, referred to as the MAIS 3+F risk, for belted drivers of age group 16 to 50 years old. The societal injury risk for the target

vehicle is the injury risk of the occupant of the target vehicle in the single-vehicle crash simulation plus the sum of the injury risks for the occupants of both the target vehicle and the given partner vehicle in the two-vehicle crash simulations. This is illustrated in Figure 3-34. Three societal injury risks were computed at each crash simulation for each occupant, societal injury risk I, societal injury risk II, and societal injury risk IIP, corresponding to the three combined injury risks for each occupant, CIR I, CIR II, and CIR IIP. Detailed equations for computation of societal injury risks are provided in the next section. It is worth noting that a small injury risk of AIS3+ is expected in impact speeds <12 mph, as such there were no simulations conducted at these lower speeds; thus the equations for Combined AIS3+ Risk below do not have a corresponding term for this low speed exposure.

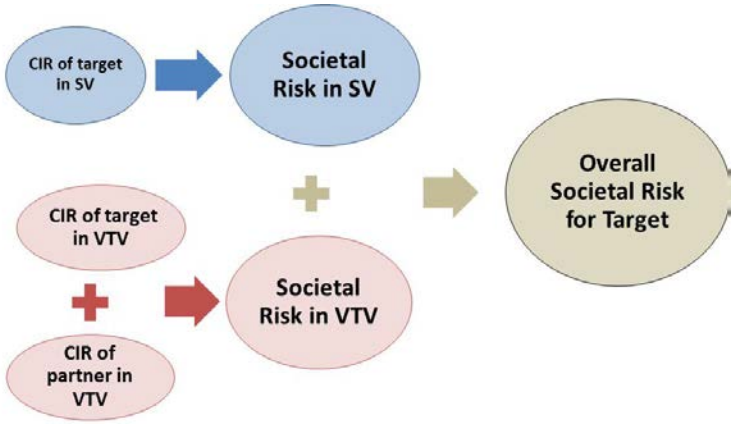

Figure 3-34. Overview of Societal Injury Risk Computation in a Given Impact

3.7.4.1 Equations for Societal Injury Risk Computation

In the equations below, "Exposure Rate" denotes crash involvement frequency and "Weighting Factor" denotes percent of occurrence. A 0.75/0.25 split between mid-sized males and small statured females was implemented based on earlier research (Laituri et al., 2003).

Societal injury risk = $\text{Injury Risk}|_{\text{1V- target vehicle}} + \text{Injury Risk}|_{\text{v2v -target and partner vehicle}}$ **Equation (1)**

where $\text{Injury Risk}|_{\text{1V- target vehicle}}$ is defined in Equation (2) and $\text{Injury Risk}|_{\text{v2v -target and partner vehicle}}$ is defined in equation (3)

Injury Risk$|_{\text{1V- target vehicles}}$ **Equation (2)**

$= \text{Weighting Factor}|_{\text{50th Male}} \times \text{Injury Risk}|_{\text{target vehicle, 50th Male}}$

$+ \text{Weighting Factor}|_{\text{5th Female}} \times \text{Injury Risk}|_{\text{target vehicle, 5th female}}$

$= 0.75 \times \text{Injury Risk}|_{\text{target vehicle, 50th Male}} + 0.25 \times \text{Injury Risk}|_{\text{target vehicle, 5th female}}$

where

Injury Risk$|_{\text{target vehicle, gender (50th Male or 5th Female)}}$

= Exposure Rate for Full Frontal|$_{\text{single vehicle}}$ x Combined AIS3+ Risk for Full Frontal|$_{\text{target vehicle, gender}}$

+ Exposure Rate for Offset Frontal|$_{\text{single vehicle}}$ x Combined AIS3+ Risk for Offset Frontal|$_{\text{target vehicle, gender}}$

+ Exposure Rate for Center Pole|$_{\text{single vehicle}}$ x Combined AIS3+ Risk for Center Pole|$_{\text{target vehicle, gender}}$

Combined AIS3+ Risk|$_{\text{target vehicle, gender, configuration (full frontal, offset frontal or center pole)}}$

= Combined Injury Risk|$_{\text{target vehicle, gender, configuration, 15mph}}$ x Exposure Rate |$_{\text{12-17mph}}$

+ Combined Injury Risk|$_{\text{target vehicle, gender, configuration, 20mph}}$ x Exposure Rate |$_{\text{17-22mph}}$

+ Combined Injury Risk|$_{\text{target vehicle, gender, configuration, 25mph}}$ x Exposure Rate |$_{\text{22-27mph}}$

+ Combined Injury Risk|$_{\text{target vehicle, gender, configuration, 30mph}}$ x Exposure Rate |$_{\text{27-32mph}}$

+ Combined Injury Risk|$_{\text{target vehicle, gender, configuration, 35mph}}$ x Exposure Rate |$_{\text{>=32mph}}$

Where

Combined Injury Risk|$_{\text{target vehicle, gender, configuration, Speed (15mph, 20mph, 25mph, 30mph or 35mph)}}$

= 1 – (1 - Injury Risk|$_{\text{target vehicle, gender, configuration, Speed, HIC15}}$)

* (1- Injury Risk|$_{\text{target vehicle, gender, configuration, Speed, Chest}}$)

* (1 - Injury Risk|$_{\text{target vehicle, gender, configuration, Speed, Femur}}$)

* (1- Injury Risk|$_{\text{target vehicle, gender, configuration, Speed, neck}}$)

Injury Risk|$_{\text{v2v -target and partner vehicle}}$ **Equation (3)**

= Weighting Factor|$_{\text{50th Male}}$ x Injury Risk|$_{\text{v2v, 50th Male}}$

+ Weighting Factor|$_{\text{5th Female}}$ x Injury Risk |$_{\text{v2v, 5th female}}$

= 0.75 x Injury Risk|$_{\text{v2v, 50th Male}}$ + 0.25 x Injury Risk |$_{\text{v2v, 5th female}}$

Injury Risk|$_{\text{v2v, gender (50th Male or 5th Female)}}$

= Exposure Rate for Full Frontal, SUV |$_{\text{v2v}}$ x Combined AIS3+ Risk for Full Frontal With SUV|$_{\text{target vehicle, gender}}$

+ Exposure Rate for Offset Frontal, SUV|$_{\text{v2v}}$ x Combined AIS3+ Risk for Offset Frontal With SUV|$_{\text{target vehicle, gender}}$

+ Exposure Rate for Full Frontal, Pickup |$_{\text{v2v}}$ x Combined AIS3+ Risk for Full Frontal With Pickup|$_{\text{target vehicle, gender}}$

+ Exposure Rate for Offset Frontal, Pickup| $_{v2v}$ x Combined AIS3+ Risk for Offset Frontal With Pickup| $_{\text{target vehicle, gender}}$

+ Exposure Rate for Full Frontal, Small PC | $_{v2v}$ x Combined AIS3+ Risk for Full Frontal With Small PC | $_{\text{target vehicle, gender}}$

+ Exposure Rate for Offset Frontal, Small PC| $_{v2v}$ x Combined AIS3+ Risk for Offset Frontal With Small PC | $_{\text{target vehicle, gender}}$

+ Exposure Rate for Full Frontal, Mid-Large PC | $_{v2v}$ x Combined AIS3+ Risk for Full Frontal With Mid-Large PC | $_{\text{target vehicle, gender}}$

+ Exposure Rate for Offset Frontal, Mid-Large PC | $_{v2v}$ x Combined AIS3+ Risk for Offset Frontal With Mid-Large PC | $_{\text{target vehicle, gender}}$

Combined AIS3+ Risk| $_{\text{target vehicle, gender, configuration (full frontal, offset frontal or center pole), partner vehicle (SUV, Pickup, small PC, mid-large PC)}}$

= Combined Injury Risk| $_{\text{target vehicle, gender, configuration, partner vehicle, 15mph}}$ x Exposure Rate |$_{\text{configuration, 12-17mph}}$

+ Combined Injury Risk| $_{\text{target vehicle, gender, configuration, partner vehicle, 20mph}}$ x Exposure Rate | $_{\text{configuration, 17-22mph}}$

+ Combined Injury Risk| $_{\text{target vehicle, gender, configuration, partner vehicle, 25mph}}$ x Exposure Rate | $_{\text{configuration, 22-27mph}}$

+ Combined Injury Risk| $_{\text{target vehicle, gender, configuration, partner vehicle, 30mph}}$ x Exposure Rate | $_{\text{configuration, 27-32mph}}$

+ Combined Injury Risk| $_{\text{target vehicle, gender, configuration, partner vehicle, 35mph}}$ x Exposure Rate | $_{\text{configuration, >=32mph}}$

Combined Injury Risk| $_{\text{target vehicle, gender, configuration, partner vehicle, Speed (15mph, 20mph, 25mph, 30mph or 35mph)}}$

= Target Vehicle Combined Injury Risk| $_{\text{target vehicle, gender, configuration, partner vehicle, Speed}}$

+ Partner Vehicle Combined Injury Risk| $_{\text{target vehicle, gender, configuration, partner vehicle, Speed}}$

Target or Partner Combined Injury Risk| $_{\text{target vehicle, gender, configuration, partner vehicle, Speed}}$

= 1 – (1 - Target or Partner Injury Risk| $_{\text{target vehicle, gender, configuration, partner, Speed, HIC15}}$)

* (1- Target or Partner Injury Risk| $_{\text{target vehicle, gender, configuration, partner, Speed, Chest}}$)

* (1 - Target or Partner Injury Risk| $_{\text{target vehicle, gender, configuration, partner, Speed, Femur}}$)

* (1- Target or Partner Injury Risk| $_{\text{target vehicle, gender, configuration, partner, Speed, neck}}$)

An example of computed societal injury risk in a two-vehicle crash is shown for three of the target vehicles in Table 3-23. In each cell, the risk is the sum of occupant risk in both the target (i.e., Taurus Baseline or LW3 or LW4) and the occupant risk in the partner vehicle (i.e., Explorer). The societal injury risk data for single- and two-vehicle crashes for the eight target vehicles (baseline and modified) are tabulated in Appendix 20.

Table 3-23. Example of Societal Injury Risk I in Target-to-Explorer Full and Offset Frontal Crash Simulations

		Taurus Baseline		LW3		LW4	
Crash Configuration	Speed (mph)	Taurus BL- 50th %ile Male	Taurus BL- 5th %ile Female	LW3- 50th %ile Male	LW3- 5th %ile Female	LW4- 50th %ile Male	LW4- 5th %ile Female
		Societal Risk (%)	Societal Risk (%)	Societal Risk (%)	Societal Risk (%)	Societal Risk (%)	Societal Risk (%)
Explorer Full	15	5.0%	9.1%	5.4%	10.1%	6.1%	8.3%
	20	8.4%	10.5%	8.2%	11.2%	10.1%	10.2%
	25	11.0%	13.0%	14.0%	14.2%	13.9%	14.2%
	30	13.6%	16.1%	16.3%	19.9%	32.2%	16.7%
	35	14.8%	18.5%	17.2%	22.6%	43.0%	21.0%
Explorer Offset	15	2.8%	8.3%	2.0%	7.0%	2.3%	6.0%
	20	3.6%	10.3%	4.1%	10.7%	5.6%	10.5%
	25	5.5%	12.8%	5.6%	12.8%	8.2%	11.7%
	30	9.0%	12.6%	8.4%	15.0%	12.0%	15.6%
	35	11.9%	15.2%	15.8%	15.9%	30.4%	18.9%

3.8 Fleet Injury Risk Calculation

To estimate the overall fleet societal injury risk, each individual risk was given a weight based on relative occurrence of the crash configuration and impact speeds in the real-world. The weights were derived from the NASS CDS data analysis. The total fleet societal injury risk for a given target was computed as the weighted sum, or accumulated, injury risks for single- and two-vehicle crashes across the simulated impact speeds and crash configurations.

3.8.1 NASS CDS Crash Configuration Weighting Factors

The distribution of crash configurations in single- and two-vehicle real-world frontal crashes, established in Section 3.2, is presented again in Table 3-24 for reference. As the study simulation matrix included only the 50 percent offset and full engagement frontal crash configurations, the 3.9 percent of the two-vehicle real-world crashes categorized as “Between Rail” configuration would be better represented with a centerline pole crash simulation. The localized deformation of the vehicle-to-pole test is representative of between rail structural engagements in frontal crashes. As such, this 3.9 percent portion “Between Rail” of two-vehicle crashes was folded into the “Between Rail” segment of the single-vehicle crashes. The revised distributions for single- and two-vehicle crashes are shown in Table 3-25 and in Table 3-26. They present the weighting factors used for the crash configuration simulated in this study.

Table 3-24. Frontal Crash Involvement: Single- and Two-Vehicle Crash Configurations: Air-Bag-Equipped Fleet Vehicles, MY 1985+ (weighted), 1998-2010 NASS CDS

						of Total	
Frontal Taxonomy	All Crashes	Single Vehicle	Two Vehicle	Single Vehicle	Two Vehicle	Single Vehicle	Two Vehicle
Between Rail	202010	97579	**104431**	**19%**	**5%**	**3.6%**	**3.9%**
FullEng	1243912	195458	**1048454**	**38%**	**48%**	**7.2%**	**38.7%**
Offset	968395	138660	**829735**	**27%**	**38%**	**5.1%**	**30.7%**
Other(Front)	143552	48420	95132	9%	4%	**1.8%**	**3.5%**
Sml Offset F&S	148376	30544	117833	6%	5%	**1.1%**	**4.4%**
Total	2706246	510661	2195584	100%	100%	**19%**	**81%**

Table 3-25. Frontal Crash Involvement: Single- and Two-Vehicle Crash Configurations: Air-Bag-Equipped Fleet Vehicles, MY 1985+ (weighted), 1998-2010 NASS CDS

With Between Rail folded into Single Vehicle						of Total	
Frontal Taxonomy	All Crashes	Single Vehicle	Two Vehicle	Single Vehicle	Two Vehicle	Single Vehicle	Two Vehicle
Between Rail	202010	202010	**0**	**40%**	**0%**	**7.5%**	**0.0%**
FullEng	1243912	195458	**1048454**	**38%**	**48%**	**7.2%**	**38.7%**
Offset	968395	138660	**829735**	**27%**	**38%**	**5.1%**	**30.7%**
Other(Front)	143552	48420	95132	9%	4%	**1.8%**	**3.5%**
Sml Offset F&S	148376	30544	117833	6%	5%	**1.1%**	**4.4%**
Total	2706246	510661	2195584	100%	100%	**23%**	**77%**

Table 3-26. Frontal Crash Population for Simulation
Air-Bag-Equipped Fleet Vehicles, MY 1985+ (weighted), 1998-2010 NASS CDS

Frontal Taxonomy	Single Vehicle	Two Vehicle
Between Rail	**7.5%**	**0.0%**
FullEng	**7.2%**	**38.7%**
Offset	**5.1%**	**30.7%**
Total	**20%**	**69%**
*Not Modeled	11%	

3.8.2 NASS CDS Impact Speed Weighting Factors

The weighting factors for each of the simulated frontal configurations at different impact speeds were established by grouping distributions of BES for crash involved passenger car that were the target vehicles in this study (see following Figures and Tables). All the target vehicles in this study were passenger cars. The physical weights of the target vehicles are presented in Table 3-27. The Taurus Baseline, LW4, Venza Baseline, Venza Low Option, and Accord Baseline vehicles fall into the category of passenger cars >3,000 lbs. The LW3, Venza High Option, and Accord Light Weight vehicles fall into the category of passenger cars <3,000 lbs.

Table 3-27. Target Vehicle Weights

	Taurus			Venza			Accord	
	Baseline	LW3	LW4	Baseline	Low Option	High Option	Baseline	Light Weight
weight (kg)	1515	1138	1515	1806	1503	1151	1670	1345
weight (lb)	3339	**2508**	3339	3980	3313	**2537**	3681	**2964**

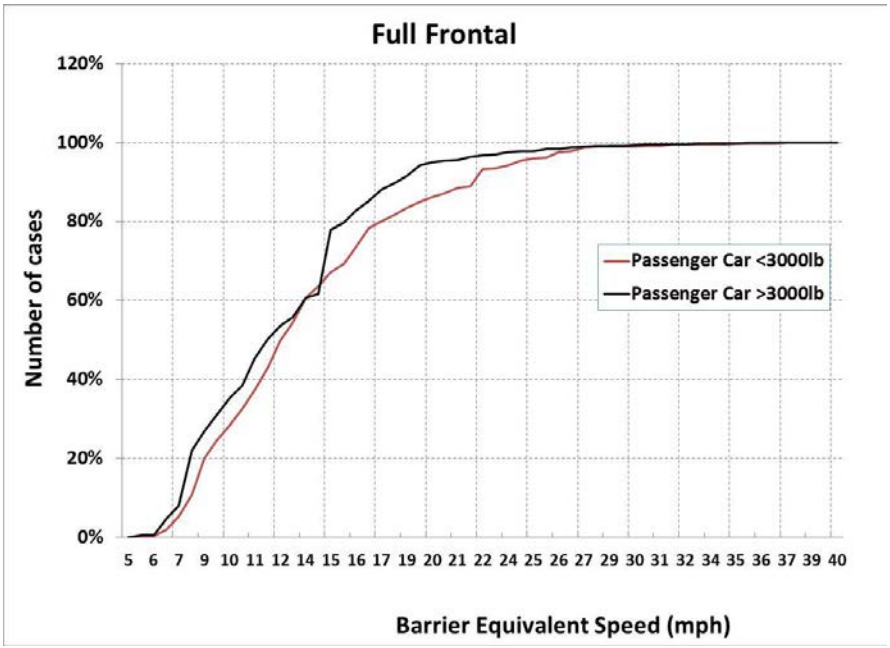

Figure 3-35. Cumulative Distribution of Full Frontal Crashes over BES

Table 3-28. Weighting Factors for Full Frontal Crash Configuration Across BES

Full Frontal				
BARRIER EQUIVALENT SPEED mph	Passenger Car >3000lb	Passenger Car <3000lb	Pickup	SUV
0-11	50%	43%	38%	40%
12-17	35%	35%	41%	42%
17-22	11%	11%	16%	10%
22-27	2%	9%	2%	5%
27-32	1%	2%	2%	3%
≥32	0%	0%	1%	0%
Total	100%	100%	100%	100%

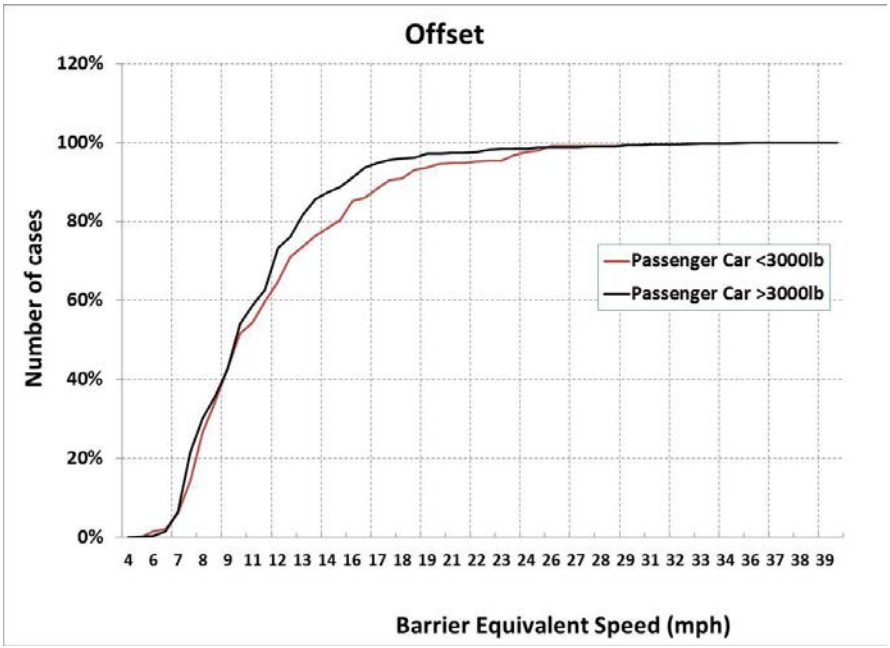

Figure 3-36. Cumulative Distribution of Offset Frontal Crashes over BES

Table 3-29. Weighting Factors for Offset Frontal Crash Configuration Across BES

Offset				
BARRIER EQUIVALENT SPEED mph	Passenger Car >3000lb	Passenger Car <3000lb	Pickup	SUV
0-11	73%	65%	45%	68%
12-17	22%	23%	43%	23%
17-22	3%	7%	6%	5%
22-27	1%	4%	2%	5%
27-32	1%	1%	3%	0%
≥32	0%	0%	2%	0%
Total	100%	100%	100%	100%

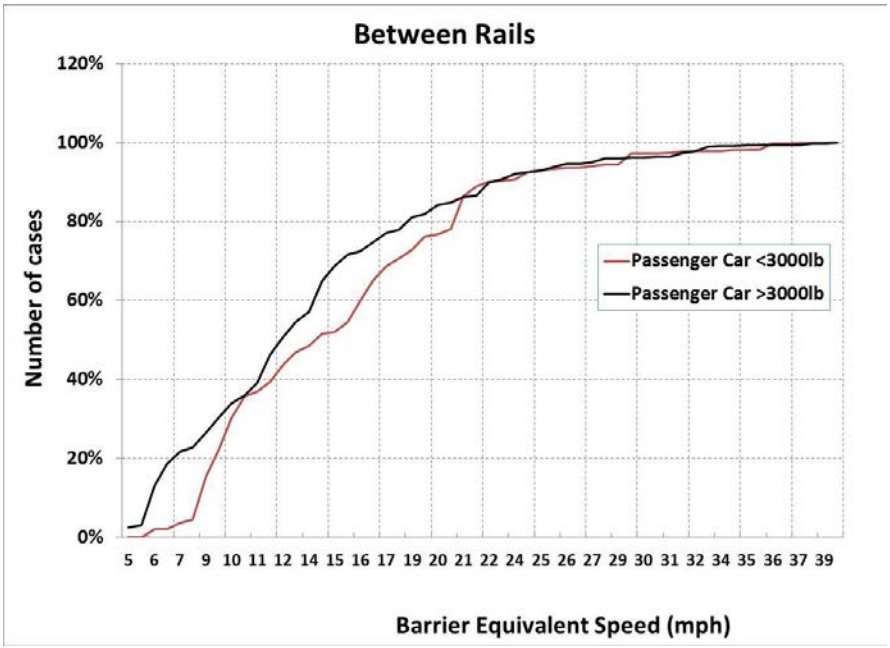

Figure 3-37. Cumulative Distribution of Between Rail Frontal Crashes over BES

Table 3-30. Weighting Factors for Between Frontal Crash Configuration Across BES

Between Rails				
BARRIER EQUIVALENT SPEED mph	Passenger Car >3000lb	Passenger Car <3000lb	Pickup	SUV
0-11	39%	37%	43%	31%
12-17	33%	23%	31%	34%
17-22	14%	26%	4%	21%
22-27	9%	7%	20%	8%
27-32	3%	4%	0%	6%
≥32	3%	2%	2%	0%
Total	100%	100%	100%	100%

3.8.3 Application of Weighting Factors for Fleet Injury Risk Calculation

For both single- and two-vehicle crash simulations, the initial weighting applied is for each crash configuration by BES, i.e., using the factors in Table 3-28, Table 3-29, and Table 3-30, for each occupant size. Example results for single-vehicle crashes are shown in Table 3-36, i.e., the entry in the cell with column title "Center Pole 50th Male" and row "Accord BL" is the sum of injury risk for the 50th male Accord BL in a centerline pole configuration at various vehicle speed weighted by the BES weighting factors for "Between Rails" configuration for a passenger car >3,000lbs from Table 3-30. As no simulations were performed at the low speed range of 0-11 mph where low serious injuries occur (around 10%), the corresponding weighting factors were not used in the analysis.

For single-vehicle crash simulations, the second weighting applied is for crash configuration. An example from Table 3-36 is the cell with column title "Total Risk 5th Female" and row "Accord BL," which is the weighted sum of injury risk for the 5th female risk in the three crashes configuration with weighting factors of the crash configuration distribution, normalized to a total of 100 percent and shown in Table 3-31.

For two-vehicle crash simulations, the second weighting applied is for crash configuration factors (shown in Table 3-31), modulated by crash exposure of vehicle class. The applied factors are presented in Table 3-32. The crash exposure by vehicle class for the crash partners for both passenger car <3,000 lbs. and >3,000 lbs. was based on the NHTSA 2010 Traffic Safety Facts (NHTSA, 2012). In this study, only the "Car-to-Car" and "Car-LT" two crashes are simulated, as highlighted in Table 3-33. For the car class, a 50/50 distribution of PCs <3,000 lbs. and PCs >3,000 lbs. and a 50/50 distribution for SUVs and pickups in the light truck (LT) class are assumed, shown in Table 3-34. The normalized weighting factors for crash exposure by vehicle class are shown in Table 3-35. In addition, no bias for frontal crash pairings as compared to other vehicle to vehicle crash modes was assumed, given the availability of crash pairing data in Traffic Safety Facts. These assumptions can be reevaluated in future development of the EFP.

Table 3-31. Crash Configuration Weighting Factors

	NASS/CDS Exposure all		
	Full Engagement	Offset Frontal	Between Rail
Single vehicle	8.10%	5.74%	8.37%
Two Vehicle	43.43%	34.37%	0.00%

Table 3-32. Weighting Factors for Crash Configuration Modulated by Vehicle Class Crash Exposure for Two-Vehicle Crash Simulation

NASS/CDS Exposure (>3000lb)							
SUV Full	SUV offset	Pickup Full	Pickup Offset	Small PC Full	Small PC Offset	Mid-Large PC Full	Mid-Large PC Offset
10.4%	8.2%	10.4%	8.25%	15.1%	11.9%	7.5%	6.0%
NASS/CDS Exposure (<3000lb)							
SUV Full	SUV offset	Pickup Full	Pickup Offset	Small PC Full	Small PC Offset	Mid-Large PC Full	Mid-Large PC Offset
10.4%	8.2%	10.4%	8.25%	7.5%	6.0%	15.1%	11.9%

Table 3-33. Two-Vehicle Crash Exposure (LT=Light Truck, HT=Heavy Truck)

Two Vehicle Crash Distributions Based on 2012 Traffic Safety Facts (DOT 811659)						
Car-to-car	LT-to-LT	HT-to-HT	Car-LT	Car-HT	LT-to-HT	Total
32.66%	16.33%	0.21%	45.22%	3.36%	2.21%	99.99%

Note: HT are heavy trucks with weight more than 10,000 lbs

Table 3-34. Crash Partner Pairings
(LC=Light PC, HC=Heavy PC, LTSUV and LTPU= Light SUV and Light PU)

Crash Partner Pairings in Study Two Vehicle Crash Simulations				
			LC/LTSUV	11.3%
LC/HC	16.3%		LC/LTPU	11.3%
LC/LC	8.2%		HC/LTSUV	11.3%
HC/HC	8.2%		HC/LTPU	11.3%
Total	**32.7%**		**Total**	**45.2%**

Table 3-35. Weighting Factors Applied- Normalized to 100 Percent

Midsize Simulations (>3000lbs) Factors			
HC/LTSUV	HC/LT PU	HC/LC	HC/HC
24.0%	24.0%	34.7%	17.3%
Total	**100.0%**		

Midsize Simulations (>3000lbs)			
HC/LT	HC/HT	HC/LC	HC/HC
11.3%	11.3%	16.3%	8.17%

Midsize Simulations (<3000lbs) Factors			
LC/LTSUV)	LC/LT PU	LC/LC	LC/HC
24.0%	24.0%	17.3%	34.7%
Total	**100.0%**		

Midsize Simulations (<3000lbs)			
LC/LTSUV	LC/LT PU	LC/LC	LC/HC
11.3%	11.3%	8.17%	16.33%

The third and last weighting factor applied for both single- and two-vehicle crashes is the 75 percent versus 25 percent relative distribution of 50th percentile male and 5th percentile female driver occupants (Laituri et al., 2003) to compute the overall or accumulated societal injury risk I in single-vehicle crashes shown in the second column of Table 3-36. An overview schematic of applying the weighting factor in single-vehicle crashes is shown in Figure 3-38. A similar approach is applied for applying weighting factors in two-vehicle crashes.

Table 3-36. Example Accumulated Societal Injury Risk in Single-Vehicle Crashes

Societal Risk I- Target Combined AIS3+ risk of Head, Neck, Chest & Femur										
	Target	Overall Risk in SV	Total Risk 50th male	Total Risk 5th female	Full Frontal 50th male	Full Frontal 5th female	Offset Frontal 50th male	Offset Frontal 5th female	Center Pole 50th male	Center Pole 5th female
Single Vehicle Crashes	Taurus BL	0.15%	0.10%	0.28%	**0.79%**	**1.79%**	**0.23%**	**0.83%**	**0.33%**	**1.11%**
	LW3	0.18%	0.14%	0.31%	**1.14%**	**2.04%**	**0.34%**	**1.03%**	**0.33%**	**0.99%**
	LW4	0.19%	0.17%	0.24%	**1.50%**	**1.66%**	**0.27%**	**0.51%**	**0.46%**	**0.88%**
	Accord BL	0.22%	0.20%	0.25%	**1.35%**	**1.87%**	**0.50%**	**0.59%**	**0.79%**	**0.78%**
	Accord LW	0.25%	0.24%	0.29%	**1.46%**	**1.91%**	**0.72%**	**0.92%**	**0.96%**	**1.00%**
	Venza BL	0.20%	0.12%	0.44%	**0.70%**	**3.12%**	**0.29%**	**0.70%**	**0.58%**	**1.72%**
	Venza Low Option	0.21%	0.14%	0.44%	**0.70%**	**2.79%**	**0.37%**	**1.10%**	**0.72%**	**1.75%**
	Venza High Option	0.22%	0.15%	0.42%	**0.71%**	**2.36%**	**0.62%**	**1.56%**	**0.68%**	**1.70%**

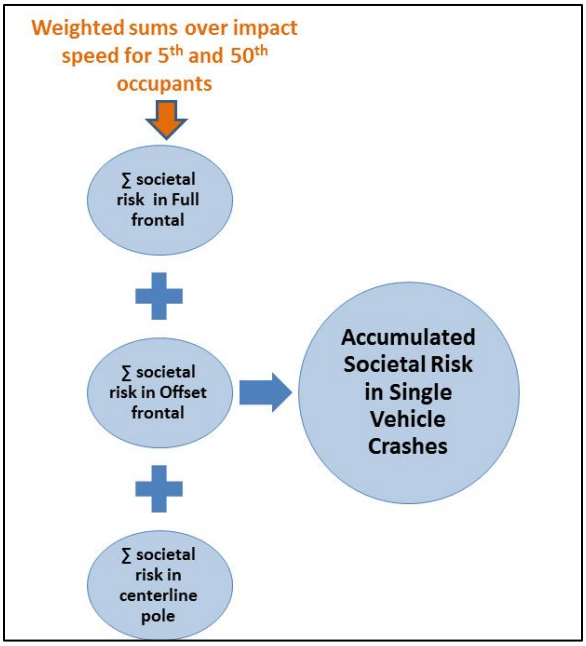

Figure 3-38. How an Individual Injury Risk Is Weighted in Single-Vehicle Crashes

4 RESULTS

4.1 Fleet Societal Injury Risk for Each Target vehicle

The societal injury risks for each target vehicle in this study are presented in Table 4-1. The societal injury risk is the sum of the injury risks for the occupants of both the target vehicle and partner vehicles in single- and two-vehicle crashes. The baseline vehicles are the Taurus, Accord, and Venza. The injury risk of the modified vehicle designs should be evaluated relative to the baseline vehicle, not relative to each other due to the fact that each modified vehicle design has different level of design and modeling accuracy. Each of the baseline vehicles, Taurus, Accord, and Venza also has a different level of modeling accuracy and level of validation efforts (Marzougui et al., 2012; Lotus Engineering Inc., 2012). The Taurus has two variants: a 25 percent mass reduced variant, LW3, and an equal mass but stiffer variant, LW4. The Venza has two variants: a 17 percent and a 36 percent mass reduced variant called Venza LWLO and Venza LWHO, respectively. The Accord has a 19 percent lighter mass variant called Accord LW. The overall injury risk combines the single-vehicle and two-vehicle risks for two occupant sizes based on the frequency of occurrence.

Three different societal injury risks have been considered. Societal injury risk I is composed of the combined injury risk of head, neck, chest, and KTH complex. Societal injury risk II is composed of the combined risk of the head, neck and the chest. This was done to isolate the effect of Knee-Thigh-Hip risk predictions based on strictly axial femur load, given that axial femur loads are very sensitive to rotation of the femur and may not capture the real risk to the KTH complex, as demonstrated in section 3.7.2.1.2. The third risk is labeled societal injury risk IIP which contains a penalty for high A-Pillar intrusion, since the A-pillar intrusion is not simulated in the occupant models. Comparing societal injury risk I and II, as can be seen in Table 4-2, the absolute value of the societal injury risk is reduced substantially if the KTH complex risks are not included. It can also be seen in the table that adding a penalty for excessive A-Pillar intrusion increases the societal injury risk over the societal injury risk II by a small amount. This reflects the fact that the observed intrusions were at the higher velocities at which the involvement rates are low.

The baseline societal injury risks (Taurus, Accord, and Venza) as predicted by the model agree reasonably with the NASS data. Prasad et al. (2010) had estimated the combined AIS3+ risk for Head, Neck, Chest, and KTH for frontal crashes in NASS to be 1.79 percent (including crashes above 64 km/h and 10 and 2 o'clock frontals, and AIS2+ KTH injuries). In the current study, the predicted risks for the baseline vehicles range from 1.25 percent to 1.56 percent for a subset of NASS frontal crashes that were simulated. Actually, the average risk for the three baseline vehicles, as estimated by this initial implementation of EFP was 1.39 percent as compared to the NASS CDS overall societal injury risk of (37,988/2,427,224= 1.57%) shown in Table 3-1. Considering the generic nature of the restraints used in this study, various assumptions and weighting factors, the predicted baseline societal injury risks are consistent with those observed in NASS.

It should be noted that because the restraint systems used in all the vehicles are generic and were not optimized for the individual vehicles, a direct comparison between the baseline vehicle risks might not be valid. But the trends from the baseline to the light weighted design due to design changes found in this study should be valid. For example, as the mass of the Taurus was reduced by 25 percent (LW3), the overall societal injury risk increased by 12 percent. The next exercise with the Taurus was LW4, in which the stiffness was increased while

the mass of the vehicle was unchanged. With the increased stiffness, there was an 18 percent increase in societal injury risk. Both the effects are discussed later (see Figure 4-1 and Figure 4-2).

It also be noted that the study was not designed to evaluate how restraints might change in response to vehicle design changes; however, using the same restraint system in the baseline and modified vehicles will help in in gaining insight on how the system needs to be changed. This was intentional and not the focus of the initial development of the methodology. Restraint technologies will be improved in the future, but for an initial analysis, this study gives a glimpse in the future of what will have to change to keep occupants safe.

The societal injury risk predicted for the baseline and the redesigned light weighted Accord are shown in Table 4-1 and Table 4-2. An increase (11%) in societal injury risk is observed with the redesigned Accord. Unlike with the Taurus, at this point a prediction cannot be made about how much of the risk increase is associated with mass reduction and how much is due to architectural design changes.

The results are similar for the Venza baseline and the two variants thereof. In as much as the two variants of the Venza have reduced mass and different architectural designs, the increase in risks cannot be attributed to any one action.

Table 4-1. Societal Injury Risk I for Single and Two-Vehicle Crashes All Target Vehicles

Societal Risk I- Target
Combined AIS3+ risk of Head, Neck, Chest & Femur

	Target	Overall Risk in SV	Total Risk 50th male	Total Risk 5th female
Single Vehicle Crashes	Taurus BL	0.15%	0.10%	0.28%
	LW3	0.18%	0.14%	0.31%
	LW4	0.19%	0.17%	0.24%
	Accord BL	0.22%	0.20%	0.25%
	Accord LW	0.25%	0.24%	0.29%
	Venza BL	0.20%	0.12%	0.44%
	Venza Low Option	0.21%	0.14%	0.44%
	Venza High Option	0.22%	0.15%	0.42%

Societal Risk I - Target + Partner
Combined AIS3+ risk of Head, Neck, Chest & Femur

	Target	Overall Risk in VTV	Total Risk 50th male	Total Risk 5th female
Two Vehicle Crashes	Taurus BL	1.10%	0.82%	1.96%
	LW3	1.23%	0.91%	2.17%
	LW4	1.29%	1.05%	2.00%
	Accord BL	1.34%	1.13%	1.98%
	Accord LW	1.48%	1.30%	2.04%
	Venza BL	1.16%	0.81%	2.20%
	Venza Low Option	1.22%	0.84%	2.35%
	Venza High Option	1.35%	0.87%	2.77%

Table 4-1 shows a breakdown of the societal injury risk (Head, Neck, Chest, Femur), by single- and two-vehicle crashes, and by occupant sizes, for each target vehicle. The risks for the 5th female percentile occupant are consistently higher than those for the 50th percentile male occupant, more so in the two-vehicle crashes and predominantly for the Venza models.

An example of such a breakdown of injury risk for the baseline Taurus, LW3 and LW4 is shown in Figure 4-1 and Figure 4-2 with the following clarification: Note that it is assumed that the 50th percentile dummy represents 75 percent of the population and the 5th percentile dummy represents 25 percent of the population (Laituri, et al. 2003). Therefore the overall risk is a weighted sum of the risks of the 50th and the 5th percentile occupants. For example:

Overall risk of the Taurus BL in SV is $0.15\% = 0.75 \times 0.10 + 0.25 \times 0.28$

Overall risk of the Taurus LW3 in SV is $0.18\% = 0.75 \times 0.14 + 0.25 \times 0.31$

Therefore, increase in Overall Risk for LW3 in SV = (0.18-0.15)/0.15 = 20%

Similarly, in two- vehicle crashes:

Overall risk of the Taurus BL in two-vehicle crashes is 1.10% = 0.75x0.82 + 0.25x1.96

Overall risk of the Taurus LW3 in two-vehicle crashes is 1.23% =0.75x0.91 + 0.25x2.17

Increase in overall Risk for LW3 = (1.23-1.10)/1.10 = 11.8%

Note that in two-vehicle crashes the risks of occupants in both vehicles are summed.

Table 4-2. Total Fleet Injury Risk
Sum of Risk in Simulated Single- and Two-Vehicle Crashes

Target Vehicle	Taurus Baseline	LW3	LW4	Accord Baseline	Accord LW	Venza Baseline	Venza Low Option	Venza High Option
Weight (lbs)	3339	2508	3339	3681	2964	3980	3313	2537
reduction		831			716		668	1444
% mass reduction		**25%**	**0%**		**19%**		**17%**	**36%**
Societal Risk I	1.25%	1.41%	1.48%	1.56%	1.73%	1.36%	1.43%	1.57%
Risk Increase		12%	18%		11%		5%	15%
Societal Risk II	1.01%	1.14%	1.22%	1.43%	1.57%	1.14%	1.20%	1.30%
Risk Increase		13%	21%		10%		5%	14%
Societal Risk IIP	1.01%	1.16%	1.23%	1.44%	1.59%			
Risk Increase		14%	21%		10%			
Societal Risk I - Target + Partner Combined AIS3+ risk of Head, Neck, Chest & Femur								
Societal Risk II - Target + Partner Combined AIS3+ risk of Head, Neck, and Chest								
Societal Risk IIP - Target + Partner Combined AIS3+ risk of Head, Neck, and Chest with A-Pillar Intrusion Penalty								

Note: *CIRIIP was not computed for the Venza models, as the occupant model incorporated the prescribed structural motion of A-pillar, and B-pillar, as such a penalty function was not warranted.*

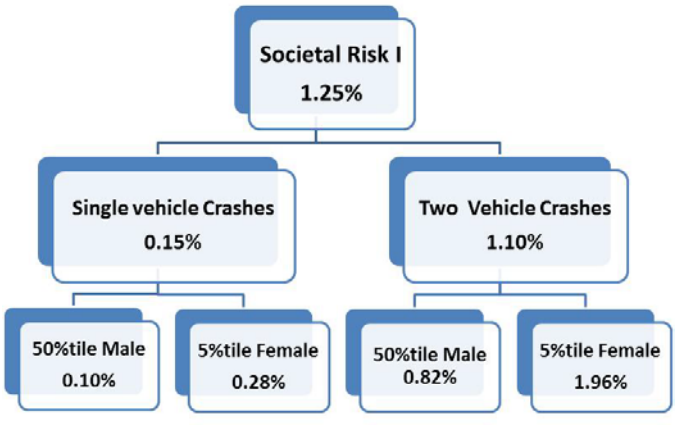

Figure 4-1. Taurus Baseline Societal Injury Risk I Computation

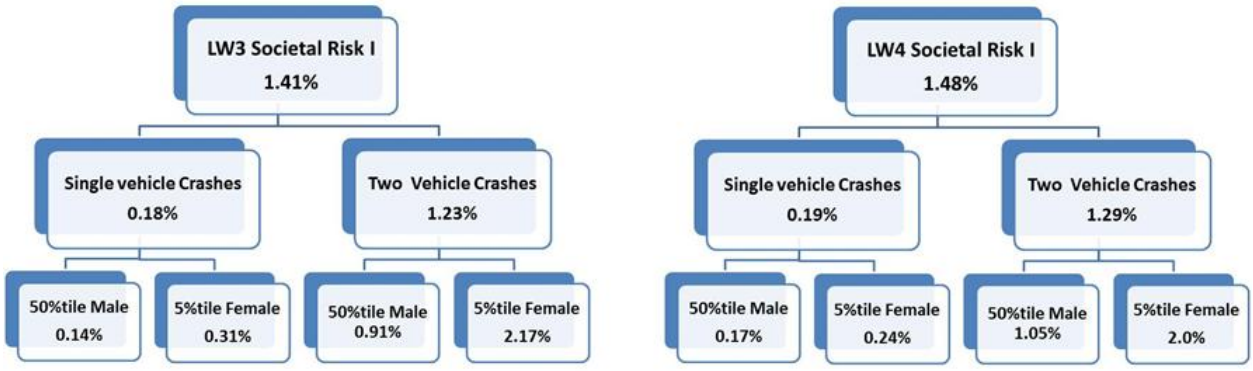

Figure 4-2. Taurus LW3 and LW4 Societal Injury Risk I Computation

Table 4-3 shows the baseline and redesigned vehicle risks if only the head, neck, and chest injury risks are considered. Obviously, the overall societal injury risk for each vehicle and its variants are lower than those predicted when the KTH risks were included. Similar to the societal injury risk I results, the societal injury risk II risks for the 5th female percentile occupant are consistently higher than those for the 50th percentile male occupant, predominantly for the Venza models.

Table 4-3. Societal Injury Risk II for Single- and Two-Vehicle Crashes for All Target Vehicles

Societal Risk II - Target Compined AIS3+ risk of Head, Neck, & Chest				
Single Vehicle Crashes	Target	Overall Risk in SV	Total Risk 50th male	Total Risk 5th female
	Taurus BL	0.12%	0.09%	0.23%
	LW3	0.14%	0.11%	0.24%
	LW4	0.15%	0.12%	0.24%
	Accord BL	0.21%	0.20%	0.24%
	Accord LW	0.24%	0.23%	0.28%
	Venza BL	0.17%	0.11%	0.38%
	Venza Low Option	0.18%	0.12%	0.34%
	Venza High Option	0.18%	0.12%	0.35%

Societal Risk II - Target + Partner Combined AIS3+ risk of Head, Neck, & Chest				
Two Vehicle Crashes	Target	Overall Risk in VTV	Total Risk 50th male	Total Risk 5th female
	Taurus BL	0.89%	0.65%	1.60%
	LW3	1.00%	0.73%	1.79%
	LW4	1.07%	0.80%	1.86%
	Accord BL	1.22%	1.02%	1.82%
	Accord LW	1.33%	1.15%	1.86%
	Venza BL	0.96%	0.64%	1.91%
	Venza Low Option	1.02%	0.69%	2.03%
	Venza High Option	1.12%	0.70%	2.38%

Table 4-4 shows the societal injury risk in which a penalty function for A-pillar intrusion is included. Comparing the risks in Table 4-3 and Table 4-4, the differences in societal injury risks are not substantial since the high intrusions are in higher velocity impacts that have low weighting factors due to their low involvement rates.

Table 4-4. Societal Injury Risk IIP for Single- and Two-Vehicle Crashes for the Taurus and Accord

Societal Risk IIP - Target Compined AIS3+ risk of Head, Neck, & Chest with A-Pillar Intrusion Penalty				
Single Vehicle Crashes	Target	Overall Risk in SV	Total Risk 50th male	Total Risk 5th female
	Taurus BL	0.12%	0.09%	0.23%
	LW3	0.14%	0.11%	0.24%
	LW4	0.15%	0.12%	0.24%
	Accord BL	0.21%	0.20%	0.24%
	Accord LW	0.24%	0.23%	0.28%

Societal Risk IIp - Target + Partner Combined AIS3+ risk of Head, Neck, & Chest with A-Pillar Intrusion Penalty				
Two Vehicle Crashes	Target	Overall Risk in VTV	Total Risk 50th male	Total Risk 5th female
	Taurus BL	0.89%	0.65%	1.61%
	LW3	1.02%	0.75%	1.82%
	LW4	1.08%	0.81%	1.87%
	Accord BL	1.23%	1.03%	1.84%
	Accord LW	1.35%	1.17%	1.88%

4.1.1 Dynamic Intrusions Considerations

Along with injury risk computation, the dynamic intrusions from LS-DYNA structural response outputs were examined specifically in light of the following limitations of the current occupant models.

- In the current implementation of the occupant environment, toe-board intrusions are modeled as prescribed structural motions in MADYMO; however A-pillar intrusions relative to the B-pillar are not fully modeled, except for the Venza occupant model to a certain degree. As such, a penalty function for A-Pillar intrusion in the two vehicle crashes was also computed and incorporated in CIR IIP, which combines the injury risk to the head, or neck, or chest.

- The structural models did not include a model of the steering column linkage system and as such corresponding intrusions were not input to the occupant models. Intrusions of the dash and toe-board during the crash can move the steering wheel from its original design location and in some cases restrict the energy absorbing feature of the steering column and also affect the interaction of the air bag with the occupant. Therefore, under conditions in which the toe-board and dash intrusions are substantially greater than those in the baseline simulations, the predicted injury risks will be less than what it would be if the intrusion effects of the steering column were modeled.

In the future the occupant simulation capabilities could be expanded to incorporate dynamic A-pillar intrusions and steering column movements. In a follow-up study, an incorporation of an additional penalty function for knee-bolster intrusion as outlined in Section 4.4 would be beneficial.

4.1.1.1 Dynamic Intrusions vs. Residual Intrusions

It is worth noting that dynamic intrusions from LS-DYNA structural response outputs are substantially higher than the post-crash residual intrusions that are reported in most crash test results. This is illustrated by a comparison of the residual and maximum intrusions for the Taurus baseline and the two design variants in the foot well area for the IIHS offset crash simulation at 35 mph, shown in Table 4-5, with corresponding measurement locations shown in Figure 4-3. FE simulations offer the advantage of providing the maximum intrusion levels into the occupant compartment since measurement of dynamic intrusions in crash tests is very challenging. This will allow a more realistic interaction of the intruding structure with the occupant.

Table 4-5. Intrusion in 35 mph IIHS Offset Configuration

	Baseline (mm)		LW3 (mm)		LW4 (mm)	
	MAX	Residual	MAX	Residual	MAX	Residual
Footrest	-133	-94	-91	-70	-151	-81
Left toepan	-205	-145	-169	-130	-237	-116
Center toepan	-205	-140	-165	-122	-252	-134
Right toepan	-203	-137	-154	-111	-223	-119

Figure 4-3. Locations for Intrusion Measurements in the IIHS Offset Configuration

4.1.1.2 Assessment of Dynamic Intrusions

Table 4-6 shows the center toe pan intrusion in vehicle-to-vehicle (VTV) crashes of the variants of the Taurus, Accord, and Venza. The partner vehicles were the fleet vehicles Explorer, Silverado, Yaris, and Taurus. Some cells are colored green, implying greater than 80 mm but less than 152.4 mm of intrusion, and some are colored red, implying greater than 152.4 mm of intrusion. The intrusions reported in this table are intrusions experienced by the target vehicles listed in the top row, e.g., the maximum toe pan intrusion in the Taurus baseline vehicle is 410 mm in a head-on, offset crash of the Taurus with the Explorer with both vehicles moving at 35 mph. Note that, at this speed with the Explorer, there is slightly less intrusion in the LW3 and substantially less intrusion in the LW4. The LW3 being lighter, but equal in stiffness to the baseline Taurus, should have lower intrusion because less energy is involved in this collision than between the baseline Taurus and the Explorer. The intrusion in the LW4 should be much less than that in the baseline Taurus, because the vehicle is stiffer. Note that in general the offset crashes are associated with greater intrusion. The lightweight Accord has substantially higher intrusions than the baseline Accord.

Table 4-7 shows the intrusion at the mid A-pillar location and Table 4-8 shows the intrusion at the knee bolster of the target vehicles shown in the top row against the partner vehicles shown in the first column. The maximum intrusions in the baseline Taurus are experienced in offset crashes against the Explorer and Silverado. Similar results are seen in the Accord baseline. The LW Accord shows substantially higher intrusions than the baseline Accord.

Table 4-6. Target Vehicle Center Toe Pan Intrusions

Target Intrusion in VTV Frontal Crashes: Maximum Center Toe Pan Intrusion (mm)									
	TARGET								
Partner	Impact Speed (mph)	Taurus Baseline	LW3	LW4	Accord Baseline	Accord LW	Venza Baseline	Venza Low Option	Venza High Option
NCAP	15	14	13	14	8	4	5	4	6
	20	39	33	23	18	4	28	10	10
	25	71	57	43	32	4	61	23	16
	30	118	99	51	52	10	91	35	16
	35	200	159	93	71	20	123	66	25
IIHS	20	51	38	16	19	3	11	6	9
	25	72	62	28	28	4	56	19	11
	30	100	84	30	32	6	105	59	15
	35	151	107	115	50	17	144	51	20
	40	205	165	250	65	60	210	96	16
Explorer Full	15	13	12	8	9	8	2	3	8
	20	26	26	19	30	30	5	19	17
	25	64	96	34	57	74	22	43	21
	30	153	182	85	107	112	22	60	36
	35	239	237	119	178	210	89	112	81
Explorer Offset	15	94	42	25	26	22	6	34	11
	20	141	124	47	48	75	17	104	27
	25	193	177	103	116	122	42	123	36
	30	291	249	159	200	208	69	192	84
	35	410	370	210	241	304	271	243	126
Silverado Full	15	15	15	10	16	16	11	13	12
	20	36	29	23	39	37	26	24	16
	25	52	56	37	63	62	64	55	31
	30	90	91	40	118	118	131	106	30
	35	137	134	53	152	220	185	147	55
Silverado Offset	15	68	54	31	29	25	55	22	6
	20	169	152	71	71	75	97	103	6
	25	242	239	80	116	150	127	129	23
	30	286	253	105	168	209	180	146	37
	35	377	347	133	220	298	231	185	118
Yaris Full	15	8	9	8	8	8	3	2	4
	20	21	20	9	17	10	6	3	9
	25	41	35	19	31	21	12	4	12
	30	80	82	28	46	51	42	11	14
	35	156	152	44	63	99	90	23	21
Yaris Offset	15	25	19	11	9	5	8	5	8
	20	47	42	29	23	28	27	15	11
	25	116	98	35	39	68	60	36	14
	30	188	167	59	58	108	75	52	22
	35	258	257	84	71	145	116	73	26
Taurus Full	15	24	22	17	10	6	3	4	5
	20	40	45	26	25	14	7	4	10
	25	73	83	40	41	45	25	10	16
	30	111	122	38	54	93	62	23	21
	35	194	177	51	76	146	98	68	81
Taurus Offset	15	41	43	12	25	11	6	5	9
	20	82	65	35	35	35	29	15	14
	25	202	139	56	48	71	86	29	18
	30	278	171	87	55	105	87	50	25
	35	310	266	134	67	154	142	100	31
Intrusions > 3.14" (80 mm) in GREEN and > 6"(152.4mm) in RED; FHWA 2004 study (AIS2+) & Laituri/Prasad study									

Table 4-7. Target Vehicle Mid A-Pillar Intrusions

Target Intrusion in VTV Frontal Crashes: Maximum Left Mid A-Pillar Intrusion (mm)									
Partner	Impact Speed (mph)	Taurus Baseline	LW3	LW4	Accord Baseline	Accord LW	Venza Baseline	Venza Low Option	Venza High Option
NCAP	15	8	8	11	9	9	3	3	4
	20	15	15	14	11	12	7	4	6
	25	34	27	21	11	11	9	8	7
	30	59	51	33	12	12	11	12	11
	35	71	69	53	15	24	11	12	13
IIHS	20	24	21	13	9	8	2	1	3
	25	26	26	23	11	8	3	3	3
	30	35	29	26	10	11	3	2	3
	35	59	40	51	17	18	11	8	2
	40	62	62	73	32	23	15	17	5
Explorer Full	15	7	7	8	11	10	3	4	3
	20	20	21	18	13	15	7	6	5
	25	45	53	30	21	31	5	7	8
	30	64	65	46	42	45	8	17	12
	35	80	88	62	79	134	7	24	18
Explorer Offset	15	20	23	21	13	19	3	3	4
	20	34	27	30	24	26	4	6	8
	25	47	48	39	49	63	5	13	10
	30	235	111	54	110	297	5	29	26
	35	421	404	93	209	527	436	84	57
Silverado Full	15	13	14	11	12	9	3	4	7
	20	33	25	25	15	19	5	5	8
	25	45	52	34	20	31	8	15	10
	30	70	75	31	51	69	17	23	11
	35	105	100	46	62	254	38	32	23
Silverado Offset	15	24	25	22	14	20	5	5	4
	20	45	42	35	28	30	7	8	7
	25	63	79	32	58	56	7	8	10
	30	234	122	48	134	241	34	12	14
	35	349	315	56	277	514	87	45	50
Yaris Full	15	6	7	8	10	11	3	3	2
	20	13	13	9	10	12	6	5	3
	25	21	22	14	10	14	8	9	3
	30	32	39	19	10	15	11	12	5
	35	63	64	31	11	27	13	13	7
Yaris Offset	15	19	15	13	8	10	3	3	2
	20	30	28	19	9	11	4	5	3
	25	32	33	23	12	19	5	7	4
	30	55	48	28	23	33	8	7	9
	35	92	80	37	35	62	12	9	11
Taurus Full	15	15	15	17	10	12	3	5	2
	20	22	27	20	10	12	5	5	4
	25	31	39	27	9	12	8	7	4
	30	42	53	28	11	13	10	11	4
	35	72	80	35	16	37	12	9	7
Taurus Offset	15	22	27	12	9	9	3	3	2
	20	31	31	24	10	9	4	6	4
	25	41	42	31	15	19	5	7	5
	30	67	59	33	27	35	5	12	4
	35	85	70	54	41	64	20	10	4
Intrusions > 5" (127 mm) in in RED; FMVSS 204 limits steering rearward displacement to 5"									

Table 4-8. Target Vehicle Knee Bolster Intrusions

Target Intrusion in VTV Frontal Crashes: Maximum Knee Bolster Area Intrusion (mm)									
Partner	Impact Speed (mph)	Taurus Baseline	LW3	LW4	Accord Baseline	Accord LW	Venza Baseline	Venza Low Option	Venza High Option
NCAP	15	18	19	22	8	6	2	3	Not Available
	20	20	22	26	10	11	8	3	
	25	21	23	29	10	11	14	5	
	30	42	33	36	12	17	17	10	
	35	63	57	39	18	30	15	9	
IIHS	20	13	13	7	8	7	2	2	
	25	17	15	12	11	6	3	3	
	30	24	18	15	8	9	10	3	
	35	53	24	30	13	13	35	6	
	40	80	58	64	32	19	59	10	
Explorer Full	15	17	17	18	9	10	3	4	
	20	19	21	24	14	13	4	8	
	25	28	33	34	31	29	5	28	
	30	51	61	34	54	49	5	40	
	35	83	86	45	101	192	46	80	
Explorer Offset	15	15	16	19	12	15	2	4	
	20	27	22	28	26	34	3	11	
	25	63	54	29	61	98	4	33	
	30	156	132	51	125	311	11	84	
	35	303	279	86	193	487	381	148	
Silverado Full	15	19	19	23	11	10	3	7	
	20	24	22	31	15	20	5	14	
	25	33	35	34	23	38	25	41	
	30	49	58	37	64	100	91	72	
	35	72	71	33	87	292	183	116	
Silverado Offset	15	17	18	21	14	17	4	6	
	20	46	41	29	35	57	29	21	
	25	83	102	27	70	105	63	46	
	30	170	124	50	147	280	126	81	
	35	252	228	49	258	470	199	145	
Yaris Full	15	17	18	16	9	11	3	3	
	20	18	19	20	10	9	4	5	
	25	20	20	24	9	13	6	9	
	30	20	24	27	9	26	10	10	
	35	53	61	31	10	58	14	10	
Yaris Offset	15	11	8	8	8	6	3	2	
	20	18	14	14	9	9	4	4	
	25	20	19	20	12	14	5	6	
	30	47	32	24	23	34	7	6	
	35	111	98	29	30	64	35	22	
Taurus Full	15	13	14	18	9	9	3	4	
	20	17	17	22	10	8	4	5	
	25	18	25	24	9	11	6	6	
	30	29	43	27	10	25	9	8	
	35	59	59	41	16	30	23	7	
Taurus Offset	15	15	15	10	8	8	3	2	
	20	20	15	18	10	7	4	4	
	25	45	28	19	15	15	5	6	
	30	86	49	23	26	30	17	6	
	35	126	106	36	35	68	48	38	
Intrusions > 4" 101.6 mm) in RED: because initial design gap between dummy and bolster is 4" - so available space is gone if >4"									

Intrusions experienced by the partner cars like the Yaris and the baseline Taurus in full frontal and offset crashes are shown in Table 4-9 and Table 4-10. The offset mode produces higher intrusions at the toe pan, and the lighter vehicles produce less intrusion than their respective baselines. The stiffer vehicle, LW4, produced higher intrusions than their baseline or lighter weight counterpart.

Table 4-9. Partner Vehicle Center Toe Pan Intrusions

Partner Intrusion in VTV Frontal Crashes: Maximum Center Toe Pan Intrusion (mm)									
Partner	Impact Speed (mph)	Taurus Baseline	LW3	LW4	Accord Baseline	Accord LW	Venza Baseline	Venza Low Option	Venza High Option
Explorer Full	15	2	2	4	4	4	2	1	2
	20	4	4	5	6	4	2	2	2
	25	5	7	8	5	4	7	3	5
	30	27	15	57	22	10	21	16	8
	35	73	33	128	44	20	60	38	15
Explorer Offset	15	2	3	6	3	3	1	1	1
	20	4	2	5	4	4	1	1	3
	25	7	5	4	7	6	7	5	6
	30	12	8	17	54	17	27	23	14
	35	81	65	148	124	60	168	67	48
Silverado Full	15	2	2	3	2	2	2	2	1
	20	3	3	4	3	2	3	3	2
	25	5	4	4	5	3	4	4	2
	30	5	5	10	7	5	3	3	2
	35	13	6	24	4	4	5	7	3
Silverado Offset	15	2	2	3	2	1	1	5	1
	20	2	2	3	2	2	1	2	1
	25	4	3	5	3	7	2	2	2
	30	26	9	26	29	18	22	7	17
	35	46	33	73	79	34	29	30	29
Yaris Full	15	9	8	14	5	5	NOT AVAILABLE		
	20	18	14	46	12	13			
	25	43	33	64	22	22			
	30	82	56	132	52	61			
	35	151	114	206	79	70			
Yaris Offset	15	9	9	16	10	6			
	20	20	17	67	17	16			
	25	68	59	165	28	33			
	30	118	101	221	73	76			
	35	202	156	354	156	124			
Taurus Full	15	19	15	8	10	10	9	7	7
	20	39	31	12	19	27	22	18	13
	25	81	44	38	29	44	61	35	23
	30	110	93	160	75	78	124	100	23
	35	195	130	264	172	117	238	214	47
Taurus Offset	15	37	42	58	23	21	31	18	20
	20	106	71	111	50	47	107	64	59
	25	208	171	166	76	57	191	128	106
	30	270	237	276	121	88	298	237	177
	35	312	275	302	188	176	351	278	168
Intrusions > 3.14" (80 mm) in GREEN and > 6"(152.4mm) in RED; FHWA 2004 study (AIS2+) & Laituri/Prasad SAE Paper No. 2006-01-1666									

Table 4-10. Partner Vehicle Knee Bolster Intrusions

Partner Intrusion in VTV Frontal Crashes: Maximum Knee Bolster Intrusion (mm)				
Partner	Impact Speed (mph)	Taurus Baseline	LW3	LW4
Explorer Full	15	8	8	13
	20	16	14	18
	25	26	29	21
	30	39	31	46
	35	67	42	78
Explorer Offset	15	5	9	17
	20	10	5	15
	25	20	14	12
	30	22	20	25
	35	93	77	131
Yaris Full	15	21	20	26
	20	27	26	30
	25	32	33	34
	30	33	33	67
	35	102	45	129
Yaris Offset	15	15	16	18
	20	20	19	57
	25	38	37	119
	30	71	71	168
	35	232	148	327
Taurus Full	15	13	13	18
	20	17	17	19
	25	19	18	19
	30	30	23	69
	35	58	36	105
Taurus Offset	15	13	16	17
	20	22	19	21
	25	47	25	46
	30	85	73	115
	35	134	100	201
Intrusions > 4" 101.6 mm) in RED: because initial design gap between dummy and bolster is 4" - so available space is gone if >4"				

Note: Knee bolster intrusions are not available for the Accord and Venza Partners, and knee bolster intrusions are not available for the Silverado.

4.2 Safety Prediction – Risk Analysis for Each Target Vehicle

In this section, details are presented and discussed for the combined and societal injury risks for each of the eight target vehicles simulated in this study. To assist in the interpretation and evaluation of trends, the results are broken down by speed and crash mode. In the figures, results pertaining to the baseline vehicles are consistently shown in red lines, results for modified designs are shown in green and blue lines, with solid lines for the 50th percentile male dummy and dotted lines for the 5th percentile female dummy.

4.2.1 Taurus Self-Protection Occupant Risk

4.2.1.1 Single-Vehicle Crashes

Compared to the Taurus baseline, the LW3 and LW4 have higher societal injury risks in both single-vehicle crashes and two-vehicle crashes. This trend is due to the LW3 being lighter and of equal front-end stiffness as shown in Figure 4-4, a plot of the barrier force versus dynamic crush of the baseline and two variants of the Taurus.

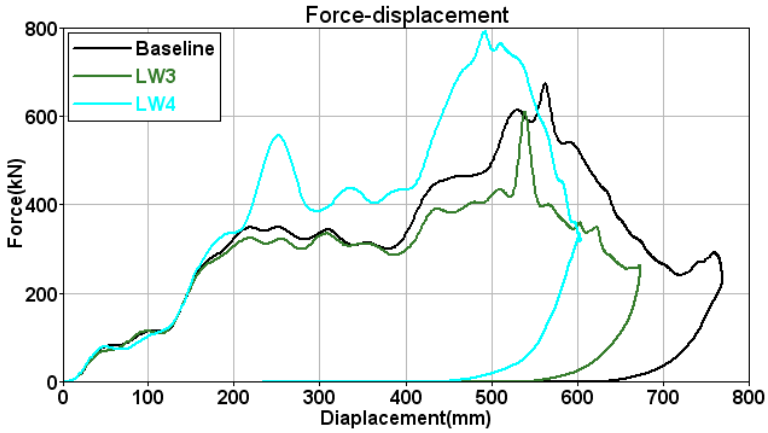

Figure 4-4. Barrier Force vs. dynamic crush of baseline Taurus, LW3 and LW4

The LW4 shows a higher injury risk in single-vehicle crashes due to higher occupant compartment accelerations in the LW4 (shown in Figure 4-5). In the Taurus simulations, the LW3 exhibits the effect of mass changes alone, and LW4 exhibits stiffness changes alone. Both variants of the Taurus have higher crash pulses than the baseline leading to higher occupant responses. In one case, LW3, the higher crash pulse is due to a lighter mass, and in the other, LW4, it is due to increased stiffness of the front-end. LW4 has the shortest crush, followed by the LW3.

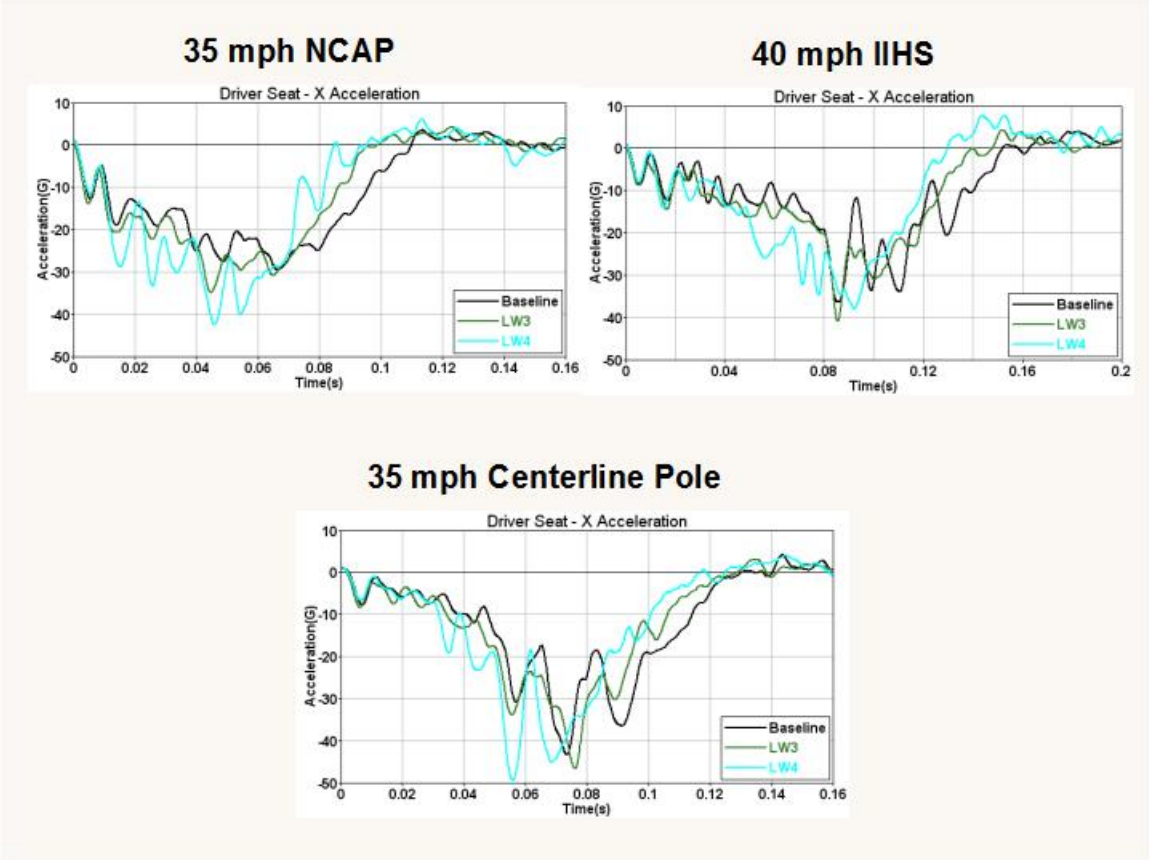

Figure 4-5. Comparison of Taurus, LW3, and LW4 Crash Pulses

The Taurus single vehicle driver injury risks show that safety in single vehicle crashes will be reduced in both the lighter (LW3) and stiffer (LW4) vehicles relative to the baseline across all impact velocities. This observation was true with and without the femur injury risks (Figure 4-6 and Figure 4-7). All drivers represented by the 5th percentile to 50th percentile dummies (close to 90%) will have higher injury risk relative to the baseline in the lighter and stiffer vehicles. In general, for all design options, the 5th percentile female driver incurred higher risk than the 50th percentile male driver.

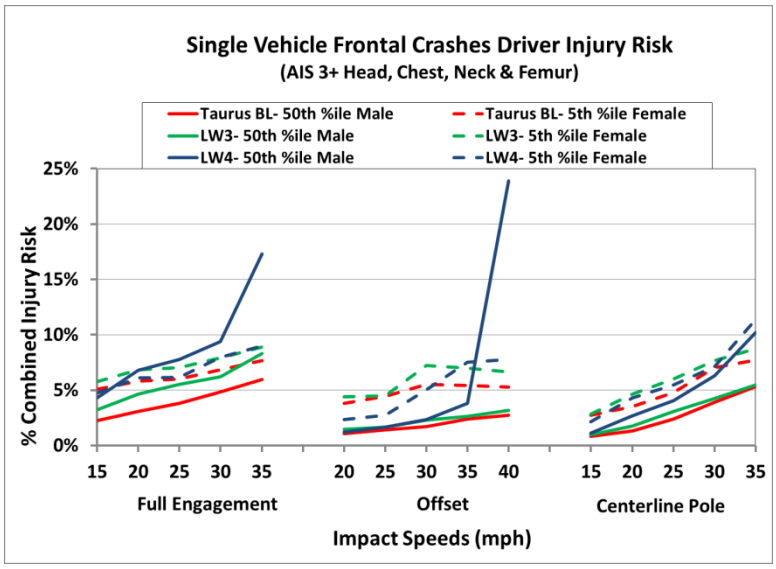

Figure 4-6. Taurus Driver Combined Injury Risk CIR I for Single-Vehicle Crashes

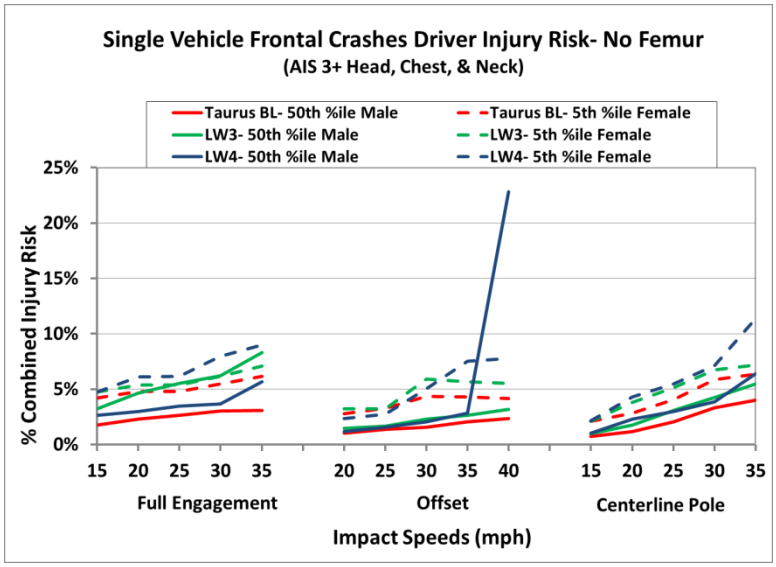

Figure 4-7. Taurus Driver Combined Injury Risk CIRII for Single-Vehicle Crashes

Particularly interesting in these single-vehicle simulations is that the lighter vehicle, LW3, has the same structural stiffness as the baseline vehicle. Being lighter, there is less energy to absorb in these collisions, and being equal in stiffness to the baseline, there is enough structure to absorb the energy. In spite of the two factors in its favor compared to the baseline vehicle, the injury risks are higher in the lighter mass vehicle across all speeds and occupant sizes. This is due to higher accelerations of the passenger compartment subjecting the occupants to higher inertial loadings.

Head strike through the air bag in the offset crash at 40 mph was observed for the 50th percentile male dummy. The hard contact with the steering wheel caused a sharp spike in the head acceleration, shown in Figure 4-8, causing the head injury risk to dominate the combined injury risk for this crash condition.

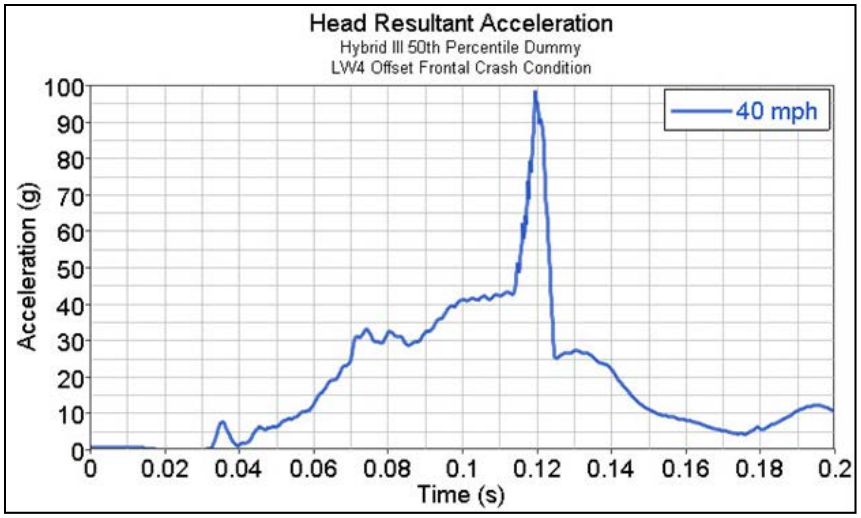

Figure 4-8. Head Resultant Acceleration for 50th Percentile Dummy in LW4 Barrier Offset Frontal Crash

The 5th percentile dummy had an elevated chest injury risk compared to the 50th percentile dummy. The restraints are designed to avoid strike through for the heavier occupants at high speeds leading to higher load limiter forces. Without an adaptive load limiter, the smaller and lighter occupants have higher chest injury risks.

4.2.1.2 Vehicle-to-Vehicle Full Engagement Self Protection

The combined injury risks for the driver in the target vehicle (baseline and lightweight Taurus designs) in full engagement frontal impacts with the four partner vehicles are shown with the femur risk in Figure 4-9 and without the femur risk in Figure 4-10. The risk in the baseline Taurus is lower than both the lighter and stiffer vehicles for all driver occupants in collisions with all partner vehicles. Figure 4-9 shows a substantial increase in risk observed when the target vehicle was struck by an Explorer or Silverado, which can be attributed to high femur loads, as this sudden increase is not seen in Figure 4-10. These high femur loads may not be representative of the real-world. In the occupant models, the knee bolster stiffness is generic and the bottoming out stiffness may not be realistic for these vehicles. The trends are generally the same in both the figures—the baseline risk is lower than those in the modified vehicles, and the 5th percentile dummy risks are higher than those of the 50th percentile dummy.

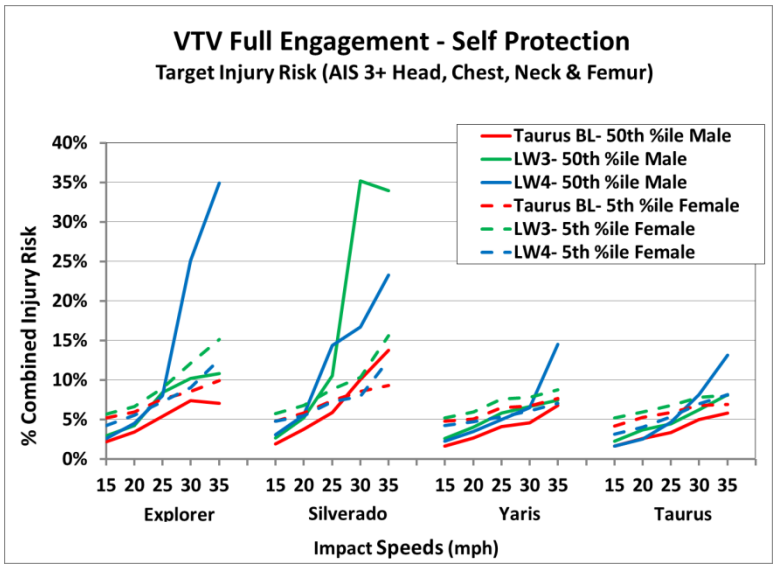

Figure 4-9. Taurus Driver Combined Injury Risk CIR I for Vehicle-to-Vehicle Full Engagement Crashes

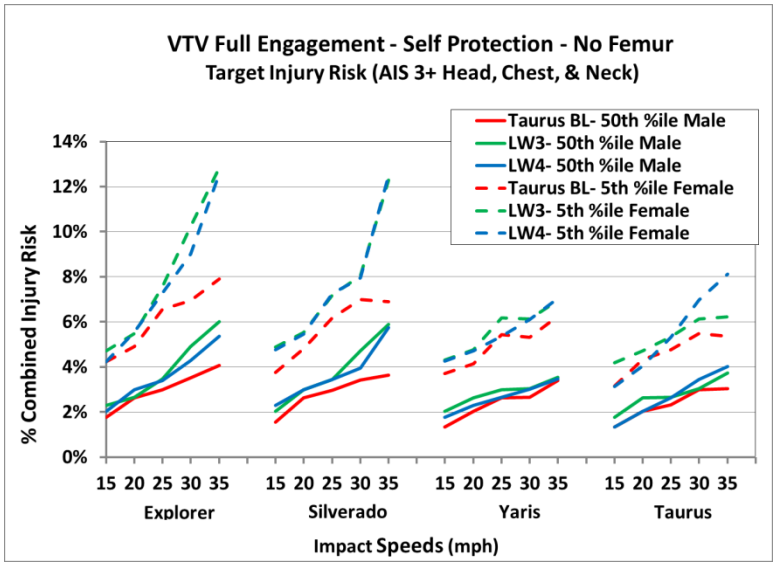

Figure 4-10. Taurus Driver Combined Injury Risk CIR II for Vehicle-to-Vehicle Full Engagement Crashes

4.2.1.3 Vehicle-to-Vehicle Offset Self Protection

The combined injury risks for the driver in the target vehicle (baseline and lightweight Taurus designs) in offset frontal impacts with the four partner vehicles are shown with the femur risk in Figure 4-11 and without the femur risk in Figure 4-12. Similar to the full engagement crashes, it is shown that the self-protection in the lighter and stiffer vehicles is reduced relative to the baseline vehicle against all four partner vehicles.

While Figure 4-12 does not include the femur risk, it still shows a high combined injury risk for the LW3 and LW4 vehicles in the 35 mph impact with the Explorer. The combined injury risk for this crash condition is driven by the head injury, as head strike through is observed in the simulation.

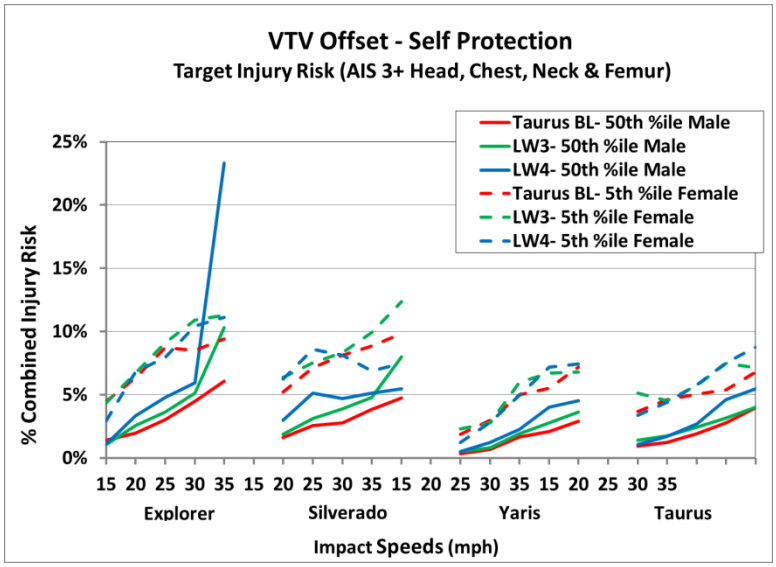

Figure 4-11. Taurus Driver Combined Injury Risk CIR I for Vehicle-to-Vehicle Offset Frontal Crashes

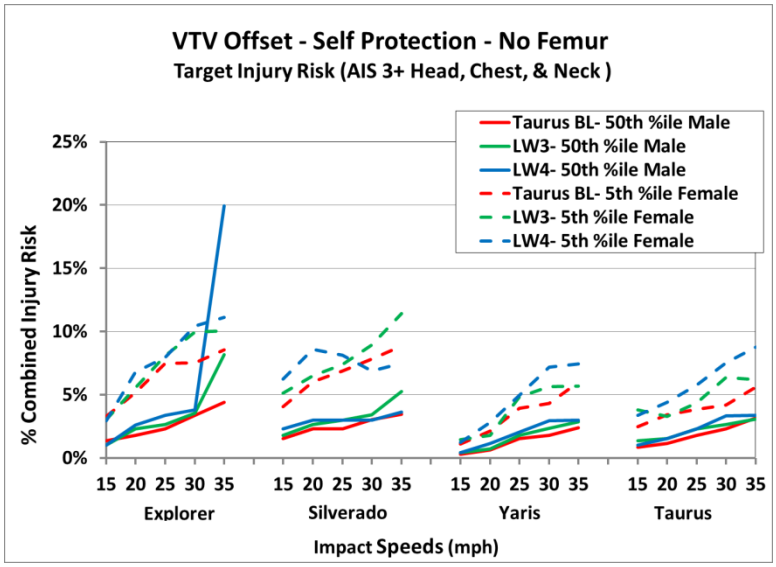

Figure 4-12. Taurus Driver Combined Injury Risk CIR II for Vehicle-to-Vehicle Offset Frontal Crashes

4.2.1.4 Summary of Taurus Self-Protection Results

Overall, both the lighter (LW3) and stiffer (LW4) Taurus vehicle design options exhibit good protection in regulatory and consumer information tests (i.e., NCAP and IIHS) as shown in the predicted injury risks in the full

engagement and offset frontal single vehicle crash simulations. However, they both exhibit higher injury risks than the baseline vehicle in all single- and two-vehicle crashes across the range of impact speeds.

4.2.2 Accord Self-Protection Occupant Risk

4.2.2.1 Single-Vehicle Crashes

The Accord study was conducted similar to the Taurus study. In this case a baseline model and one lightweight model were developed. The lightweight model involved design modifications and material substitutions. For the single-vehicle crashes, the Accord data follow similar trends as those found in the Taurus study, in particular that the lighter vehicle showed higher injury risks than the baseline vehicle for both sizes of occupants. These results are shown in Figure 4-13 and Figure 4-14.

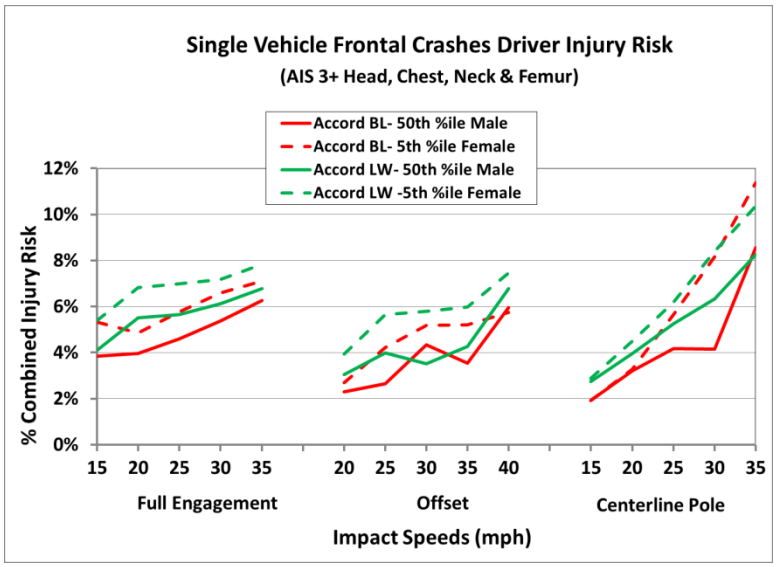

Figure 4-13. Accord Driver Combined Injury Risk CIR I for Single-Vehicle Crashes

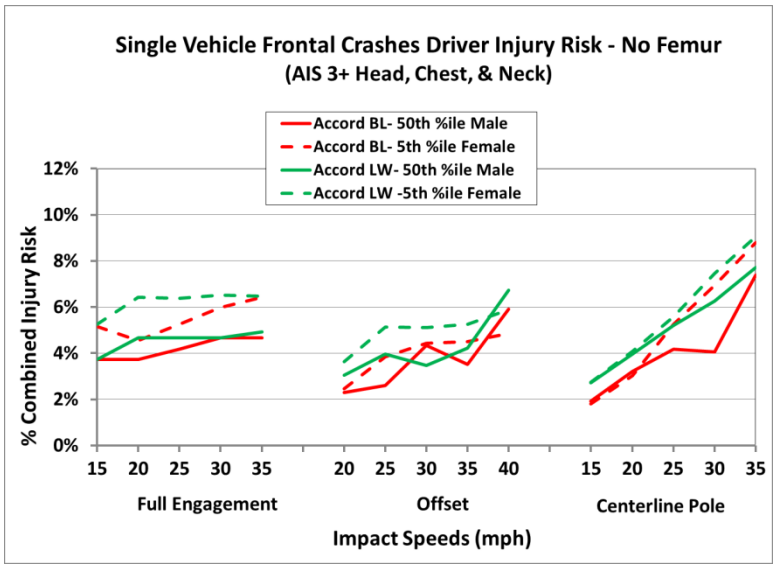

Figure 4-14. Accord Driver Combined Injury Risk CIR II for Single-Vehicle Crashes

An anomaly noticed in the Accord simulations was at 30 mph in the single vehicle offset mode. The baseline simulation showed a higher combined injury risk than at 35 mph for the 50th percentile dummy. The high injury risk was traced to higher chest deflections at 30 mph than at 35 mph (Figure 4-15). The higher chest deflection was a result of the shoulder belt load developing a second peak, as shown in Figure 4-16, highlighted by a red oval. The type of load limiting used in the Accord is known as a digressive load limiter in which a high load is achieved early on in the crash followed by a lower load level. As a result of a combination of the crash pulse, first load peak, and crash severity, it is possible that the shoulder belt load may not go over the first load level, resulting in higher chest deflections than if it had gone into the second lower load level. This is a generic restraint model for this class of vehicles to handle high speed testing and getting good safety ratings. Restraint optimization studies are needed to minimize injury risks across all speeds—low to high—and for different sized occupants.

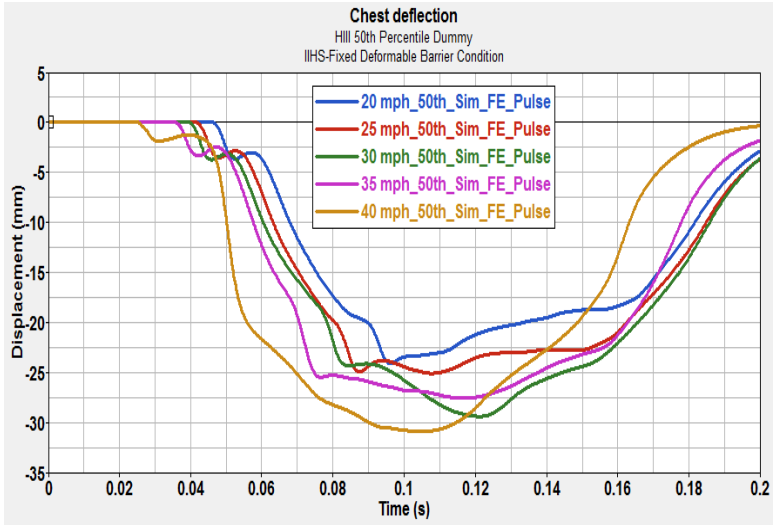

Figure 4-15. Chest Deflection of 50th Percentile Dummy in Accord Single-Vehicle Offset Crashes

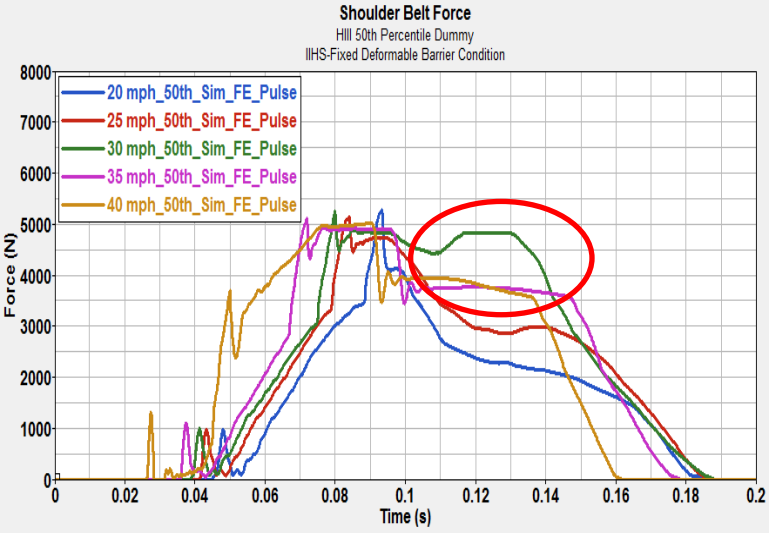

Figure 4-16. Shoulder Belt Forces in Accord Single-Vehicle Offset Crashes

4.2.2.2 Vehicle-to-Vehicle Full Engagement Self Protection

The Accord also followed similar trends as the Taurus in the vehicle-to-vehicle full engagement simulations, as shown in Figure 4-17 and Figure 4-18. Higher combined injury risks were observed for the lightweight Accord as compared to the baseline Accord. Additionally, the 5th percentile dummy showed higher injury risk as compared to the 50th percentile dummy. At the higher speeds, which are representative of the standard configurations, both the baseline and lightweight Accord exhibit similar risk.

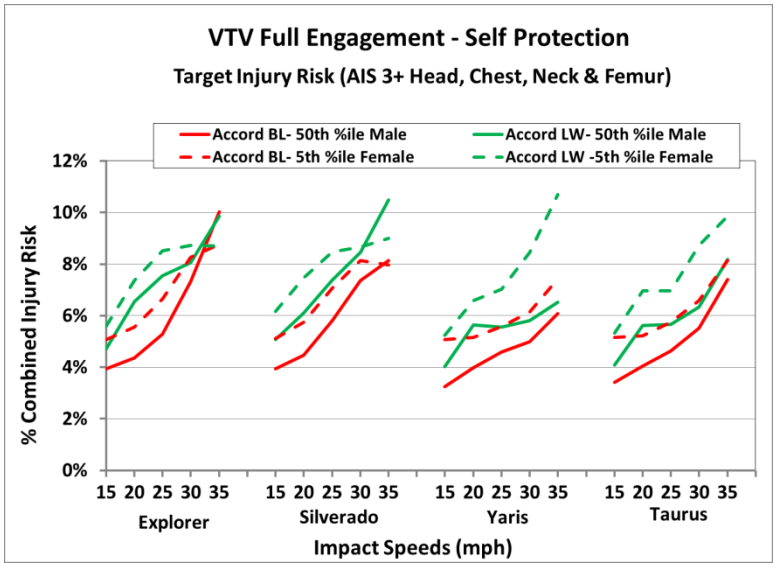

Figure 4-17. Accord Driver Combined Injury Risk CIR I for Vehicle-to-Vehicle Full Engagement Crashes

While the baseline Accord generally shows lower occupant risk than the lightweight Accord for CIR II, this trend was not as consistent in the vehicle-to-vehicle full engagement crash simulation against the Explorer and the

Silverado, as shown in Figure 4-18. Investigation of the FE simulations indicated that the dynamic mid A-Pillar intrusion of the lightweight Accord in the full engagement crashes at 35 mph against the Explorer and Silverado were 134 mm and 254 mm, respectively (shown in Table 4-7) and this should result in higher injury risks in the Accord in crashes with the Explorer and Silverado as compared to the crash with the Yaris and Taurus.

Note that the dynamic intrusions are substantially higher than the post-crash residual intrusions, which are reported in most crash test results. The predicted intrusions for the lightweight Accord in vehicle-to-vehicle crashes were higher than those predicted for the baseline Accord—79 mm and 62 mm. As noted earlier, the lightweight Accord was designed for the regulatory and consumer information crash requirements only and vehicle-to-vehicle crashes were not considered.

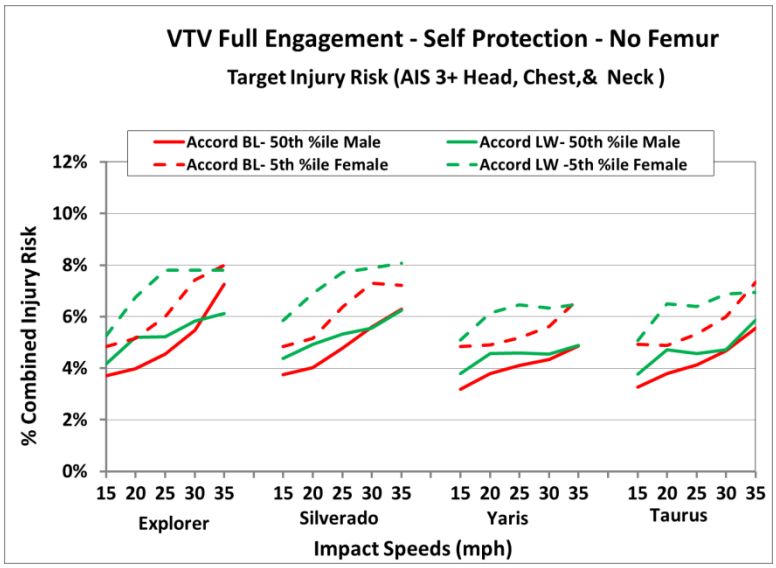

Figure 4-18. Accord Driver Combined Injury Risk CIR II for Vehicle-to-Vehicle Full Engagement Crashes

CIR IIP which combines the injury risk to the head, or neck, or chest, and includes a penalty function for A-Pillar intrusion in two-vehicle crashes is presented in Figure 4-19 for the Accord vehicles in the full engagement crashes. CIR IIP provides more realistic injury risk values where the lightweight Accord exhibits higher injury risks than the baseline vehicle in the crashes with the Explorer and Silverado across the range of impact speeds as compared to the baseline.

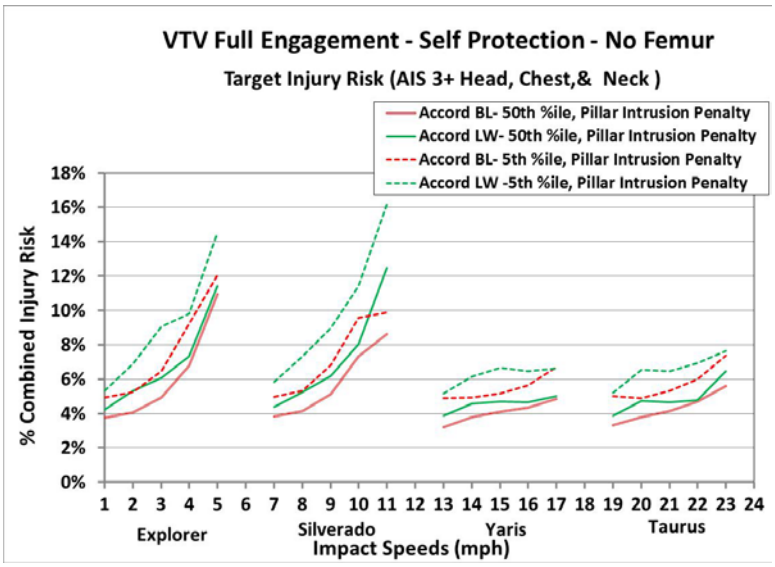

Figure 4-19. Accord Driver Combined Injury Risk CIR IIP for Vehicle-to-Vehicle Full Engagement Crashes

4.2.2.3 Vehicle-to-Vehicle Offset Self Protection

Figure 4-20 and Figure 4-21 show the combined injury risks CIR I and CIR II for the Accord occupant in vehicle-to-vehicle offset crashes, with and without the femur risk. While the baseline Accord generally shows lower occupant risk than the lightweight Accord, this trend was reversed in the offset crashes against the Explorer and the Silverado, as shown in these figures. The combined injury risks in the baseline vehicle impacting the Explorer and the Silverado were substantially higher than those of the lighter vehicle, Yaris, and Taurus. This counter trend led to further investigation of the structural response data.

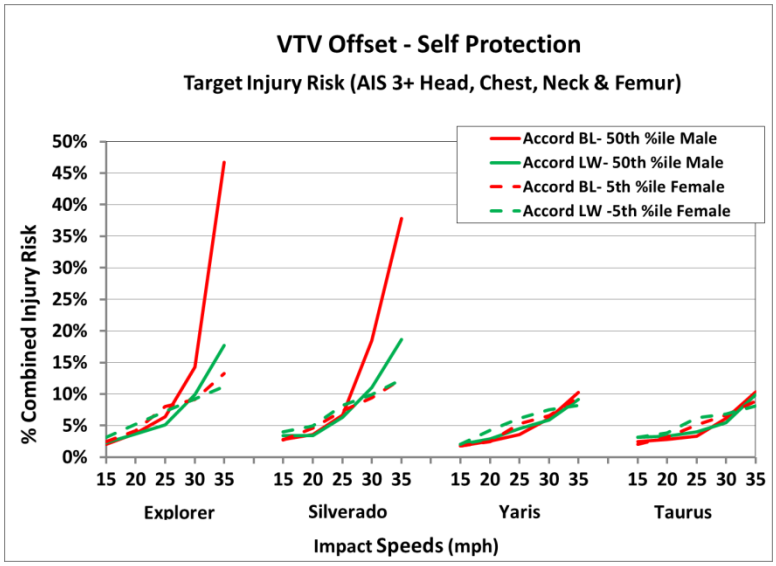

Figure 4-20. Accord Driver Combined Injury Risk CIR I for Vehicle-to-Vehicle Offset Crashes

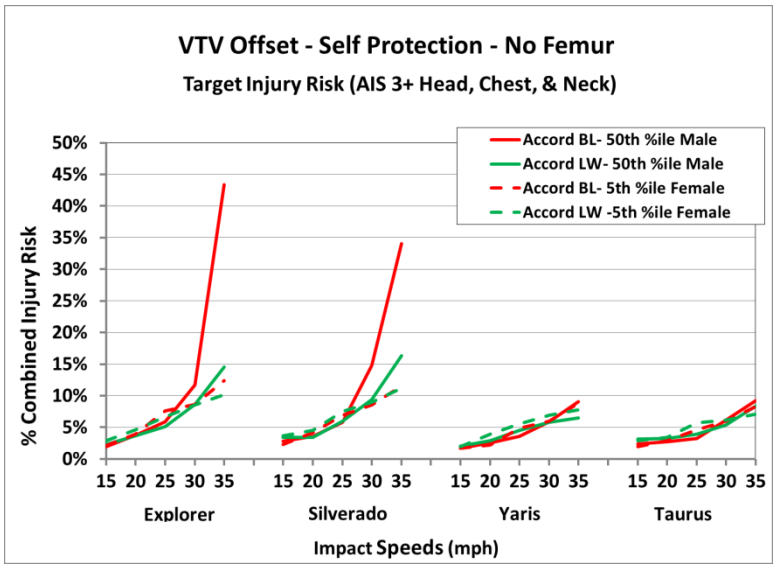

Figure 4-21. Accord Driver Combined Injury Risk CIR II for Vehicle-to-Vehicle Offset Crashes

Investigation of the FE simulations indicated that the mid A-Pillar intrusion of the lightweight Accord in the offset crashes at 30 and 35 mph against the Explorer were 297 mm and 527 mm, respectively (shown in Table 4-7) the effect of which is not reflected in the in the CIRII in injury risk shown in Figure 4-21.

These predicted intrusions were substantially higher than those in the baseline Accord—110 mm and 209 mm. With such high intrusions in the lighter Accord, the occupant responses predicted by the model are not expected to be realistic, since these intrusions were not included in the occupant model. Similar intrusion results were noted against the Silverado and explain the noted anomaly in the combined injury risks CIR I and CIR II.

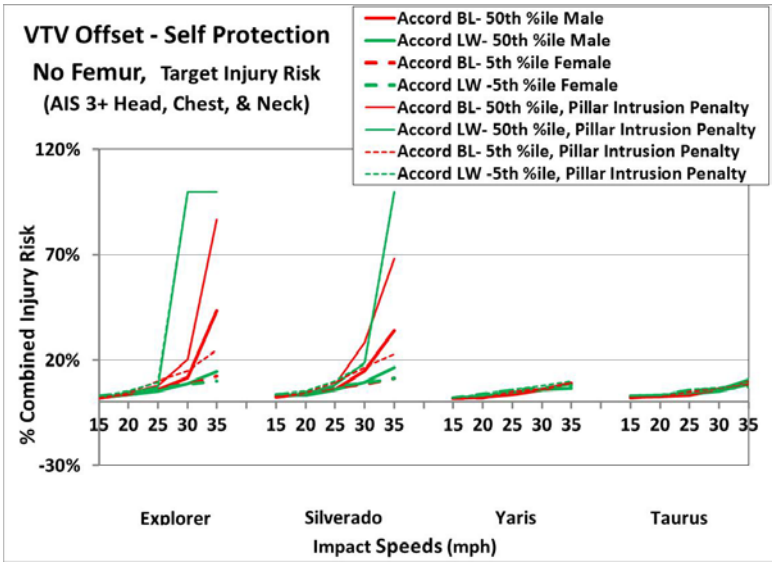

Figure 4-22. Accord Driver Combined Injury Risk CIR II and CIR IIP for Vehicle-to-Vehicle Offset Crashes

The combined injury risk CIR IIP, which combines the injury risk to the head, or neck, or chest, and includes a penalty function for A-Pillar intrusion in two-vehicle crashes is presented in Figure 4-22 for the Accord vehicles. CIR IIP provides more realistic injury risk values where the lightweight Accord exhibits higher injury risks than the baseline vehicle in the two-vehicle offset crashes across the range of impact speeds as compared to the baseline.

4.2.2.4 Summary of Accord Self-Protection Results

The baseline and lightweight Accord models exhibit good protection in regulatory and consumer information tests (i.e., NCAP and IIHS) as shown in the predicted injury risks in the full engagement and offset frontal single vehicle crash simulations. However, the lightweight Accord showed higher injury risks in single-vehicle and vehicle-to-vehicle crashes across the range of impact speeds simulated, especially when a penalty function addressing high levels of intrusions at the mid A-pillar is applied to the combined injury risk.

4.2.3 Venza Self-Protection Occupant Risk

The results for the Venza variants, the baseline, Light-Weighted Low Option (LWLO), and Light-Weighted High Option (LWHO), are presented in the following sections.

4.2.3.1 Single-Vehicle Crashes

Based on the crash pulses reported for the three versions of the Venza in full frontal rigid wall configurations, the modified vehicles were apparently designed to crash pulses similar to those of the baseline, as shown in Figure 4-23.

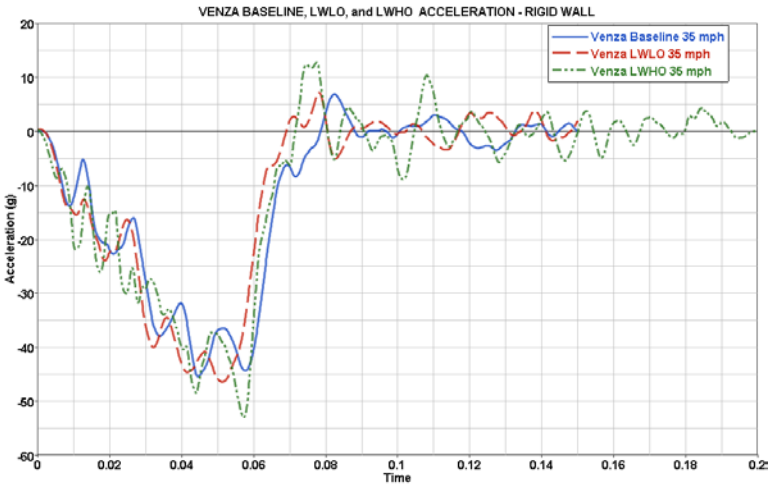

Figure 4-23. Venza Baseline, LWLO, LWHO Crash Pulses – 35 mph Rigid Barrier

The crash pulses into an offset deformable barrier of the type used by IIHS are shown in Figure 4-24. The crash pulses for the baseline and LWLO are somewhat similar; the crash pulse of the LWHO has a different shape—it is higher than both the baseline and the LWLO early on in the crash and has a plateau after 50 ms into the crash.

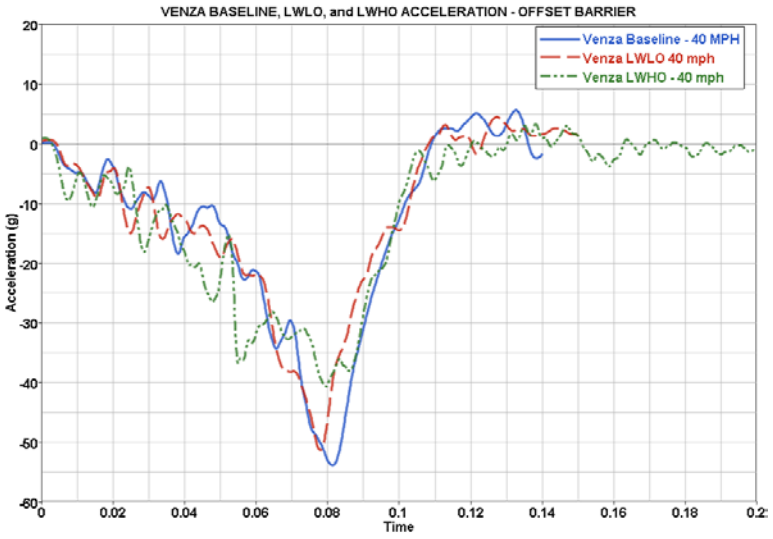

Figure 4-24. Venza Baseline, LWLO, LWHO Crash Pulses – 40 mph Offset Barrier

Figure 4-25 shows the crash pulses at various initial velocities of the LWHO vehicle against the IIHS barrier in the offset mode. Note that there is an anomalous behavior of the crash pulse in the 0 to 30 ms time frame for the 20 and 25 mph crashes, as it is mostly positive. As a result, the level of confidence in the occupant responses driven by these crash pulses is low. However, in the report evaluating the structure and crashworthiness of the Venza FEM, there was no correlation of the FEM outputs with available offset test conducted by IIHS, CEF0903-2009 MY Toyota Venza. A comparison of the crash pulses is shown in Figure 4-26. It can be seen the FE results are substantially stiffer than those from the test.

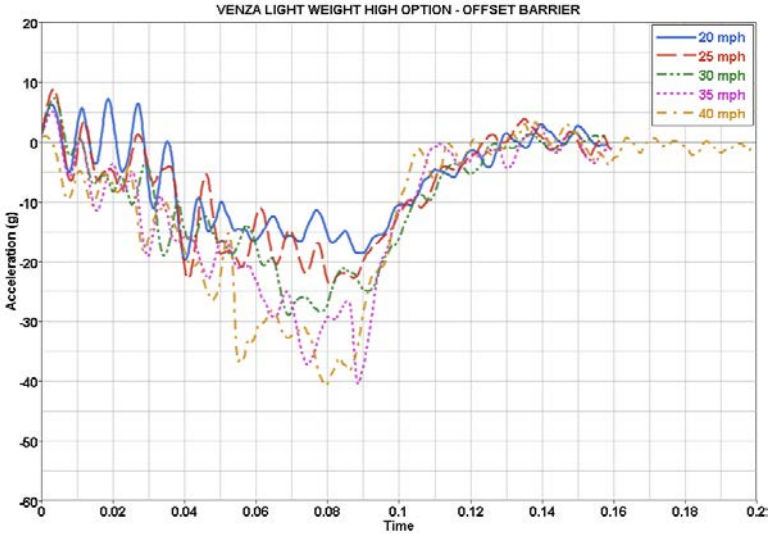

Figure 4-25. Venza LWHO Offset Barrier Crash Pulses at Various Speeds

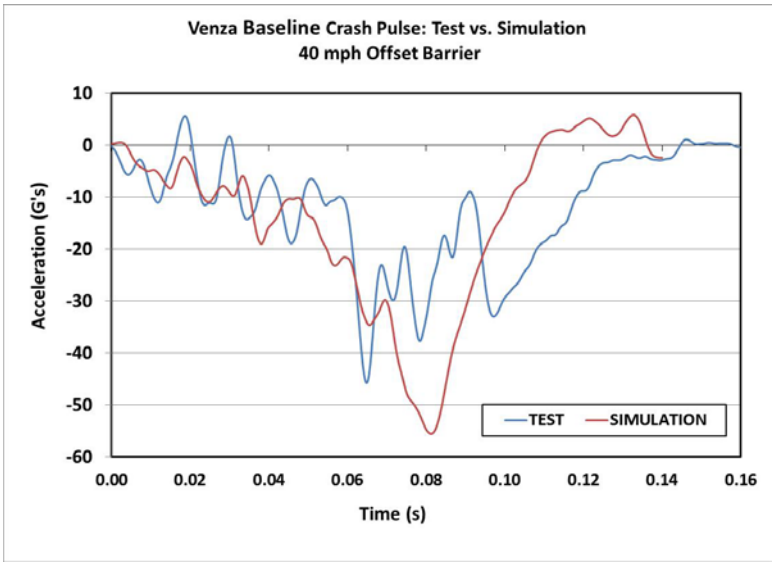

Figure 4-26. Venza Baseline 40 mph Offset Barrier FEM Versus IIHS Test Crash Pulse (CEF0903-2009 MY Toyota Venza)

The combined injury risk, including the femur, for the three Venza designs in single-vehicle crash configurations are shown in Figure 4-27. The combined injury risk in the three Venza models in the full engagement crash simulations are very similar, as would be expected from the similarities of the crash pulses shown in Figure 4-23. The risk is slightly higher in the LWLO at the higher speeds. The combined injury risk in the offset crashes seems to follow the crash pulses shown in Figure 4-24. Due to the anomalous behavior of the predicted crash pulses at 20 and 25 mph, the confidence level in the injury risk predictions for these simulations is not very high.

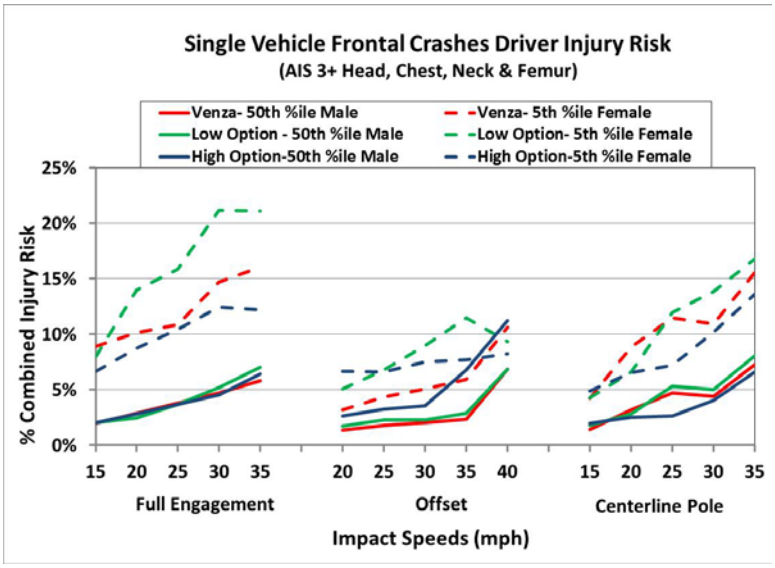

Figure 4-27. Combined Injury Risk CIR I in Venza in Single-Vehicle Crashes

In centerline pole impacts the baseline and the LWLO have similar injury risks, but the LWHO has substantially lower injury risk at 25 mph. This behavior can be traced to the dissimilar crash pulse of the LWHO in this crash mode, as shown in Figure 4-28. Unlike in the baseline and LWLO models, the acceleration of the LWHO drops

substantially between 46 ms and 54 ms before picking up again. However, at the 25 mph impact speed, the energy was not enough for the crash pulse to rise again to higher levels as the other vehicles did. Essentially the vehicle pulse was substantially softer than the pulses of the other Venza models at this velocity and as such a lower injury risk is predicted as shown in Figure 4-27, contrary to what is expected.

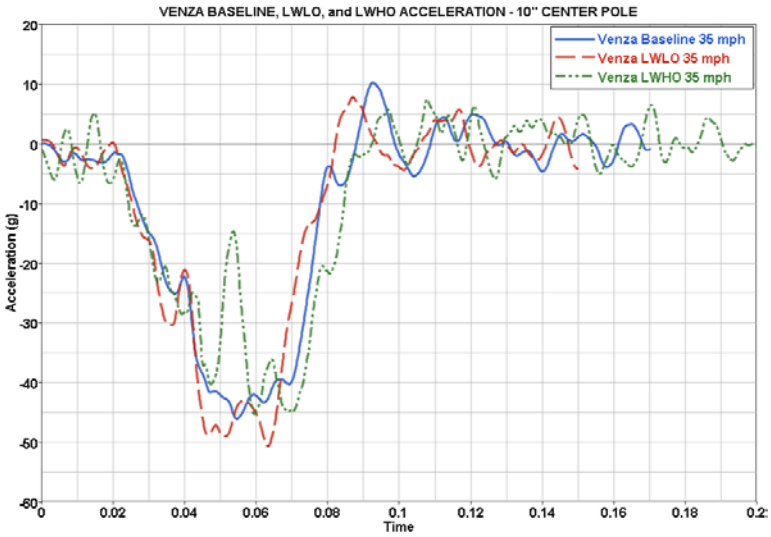

Figure 4-28. Venza Baseline, LWLO, LWHO Crash Pulses – 35 mph Centerline Pole

4.2.3.2 Vehicle-to-Vehicle Full Engagement Self Protection

The combined injury risks in the three Venza models in full engagement crashes against the Explorer, Silverado, Yaris, and Taurus are shown in Figure 4-29. The baseline Venza was shown to have lower occupant injury risks than the LWLO and LWHO designs. The injury risk in the LWHO was substantially higher than in the other two designs against the Explorer and the Silverado. In these collisions, the elevated risks to the LWHO occupants were due to increases in chest and head risks.

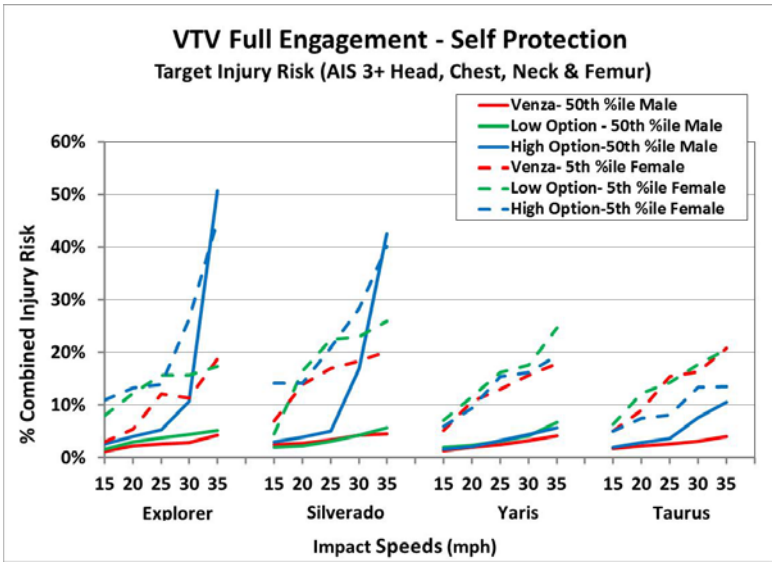

Figure 4-29. Combined Injury Risk CIR I in Venza Vehicle-to-Vehicle Full Engagement Crashes

4.2.3.3 Vehicle-to-Vehicle Offset Self-Protection

The combined injury risks in the three Venza models in offset crashes against the Explorer, Silverado, Yaris, and Taurus are shown in Figure 4-30. Similar to the Venza results for the vehicle-to-vehicle full engagement crashes, the baseline Venza was shown to have lower occupant injury risks than the LWLO and LWHO designs. The injury risk in the LWHO was substantially higher than in the other two designs against the Explorer and the Silverado. In these collisions, the elevated risks to the LWHO occupants were due to increases in chest and head risks.

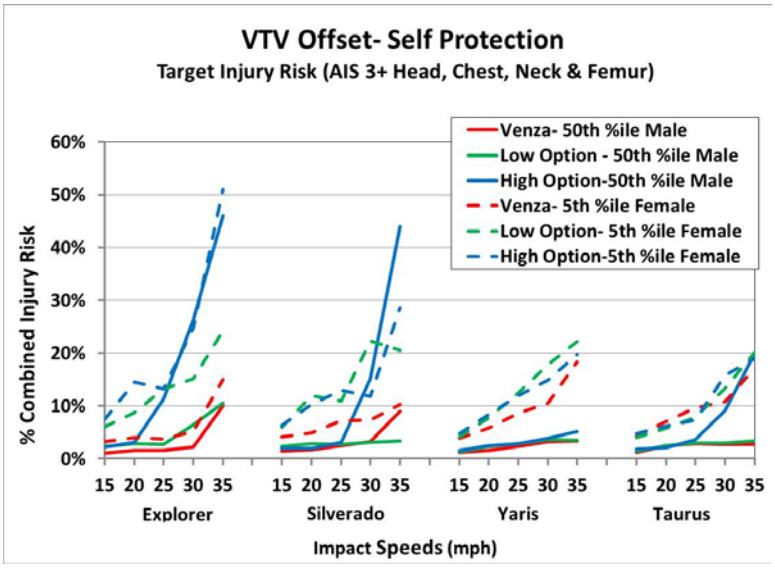

Figure 4-30. Combined Injury Risk CIR I in Venza Vehicle-to-Vehicle Offset Crashes

Several of the Venza finite element structural simulations for the two-vehicle full engagement and offset configuration terminated early at the higher impact speeds. As such, the occupant simulations may not represent the real physical events that are being simulated and, correspondingly, the computed injury risks would be questionable. In these simulations that terminated early, specifically the Venza Low Option offset crash into the Yaris at 35 mph and the Venza Baseline full engagement crashes into the Silverado at 30 and 35 mph, the injury risks were set to the values computed at the lower speeds, and are thus conservative, i.e., estimated to be lower than expected.

Due to limited time and test data availability, the Venza occupant model development did not undergo as rigorous validation and robustness checks as the other occupant models used in this study, in particular for the 5th percentile female dummy. The interior geometry was not available and contact stiffnesses were generic and not tuned to the particular vehicle. In some cases air bag interaction with the dummies were anomalous due to interaction with the neck for the 5th percentile dummy. Further investigation of anomalies showed that the 5th percentile responses are sensitive to the air bag and pretensioner firing time.

As a result of the anomalies in the structural and occupant simulations, there is not the expected monotonic increase in risk with increased impact speeds as shown in Figure 4-27 and Figure 4-36. Although the resulting societal injury risk may be slightly affected, the overall trends still hold.

4.2.3.4 Summary of Venza Self-Protection Results

Based on the results presented in the preceding sections, the two lightweight Venza designs are somewhat neutral in terms of combined injury risk to its occupants in single-vehicle crashes based on the simulation results. The lighter vehicles are expected to have higher injury risks in vehicle-to-vehicle crashes. However, there were anomalies in the predicted crash pulses in the models, which decrease confidence in the computed injury risks. Improved fidelity of both the structural and occupant models would affect the results. The result discussed so far can be considered preliminary as this is an ongoing study.

4.3 Partner Injury Risk in Vehicle-to-Vehicle Crashes

4.3.1 Taurus Partner Injury Risk in Vehicle-to-Vehicle Crashes

Figure 4-31 and Figure 4-32 show the combined injury risks in the baseline Taurus and Yaris partner vehicles in the full engagement and offset configurations when impacted by the baseline Taurus, LW3, and LW4 target vehicles. The injury risks in the Yaris and baseline Taurus are somewhat lower when impacted by the lighter weight Taurus, LW3, in both full engagement and offset crashes relative to being impacted by the baseline Taurus. The LW4 model, being a stiffer vehicle than the baseline Taurus and the LW3 Taurus, causes greater injury risk in the partner vehicles than the baseline Taurus. These trends are similar for the 50th percentile male driver and the 5th percentile female driver.

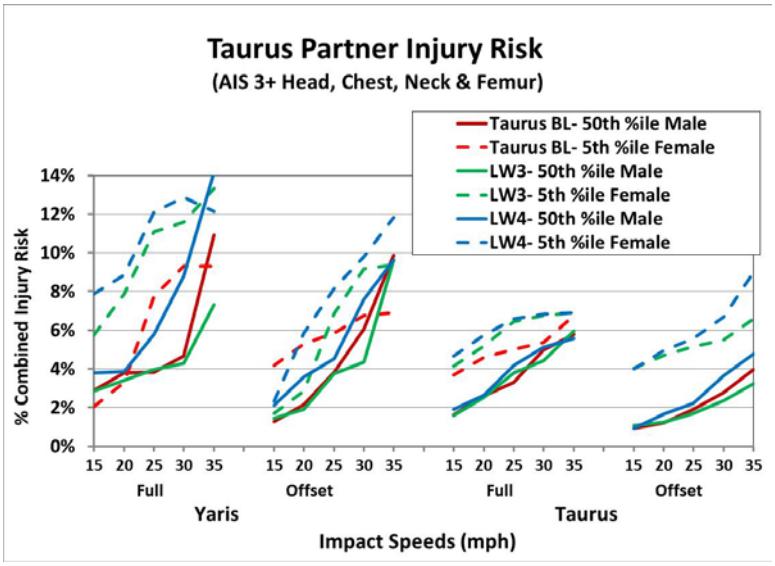

Figure 4-31. Combined Injury Risk CIR I for Partner Vehicle Hit by Taurus Vehicles

Comparing Figure 4-31 with Figure 4-32 and Figure 4-33, it appears the bigger differences in risk in the partner for the 5th percentile female driver are more driven by the risk computed from the femur loads.

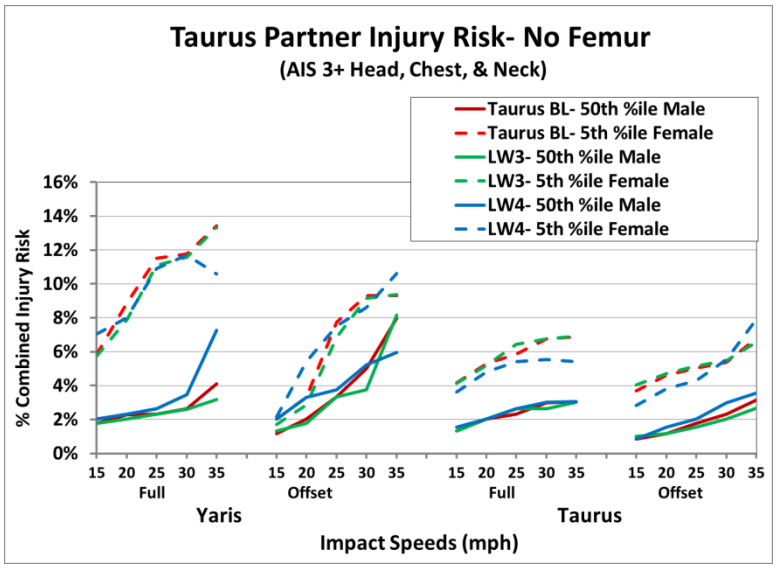

Figure 4-32. Combined Injury Risk CIR II for Partner Yaris and Taurus When Hit by Taurus Vehicles

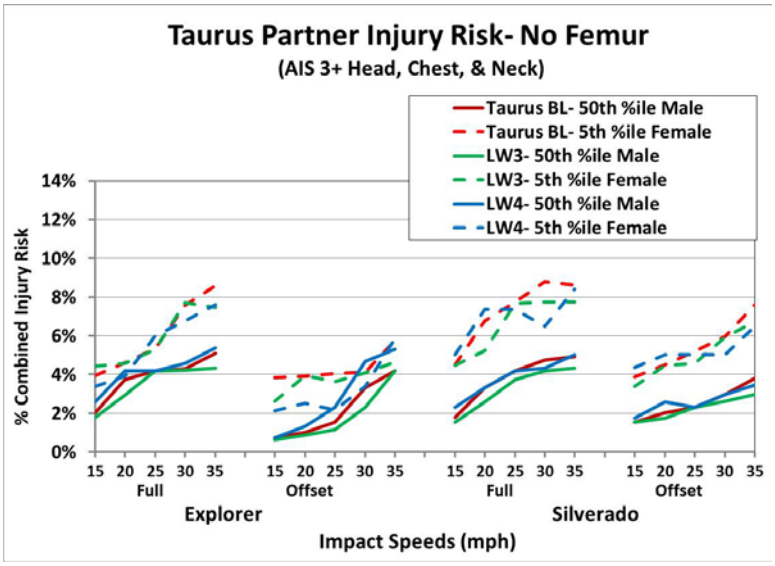

Figure 4-33. Combined Injury Risk CIR II for Partner Explorer and Silverado When Hit by Taurus Vehicles

4.3.2 Accord Partner Injury Risk in Vehicle-to-Vehicle Crashes

The partner vehicle occupant risks in crashes against the Accord and the lightweight Accord have been also computed for crashes against the Explorer, Yaris, and baseline Taurus. The combined injury risks are shown in Figure 4-34 and Figure 4-35. As expected, these figures show that the lighter weight Accord reduces the risk in the partner vehicles when compared to that from the baseline Accord. There is a sharp increase in partner risk for the Yaris in the offset crashes at the higher impact speeds with both the baseline and light weight Accord as shown in the figures below. The Accord is heavier and stiffer than the smaller Yaris. At the higher delta-V's a

large amount of energy has to be absorbed by the Yaris and it is beyond the vehicle's capability. It is worth noting that the lighter weight Accord gives slightly better results.

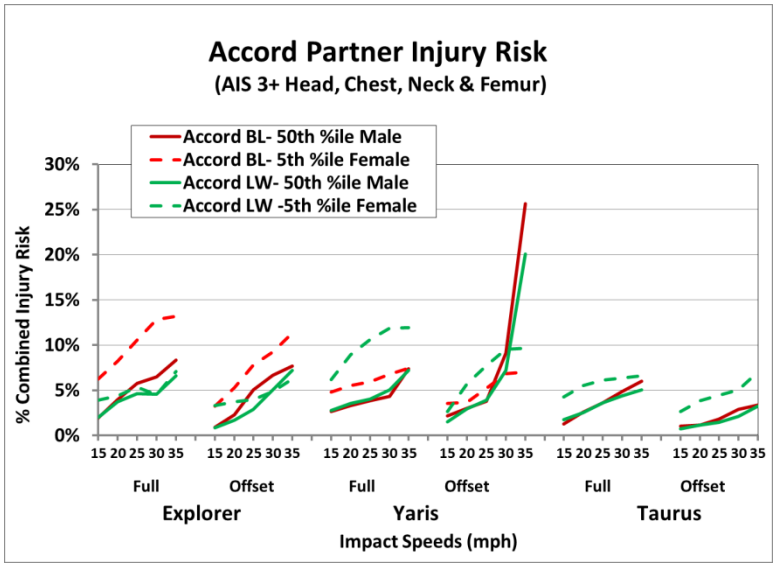

Figure 4-34. Combined Injury Risk CIR I for Partner Vehicle Hit by Accord

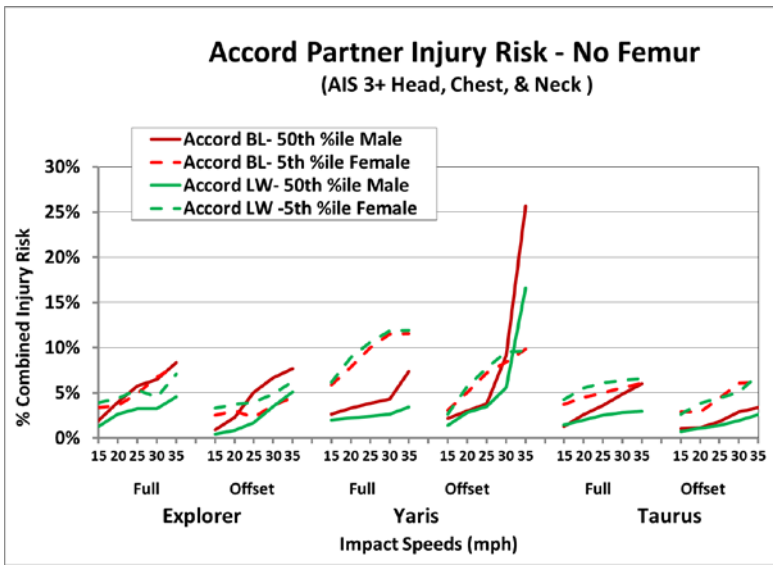

Figure 4-35. Combined Injury Risk CIR II for Partner Vehicle Hit by Accord

4.3.3 Venza Partner Injury Risk in Vehicle-to-Vehicle Crashes

The partner vehicle occupant risks in crashes against the Venza variants—the baseline, low option, and high option—have been also computed for crashes against the Explorer, Silverado, Yaris, and baseline Taurus. The combined injury risks are shown in Figure 4-36 through Figure 4-39.

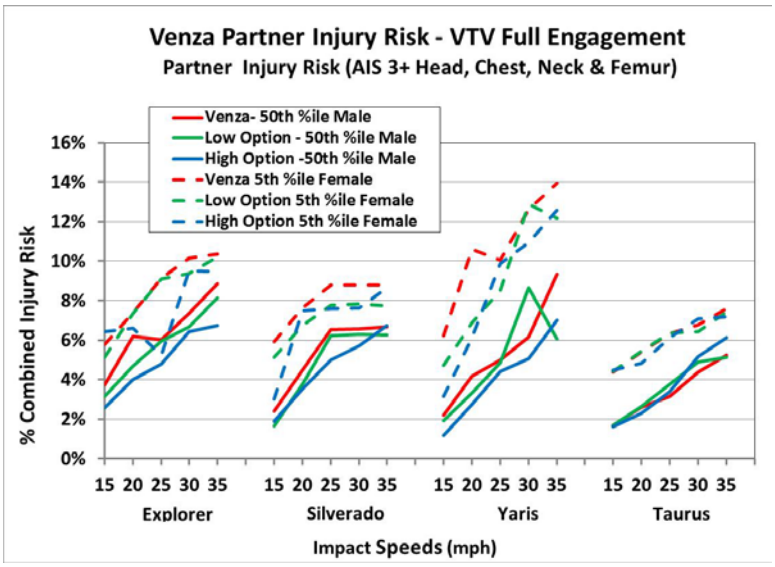

Figure 4-36. Combined Injury Risk CIR I for Partner Vehicles Hit by Venza in Full Engagement Two-Vehicle Crashes

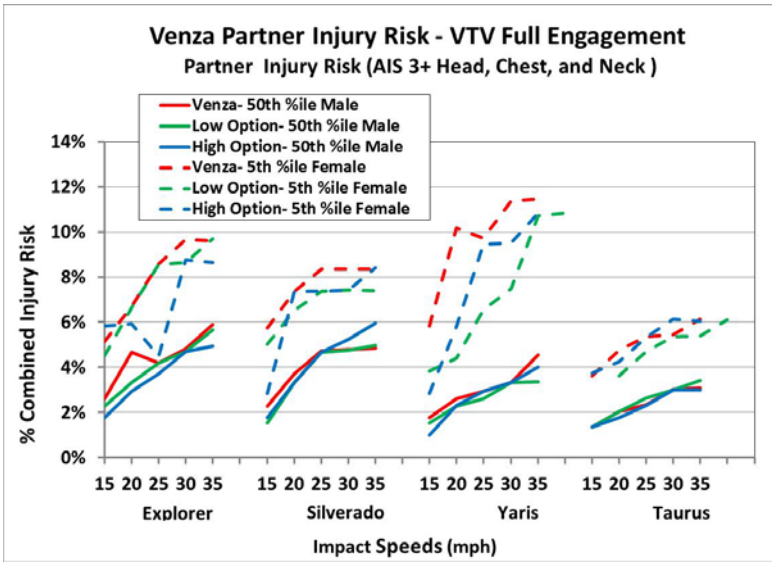

Figure 4-37. Combined Injury Risk CIR II for Partner Vehicles Hit by Venza in Full Engagement Two-Vehicle Crashes

Further investigation is needed to explain the drop in femur loads for the Yaris occupants in the full engagement crashes with the Venza Low Option at 35 mph and the drop in the Explorer 5th percentile dummy occupant responses in the offset and full engagement crashes with the Venza High Option at 25 mph.

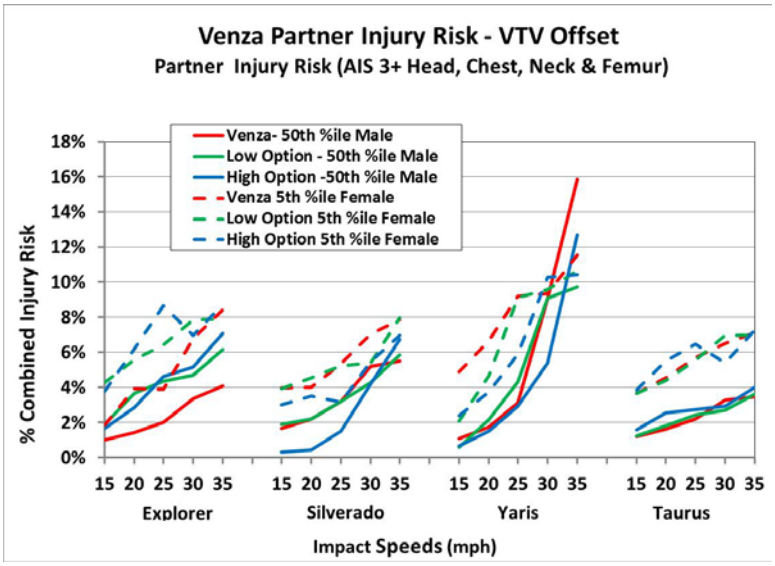

Figure 4-38. Combined Injury Risk CIR I for Partner Vehicles Hit by Venza in Frontal Offset Two-Vehicle Crashes

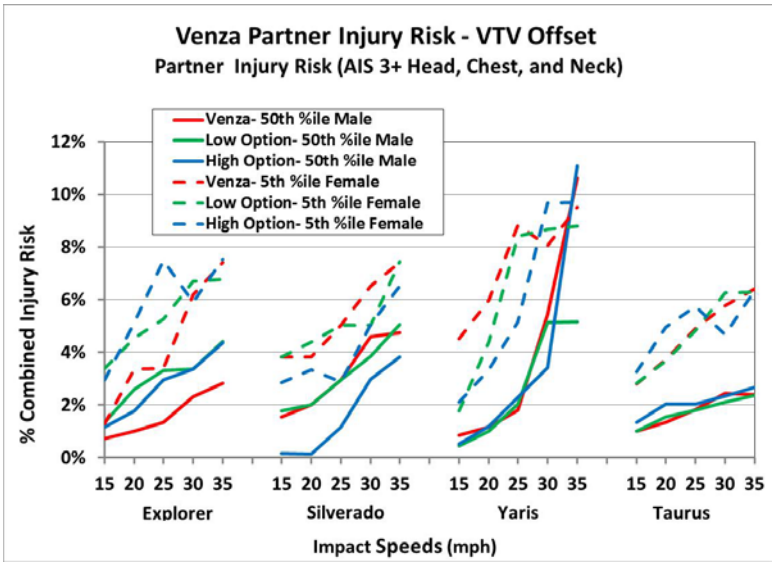

Figure 4-39. Combined Injury Risk CIR II for Partner Vehicles Hit by Venza in Frontal Offset Two-Vehicle Crashes

4.4 Limitations of Current Occupant Models

4.4.1 Steering Column Linkage System

The structural models did not include a model of the steering column linkage system and as such corresponding intrusions were not input to the occupant models. Intrusions of the dash and toe-board during the crash can move the steering wheel from its original design location and in some cases restrict the energy absorbing feature of the steering column and also affect the interaction of the air bag with the occupant. Therefore, under conditions in which the toe-board and dash intrusions are substantially greater than those in the baseline simulations, the

predicted injury risks will be less than what it would be if the intrusion effects of the steering column were modeled. In the future the occupant simulation capabilities could be expanded to incorporate dynamic A-pillar intrusions and steering column movements. In the near term, an additional penalty function for knee-bolster intrusion as outlined below would be beneficial.

4.4.2 Penalty Function for Knee-Bolster Intrusions

A choice of the penalty function, based on a common initial design guideline in industry of 101.6 mm (4") for controlling the lower body kinematics of the dummy in the unbelted mode (Daniel, 1995) would be as follows:

1. If the knee bolster intrusion is ≥ 101.6 mm, double the calculated femur risk.
2. Use linear interpolation of the risk for intrusions between 0 to 101.6 mm.

The 101.6 mm intrusion as a cut-off is predicated on the initial gap between the dummy knee and the knee bolster.

4.4.3 5th Percentile Dummy Responses

As noted in Section 3.5.1, the restraint systems used in the models for the various vehicles are generic, although the models have been validated to available crash test data. Very little data showing the responses of the 5th percentile dummy in the driver position are available, making it difficult to check the results of the simulations. However, the predicted trends are reasonable. The various simulations predicted that the small sized occupants represented by the 5th percentile anthropomorphic test device (ATD) in the forward most seated position was generally at a higher risk of injury than the average adult male represented by the 50th percentile male dummy.

4.4.4 Structural Response Inputs into the Occupant Models

The occupant models have been driven by occupant compartment accelerations and intrusions from the FE models of the vehicles. Although these FE structural model results have been compared with available crash test data for being reasonable, it was beyond the scope of this study to further verify the structural models for all the crash velocities used to simulate the real-world crash environment. In detailed descriptions of model results earlier in this report, anomalies in structural responses for some of the simulations have been pointed out.

4.4.5 Restraint System Assumptions

As mentioned earlier in the report, generic restraint systems have been used in this study, and no attempts at optimizing the restraints for individual vehicles were made. However, the goal of the study was to identify changes in occupant risks from the baseline vehicle as mass, stiffness or vehicle architecture were changed. The trends predicted in this study are believed to be valid although the absolute risks for the baseline vehicle design may not be accurate.

It is important to note that the restraint systems were not optimized in this study for the baseline or design variant vehicles. The design variants met or far exceeded the frontal regulations currently in effect, and yielded simulation results that would have garnered good ratings from the IIHS moderate overlap and NHTSA's NCAP frontal testing. However, current regulation and consumer information testing does not require a manufacturer to design a vehicle for optimum performance across all speeds and against all partner vehicles and objects.

Simulation studies based on the EFP approach could lead to the development of strategies for further reduction of societal injury risks across all speeds and objects contacted.

5 SUMMARY

The NCAC has developed and demonstrated the feasibility of EFP with initial implementation to frontal crash modes. EFP is a systems modeling and simulation methodology which uses finite element analysis and rigid body dynamics, in combination with real-world crash and test data, to evaluate self-protection, i.e., crashworthiness, partner-protection, i.e., compatibility, and fleet effects of vehicle designs. This is all achieved in a virtual environment to help design future vehicles that will substantially improve societal benefits.

In the current study three baseline vehicles and five variants were studied. The baseline societal injury risks in frontal crashes (for Taurus, Accord, and Venza) as predicted by the model agree reasonably with the NASS data. Prasad et al. had estimated the combined AIS3+ risk for Head, Neck, Chest, and KTH for frontal crashes in NASS to be 1.79 percent (including crashes above 64 km/h and 10 and 2 o'clock frontals, and AIS2+ KTH injuries) (Prasad, et al. 2010). In the current study, the predicted serious injury risks for the baseline vehicles range from 1.25 percent to 1.56 percent for a subset of NASS frontal crashes that were simulated. The average risk for the three baseline vehicles, as estimated by this initial implementation of EFP was 1.39 percent as compared to the NASS CDS overall societal injury risk of 1.5 percent shown in Table 3-4. Considering the generic nature of the restraints used in this study, various assumptions and weighting factors, the predicted baseline societal injury risks are consistent with those observed in NASS.

Overall, the main observation from the initial application of EFP to frontal crashes is that there was an increase in societal injury risk for the light-weighted vehicle designs as compared to their corresponding baselines, as shown in Table 4-2. This trend was observed for the two simple design variants of the proof-of-concept midsize vehicle as well as the lightweight vehicle design concepts developed through projects sponsored by NHTSA, EPA, and CARB. Although the same restraint systems were used for both the baseline and lightweight vehicles, future trends are not expected to be different than those observed in this study. It is anticipated that optimized restraint systems will be implemented for both the baselines and their lightweight designs to meet the existing regulatory and consumer information test requirements. However, in the absence of additional performance requirements, relatively increased societal injury risks for the lighter vehicles are still anticipated in real-world interactions with the fleet. When a lightweight design crashes into a heavier design of the same size, the lightweight vehicle will still undergo higher delta-V than the heavier counterpart. As a result, the risk of injury in the lighter vehicle will always be higher than that in the heavier vehicle with equivalent restraint systems. Moreover, with the aging population in the United States and the proven increase in injury risk for older occupants, it is expected that the study findings would be amplified for the aging population. Future studies could incorporate the older driving population in the societal injury risk computation.

5.1 Results Summary

5.1.1 Taurus

With the first baseline, the Taurus, the effect of mass reduction without changing the baseline stiffness and the effect of increasing its stiffness without increasing mass were studied. Both the variants of the baseline were subjected to three modes of single-vehicle crashes and two modes of two-vehicle crashes against four vehicles selected to represent the composition of the existing car and LTV fleets in the United States. The four vehicles selected to represent the current fleet were an average mass heavy car, the Taurus; an average light car, the Yaris; an average heavy LTV, the Silverado; and an average LTV, the Explorer. The societal injury risks, i.e., risk to its own occupant and risks to the occupants of the partner vehicles, against which it crashes, were estimated for the baseline and the two variants. As the mass of the Taurus was reduced by 25 percent (831 lbs.) strictly due to material substitution, there was an increase in overall societal injury risk (sum of risk in single and two-vehicle crashes) of 12 percent. This corresponds to a 1.45 percent increase in societal injury risk of serious injuries per 100 lbs. mass reduction in the baseline Taurus. The effect of stiffness increased through the exercise of replacing the regular steel with high strength steel while maintaining the mass in the baseline Taurus resulted in an increase of overall societal injury risk by 18 percent.

Details of the Taurus simulation results are shown in Figure 4-6 and Figure 4-7 for single-vehicle crashes, Figure 4-9 to Figure 4-12 for self-protection in two-vehicle crashes, and Figure 4-31 to Figure 4-33 for partner protection in two-vehicle crashes. The results shown in these figures were weighted by the event frequencies expected in NASS and the societal injury risks were calculated as described in Section 3.7 and presented in Table 4-1 to Table 4-3. With the simulation results of the Taurus baseline and its variants, the proof-of-concept evaluating the societal effects of a new vehicle design in a virtual fleet environment has been demonstrated. In the present study, only the frontal crash environment has been addressed, but there are no anticipated limitations in extending the analysis to include other crash modes.

5.1.2 Accord and Venza

Other vehicles studied were the baseline Honda Accord and one variant, which was redesigned using lighter and stronger material and modified architecture to reduce vehicle mass. A third set of vehicles studied were a baseline Toyota Venza and two variants. Detailed results of both the Accord and Venza simulation studies are in the main text of this report and are also summarized in Table 4-1 to Table 4-3. Details of the single-vehicle and two-vehicle crashes for the Accord are shown in Figure 4-13 to Figure 4-22. Details of the single-vehicle and two-vehicle crashes for the Venza and variants are shown in Figure 4-23 to Figure 4-30.

For the Accord light-weighted design, where the baseline was 19 percent (716 lbs.) lighter, there was an increase in overall societal injury risk by 11 percent, which corresponds to a 1.57 percent increase in societal injury risk of serious injuries per 100 lbs. For the Venza low and high option designs, where the baseline was 17 percent and 36 percent (668 lbs. and 1444 lbs.) lighter, there an increase in overall societal injury risk by 5 and 15 percent, which corresponds to a 0.8 percent and 1.04 percent increase in societal injury risk of serious injuries per 100 lbs. These estimates rely on the crash pulses used to drive the occupant models at various speeds and crash configurations. As mentioned earlier in this report, anomalies have been pointed out in both the structural and occupant responses

of the Venza simulations, which require further improvements in the fidelity of the models which would affect these results. The result discussed so far can be considered preliminary as this is an ongoing study.

5.1.3 Level of Simulation Effort

Over 530 FE full vehicle simulations were conducted in this study, which included around 90 simulations for extended FE vehicle model development and verification in frontal crash configuration. The results of the FE simulations were input into occupant simulation models to estimate injury risks to various parts of the human body. Over 1770 rigid body occupant simulations were conducted for this study, including over 250 runs to develop and establish baseline models. The simulation matrix was aimed at replicating the frontal crash environment in NASS in terms of the distribution of frontal crash configurations (single-vehicle and two-vehicle crashes), crash velocities, and occupant sizes.

6 CONCLUSIONS

A new and operative method for **E**valuating overall **F**leet crash **P**rotection for new vehicles using crash simulation was developed and demonstrated for frontal crash modes. EFP, a systems modeling and simulation methodology, uses finite element analysis and rigid body dynamics in combination with real-world crash and test data to evaluate self-protection, i.e., crashworthiness, and partner-protection, i.e., compatibility, and fleet effects of vehicle designs.

The initial implementation of methodology to frontal crashes and proof-of-concept results demonstrated EFP's capability of using crash simulations to evaluate the crash safety for an existing or new vehicle design at different crash configuration and speeds representing the real-world. Changes in overall societal, target, or partner injury risk between baseline and modified vehicle designs in frontal crashes could be established and evaluated to guide future safety research efforts. With further development, EFP can be extended to include other crash modes like side and rear impacts.

This study was aimed at determining if the fleet modeling process would lead to predictions of societal injury risks that are close to those observed in the current fleet, and if effects of design changes to a baseline vehicle can be detected. Due to time and model availability constraints, the study concentrated on only frontal impacts as a "proof-of-concept." The results indicate that the concept has been proven out in terms of the model predicting the real-world experience and its sensitivity to vehicle design changes for frontal impacts, the most important crash mode in frequency of occurrence and incidence of serious to fatal injuries. The main limitation for the frontal implementation of EFP is the availability of newer fleet vehicle FE models. The current FEMs representing the fleet span model years 2001-2012, thus the results are more representative of transitional fleet safety effects. However, as more vehicle models become available, they can replace the current ones used. As light-weighted vehicles become more available in the fleet and corresponding validated FEM model of such vehicles are developed, EFP can used to assess the fleet performance and societal injury risk of a more modern fleet.

EFP advances the state of the art of systems modeling in crash safety simulations and address limitations identified for the previous system modeling efforts. This method can serve as a powerful tool to assess and introduce particular designs in the fleet and make corresponding decisions on a societal level.

6.1 EFP Insights and Potential Refinements

6.1.1 Safety Performance Insights from Initial Application of Methodology

1. EFP allows safety evaluation of a vehicle at different crash configuration and speeds representing the real-world.
2. Using the Taurus vehicle models, EFP was able to isolate the effect of mass and stiffness changes in vehicle designs on total societal injury risk. This could not have been achieved by physical experimentation.
3. EFP highlighted the importance of performance of vehicle crashworthiness at the lower speeds that are predominant in the real-world as compared with the traditional speeds at which vehicles are tested for regulatory compliance and consumer information.
4. EFP highlighted the importance of restraint systems designed to perform well across range of occupant size
5. EFP allow evaluation of self-protection in single- and two-vehicle crashes. EFP also allows concurrent evaluation of partner protection in two-vehicle crashes at multiple configurations and speeds. The two-vehicle crashes evaluate changes due to vehicle weight (delta-V) and changes due to stiffness (peak G) that are not evaluated in regulatory and consumer information testing.
6. EFP highlighted the importance of accounting for both compartment accelerations and intrusions for better prediction of occupant injury risks. EFP also provides a framework for assessing effects of both in a virtual environment.

6.1.2 CAE Process Insights from Methodology

1. The current vehicle structural model constructs using finite element analysis have been proven to be sufficiently useful and robust to be used to simulate the field accident data in a virtual environment.
2. Restraint systems are critical in evaluating occupant safety in a virtual environment.

6.1.3 Potential Refinements of EFP

1. Incorporate steering column and A-pillar intrusion inputs into occupant model.
2. Develop and incorporate advanced air bag and belt strategies (such as adaptive systems and other advancements in restraint technology, such as inflatable belt systems and advanced load limiting strategies).
3. Perform checks of the “5-30” air bag firing guideline against actual firing times recorded in available frontal-offset and pole crash tests. Investigate obtaining air bag firing times from real-world EDR data which could provide the firing time for both the first and second deployment stages as a function of crash mode, delta-V, and occupant position.
4. Develop FEMs of additional vehicle segments to evaluate a broader cross section of the vehicle fleet: compact car segment, e.g., Corolla/Civic/Focus; Hybrid Electric and/or Electric, e.g., Volt/Prius/Hybrid Camry; CUVs, e.g., Venza (NHTSA has separated CUV as a separate vehicle category in a recent study (Kahane 2012) and market is expected to grow in the small CUV category, e.g., C-Max); and over 8,500 GVWR trucks, e.g., F250/Suburban. Also, include FEMs of newer and higher volume mid-size car and small car in the fleet as those become available.

5. Currently, EFP provides useful safety performance trends and insights between different target vehicles (e.g., baseline and redesigned vehicles). Establishing more direct correlation between fleet model and real-world crash data will make EFP a more powerful tool. Further analysis of the crash environment and verification of predicted risk could be performed.
6. Investigate combining the occupant and the vehicle structure in the same simulation environment, e.g., finite element. This approach would have the potential of increased efficiency and robustness of EFP.

6.1.4 Potential Expansions of EFP

With further development, the EFP methodology can be extended to apply to multiple crash environments, e.g., side and rear impacts.

6.2 Potential Applications of Current EFP

In its current implementation, EFP can be effectively used as a tool for many potential applications.

1. EFP can be applied to evaluate both structural and restraint countermeasures that further reduce societal risk in frontal crashes. On the structural side, analysis of the effects of structural simulation outputs on corresponding societal could provide valuable input on which front end designs provide improved societal benefits. On the restraints system side, EFP provides a virtual tool to evaluate advanced restraint concepts and strategies.
2. EFP provides a tool to evaluate the effects of proportional changes in the fleet mix, e.g., effect of the expected increase/decrease in any vehicle segment.
3. EFP provides a tool to evaluate the effects of fleet changes, e.g., the effect of the interaction of new designs with each other, e.g., interaction between light-weighted vehicles.
4. EFP provides a tool to evaluate the effects demographic changes, i.e., evaluate the effect of the U.S. aging population. This will require the introduction of appropriate injury risk functions and the investigation of differences in crash involvements for the older populations when compared to the younger driver population used for the initial EFP feasibility study.
5. EFP serves as a new tool to evaluate advanced safety concepts for frontal crash configurations and determine the corresponding net societal benefits. The following are some suggested concepts for consideration:
    a. Effects of pre-impact braking;
    b. Effects of external inflatable structures or any pre-crash adaptation of the structure; and
    c. Adaptive restraints.
6. EFP can be used to evaluate advanced restraints for right front passengers.
7. EFP can be used to study rear seat safety both relative to crash exposure as addressed in the weighting factors and restraint system as addressed by the occupant modeling.
8. EFP can be used to evaluate active/passive integration, examples such occupant pre-position, firing air bag before contact, and changing structural characteristic before contact.
9. EFP could be applied to estimate societal effects from predicted changes in crash topologies, for example, changes due to effectiveness of crash avoidance technologies. New technologies, e.g., automatic emergency braking, could produce different impact speed distributions in future fleets. Likewise, as Lane Departure Warning and automated lane-keeping systems are more widely deployed, lower incidence of

single vehicle, road departure crashes into fixed objects, e.g., poles, would potentially result. Once established by the safety community, effectiveness estimates of new crash avoidance technologies could be used to predict the crash environment in the future.

7 REFERENCES

Augenstein, J., Digges, K., Bahouth, G., Dalmotas, D., Perdeck, E., & Stratton, J. (2005). Investigation of the performance of safety systems for protection of the elderly. *49th Annual Proceedings Association for the Advancement of Automotive Medicine.* Boston, Massachusetts, September 12-14, 2005.

Battacharya, A., Sticher, G., &Subramanian, A.. (2007, July). Shifting Battlegrounds in the passenger car market. The Boston Consulting Group. July 2007. Retrieved from www.bcgsea.com/documents/file15072.pdf.

Brooke, L., & Evans, H. (2009, March). Lighten Up! Automakers and suppliers accelerate their efforts to reduce vehicle weight by engineering them for greater use of lighter, stronger materials. Warrendale, PA: Automotive Engineering, International

Daniel, R. P. (1995). The Use of Hybrid III Legs in Developing Ford's Knee Bolster Parameters. *Proceedings of the International Conference on Pelvic and Lower Extremity Injuries.* Washington, DC, December 4-6, 1995.

Digges, K., Dalmotas, D., & Prasad, P. (2013). An NCAP star rating system for older drivers. *23rd Enhanced Safety of Vehicles Technical Conference, Paper No. 13-0064.* Seoul, Korea, May 27-30, 2013.

Doggett, S. (2011, November). Compact Cars Are Bigger and Heavier Than Ever . *Edmunds.com Reports.* Retrieved at http://blogs.edmunds.com/greencaradvisor/2010/11/compact-cars-are-bigger-and-heavier-than-ever-edmundscom-reports.html

Federal Register, 73 FR 40016. (2008). Consumer Information: New Car Assessment Program.

FEV GmbH. (2012, August). Light-Duty Vehicle Mass Reduction and Cost Analysis - Midsize Crossover Utility Vehicle. Washington, DC: Environment Protection Agency. August 2012. Available at www.epa.gov/otaq/climate/documents/420r12026.pdf

Ford Motor Company. (1978). *Safety Systems Optimization Model.* (Report No. DOT HS 6 01 446). Washington, DC: National Highway Traffic Safety Administration.

Kahane, C. J. (2012). *Relationships Between Fatality Risk, Mass, and Footprint in Model Year 2000-2007 Passenger Cars and LTVs - Final Report.* (Report No. DOT HS 811 665). Washington, DC: National Highway Traffic Safety Administration.

Kellendonk, G., Van Der Zweep, C., & Mooi, H. Evaluation of accident parameters in a numerical fleet for assessing compatibility. *SAE transactions 114, no. 6* , 2005: 707-717.

Kuchar, A. (2000). A systems modeling methodology for estimation of harm in the automotive accident environment. Thesis (M.S.). Medford, MA: Tufts University.

Kuchar, A. C., Greif, R., & Neat, G. W. (2000). A Systems Modeling Methodology for Estimation of Harm in the Automotive Accident Environment. *ASME Applied Mechanics Division-Publications-AMD 246,*: 81-92.

Kuppa, S., Wang, J., Haffner, M., & Eppinger, R. (2001). Lower Extremity Injuries and Associated Injury Criteria. *17th International Technical Conference on the Enhanced Safety of Vehicles.* Amsterdam, The Netherlands, June 4-7, 2001.

Laituri, T. R., Kachnowski, B. P., Prasad, P., Sullivan, K., & Przybylo, P. A. (2003). A Theoretical, Risk Assessment Procedure for In-Position Drivers Involved in Full-Engagement Frontal Impacts. (SAE Report No. 2003-01-1354). Warrendale, PA: Society of Automotive Engineers.

Lotus Engineering Inc. (2010, March). An Assessment of Mass Reduction Opportunities for a 2017 – 2020 Model Year Vehicle Program. Ann Arbor, MI: Author.

Lotus Engineering Inc. 2012, August 31). Evaluating the Structure and Crashworthiness of a 2020 Model-Year, Mass-Reduced Crossover Vehicle Using FEA Modeling. Sacremento, CA: California Air Resources Board. Available at .

www.epa.gov/otaq/climate/documents/final-arb-phase2-rpt-r1.pdf

Lu, S. (2006, January). Vehicle Survivability and Travel Mileage Schedules. (Report No. DOT HS 809 952). Washington, DC: National Highway Traffic Safety Administration. Avalable at . www-nrd.nhtsa.dot.gov/Pubs/809952.pdf

Market Data Center. (2013, February 1). http://online.wsj.com/mdc/public/page/2_3022-autosales.html.

Marzougui, D., Samaha, R. R., Cui, C., & Kan, C-D. (2012, July). Extended Validation of the Finite Element Model for the 2001 Ford Taurus Passenger Sedan. (Report No. NCAC 2012-W-004). Ashburn, VA: National Crash Analysis Center. Available at www.ncac.gwu.edu/research/pubs/NCAC-2012-W-004.pdf

Medford, R. (2011, February). Opening Speech for the NHTSA Workshop on Vehicle Mass-Size-Safety. *NHTSA Mass-Size-Safety Symposium.* Washington, DC: National Highway Traffic Safety Administration.. Available at www.nhtsa.gov/staticfiles/administration/pdf/presentations_speeches/Medford_Mass-Safety_Workshop_02252011.pdf

NHTSA. (2006). Final Regulatory Evaluation: Amendment to FMVSS No. 208 5th Percentile Female Belted Frontal Rigid Barrier 56 km/h (35 mph) Test. Washington, DC: National Highway Traffic Safety Administration.

NHTSA. (2013)*Research Supporting 2017-2025 CAFE Final Rule.* Web page. Washington, DC: National Highway Traffic Safety Administration. Available at www.nhtsa.gov/Laws+&+Regulations/CAFE+-+Fuel+Economy/Research+Supporting+2017-2025+CAFE+Final+Rule

NHTSA. (2012). *Traffic Safety Facts 2010: A Compilation of Motor Vehicle Crash Data from the Fatality Analysis Reporting System and the General Estimates System.* (Report No. DOT HS 811 659). Washington, DC: Author. Available at www-nrd.nhtsa.dot.gov/Pubs/811659.pdf.

Pintar, F. A., Yoganandan, N., & Maiman, D. J.. (2008). Injury Mechanisms and Severity in Narrow Offset Frontal Impacts. *Proceedings of the52nd AnnualConference of the Association for the Advancement of Automotive Medicine.* San Diego, CA, October 6-8, 2008.

Prasad, P., Mertz, H., Dalmotas, D. J., Augenstein, S., & Digges, K. (2010).. Evaluation of the Field Relevance of Several Injury Risk Functions. *Stapp Car Crash Journal*, Vol. 54, Paper No. 10S-44. Warrendale, PA: Society of Automotive Engineers.

Scullion, P.,Morgan, R. M., Mohan, P., Kan, C-D., Shanks, K., Jin, W., & Tangirala, R. A. (2010). . A Reexamination of the Small Overlap Frontal Crash. 54th *Proceedings of the Association for the Advancement of Automotive Medicine,* Las Vegas, Nevada, October, 2010.

Sherwood, C. P., Nolan, J. M., & Zuby, D. S. (2009).. Characteristics of Small Overlap Crashes. *21st International Technical Conference on the Enhanced Safety of Vehicles*, Stuttgart, Germany, June 15-19, 2009.

Singh, H., Kabeer, B., Jansohn, W., Davies, J., Kan, C-D., Kramer, D., Marzougui; D., Morgan, R. M., Quong, S., & Wood, I. (2012, August). *Mass reduction for light-duty vehicles for model years 2017-2025.* (Report

No. DOT HS 811 666). Washington, DC: National Highway Traffic Safety Administration. Available at ftp://ftp.nhtsa.dot.gov/CAFE/2017-25_Final/811666.pdf.

Sullivan, K., Henry, S., Laituri, T. R.. (2008). A Frontal Impact Taxonomy for USA Field Data. (SAE Paper No. 2008-01-0526). Warrendale, PA: Society of Automotive Engineers.

Van Der Zweep, C. D., Kellendonk, G., & Lemmen, P. (2005).. Evaluation of fleet systems model for vehicle compatibility. *International Journal of Crashworthiness 10, no. 5*: 483-494.

White Jr., P. K., Pilkey, W. D., & Sieveka, E. M. (1986). *Enhancement of the Capabilities of the Safety Systems Optimization Model.* Final Report, DTRS-57--85-C00007. Washington, DC: Transportation Systems Cent, U. S. Department of Transportation.

Zhou, Q., Rouhana, S. W., & Melvin, J. W. (1996).. Age Effects of Thoracic Injury Tolerance. (SAE Paper No. 962421). Warrendale, PA: Society of Automotive Engineers.

DOT HS 812 051A
August 2014

U.S. Department
of Transportation
**National Highway
Traffic Safety
Administration**

www.nhtsa.gov

10947a-072814-v2a